



University of
Stavanger

Faculty of Science and Technology

Master thesis

Study program/Specialization: Petroleum Geoscience Engineering	Autumn semester, 2021 Open
Writer: Bartosz Grudziński (Writer's signature)
Faculty supervisor: Dora Luz Marin Restrepo External supervisor(s): Józef Dziegielowski	
Thesis title: Tectonostratigraphic evolution of the upper Paleozoic of the Sele High and its adjacent basins.	
Credits (ECTS): 30	
Key words: Central North Sea Zechstein Group Rotliegend Group Upper Paleozoic	Pages: Stavanger, 15/12/2021

Copyright
by
Bartosz Grudziński
2021

**Tectonostratigraphic evolution of the upper Paleozoic of the Sele
High and its adjacent basins**

by

Bartosz Grudziński

MSc thesis

Presented to the Faculty of Science and Technology

The University of Stavanger

December 2021

Acknowledgements

To begin with, I would like to thank my supervisor, Dora Luiz Marín Restrepo, for the guidance and valuable comments throughout the process of writing this thesis.

I would also like to thank Józef Dziegielowski for interesting conversations, insight into the industry and for providing me with a fresh and different outlook on this paper.

Moreover, I would also like to express my gratitude towards my classmates, family and friends for constant support, good laughs and being helpful.

Abstract

The main focus of this study is to improve the understanding of the timing of the tectonic activity and its control over the distribution of the upper Paleozoic strata in the chosen study area. The study area is located approximately 150 km south-west from Stavanger and covers t includes Sele High and the northernmost part of the Danish-Norwegian basin, northernmost part of Jæren High and the entire Southeastern bank of Ling Depression.

This thesis utilizes 2D and 3D seismic volumes to generate time surface maps of the top Zechstein, top Rotliegend and bottom Rotliegend horizons. As well as well log data and open-source Norwegian Petroleum Directorate well reports in order to study lateral and vertical facies variation of the Zechstein and Rotliegend Groups. In the study area The Zechstein Group assemble variety of evaporitic and siliciclastic rocks. However, in the study area its succession consists mainly of halite except 8/3-1 well. The Rotliegend Group in the study area includes packages of siltstone, sandstone, and shales. Rotliegend is homogenously distributed over the study area. The older Upper Paleozoic rocks were encountered only 7/3-1 well and 17/12-2. In the well 7/3-1 below the Rotliegend GP the carbonates were encountered. While the 17/12-2 well presents Devonian sandstone. However, since those two upper Paleozoic sections are barren of fossils, therefore their exact age is uncertain. Based on the interpretation of the seismic images the three fault groups were distinguished, of the subsequent strikes N-S, NE-SW, W-E. These fault groups appear to crosscut the Rotliegend without showing sign of syn-sedimentary deposition. However, in some of the interpreted cross-sections the thickening of pre-Rotliegend strata is visible along the the N-S and NE-SW. Therefore the study area was subjected under two main extensional events: the Late Devonian-Early Carboniferous, late Permian to Early-Triassic.

Table of contents

Acknowledgements.....	i
Abstract.....	ii
Table of contents.....	iii
List of figures.....	v
List of tables.....	viii
1. Introduction.....	1
1.1 Previous studies.....	1
1.2 Knowledge gap.....	2
1.3 Aim and objective of the study	2
1.4 Location.....	3
1.5 Geological setting.....	3
1.5.1 Tectonics.....	4
1.5.2 Paleogeography, depositional environment and stratigraphy	7
2. Dataset.....	15
3. Methodology.....	16
3.1 Seismic well tie	16
3.2 Seismic interpretation.....	18
3.3 Seismic attributes	19
4. Results.....	20
4.1 Fault families.....	20
4.2 Seismic unit description	21
4.2.1 Seismic unit 1 (SU 1): Top Zechstein to Top Rotliegend (Zechstein Group).....	21
4.2.2 Seismic unit 2 (SU 2): Top Rotliegend to Bottom Rotliegend (Rotliegend Group).....	34
4.2.3 Seismic unit 3 (SU 3): Bottom Rotliegend to Bottom Devonian or Carboniferous	44
5. Discussion.....	51
5.1 Tectonostratigraphic evolution of SU 1	51

5.2 Tectonostratigraphic evolution of SU 2	51
5.3 Tectonostratigraphic evolution of SU 3	51
5.4 Tectonostratigraphic evolution of SU 4	53
6. Conclusions.....	55
References.....	56
Appendices.....	60
Appendix 1: Table of wells	60
Appendix 2: Table of seismic quality	63
Appendix 3: Table of lithology	66
Appendix 4: Table of cores	68
Appendix 5: Table of geochemical data.....	70

List of figures

Figure 1: Location map of the Central North Sea with the study area marked in red – including the structural elements from the Norwegian sector, 3D seismic cubes and 2D seismic lines (NPD, 2021).	3
Figure 2: a) Triassic rift pattern of the North Sea with marked major first, second and third order faults. Evans et al., 2003. b) Middle to Late Jurassic pattern of the North Sea with marked major first, second and third order faults. Evans et al., 2003. c) Late Jurassic to Cretaceous rift pattern of the North Sea with marked major first, second and third order faults (Evans et al., 2003).	6
Figure 3: Lithostratigraphic graph with marked main well tops, seismic units and main tectonic events.....	7
Figure 4: a) Palinspastic global map of the Devonian period (Evans et al., 2003) b) Simplified map of NW Europe and its Devonian tectonic and sedimentary setting with the study area marked with red rectangle (modified after K.W Glennie et al. 2005).....	9
Figure 5: Depositional environment models for Lower Devonian, Middle Devonian with distinction between dry and wet periods and Upper Devonian of the Old Red Group with marked typical architectural elements for each period (Evans et al., 2003).	10
Figure 6: a) Palinspastic global map of the Early Carboniferous period (Evans et al., 2003). b) Simplified map of NW Europe and its Early Carboniferous tectonic and sedimentary setting with the study area marked with a red rectangle (modified after Glennie et al., 2005).....	11
Figure 7: a) Palinspastic global map of the Late Carboniferous period (Evans et al., 2003). b) Simplified map of NW Europe and its Late Carboniferous tectonic and sedimentary setting with the study area marked with a red rectangle (modified after Glennie et al., 2005).....	12
Figure 8: a) Palinspastic global map of the Permian period. (Evans et al., 2003). b) Simplified Permian tectonic setting map with marked variance of the depositional environments during I) Early Upper Rotliegend 2 deposition II) Late Upper Rotliegend 2 2 deposition III) Zechstein deposition – with the study area marked with a red rectangle (Glennie et al., 2003).	14
Figure 9: Map of the main Zechstein’s structural elements with marked limits of Zechstein rocks and and with averaged and restored initial thickness of all the Zechstein’s facies (Glennie et al., 2003).	14
Figure 10: Synthetic well ties for 7/3-1 and 17/4-1 well with the predefined Ricker wavelet used for each seismic well tie.	17

Figure 11: Time structural map of the Top Zechstein.	23
Figure 12: Top Rotliegend with marked fault groups.....	24
Figure 13: Time thickness map of seismic1 (SU 1), Top Zechstein to Top Rotliegend (Zechstein Group with marked Northern and Southern depocenter (black) and structurally elevated high (blue)).....	25
Figure 15: Well log response for 6/3-2 with interpreted lithology of the seismic unit 1 (SU 1): Top Zechstein to Top Rotliegend (Zechstein Group).	27
Figure 14: Well log response for 15/12-3 with interpreted lithology of the seismic unit 1 (SU 1): Top Zechstein to Top Rotliegend (Zechstein Group).....	27
Figure 16: Well log response for 16/8-3S with interpreted lithology of the seismic unit 1 (SU 1): Top Zechstein to Top Rotliegend (Zechstein Group).....	28
Figure 17: Well log response for 7/3-1 with interpreted lithology of the seismic unit 1 (SU 1): Top Zechstein to Top Rotliegend (Zechstein Group).	28
Figure 18: Well log response for 17/4-1 with interpreted lithology of the seismic unit 1 (SU 1): Top Zechstein to Top Rotliegend (Zechstein Group).....	29
Figure 19: Well log response for 17/11-1 with interpreted lithology of the seismic unit 1 (SU 1): Top Zechstein to Top Rotliegend (Zechstein Group).....	29
Figure 20: Well log response for 17/12-2 with interpreted lithology of the seismic unit 1 (SU 1): Top Zechstein to Top Rotliegend (Zechstein Group).....	30
Figure 21: Well log response for 8/3-1 with interpreted lithology of the seismic unit 1 (SU 1): Top Zechstein to Top Rotliegend (Zechstein Group).	30
Figure 22: Structural correlation of the seismic unit 1 (SU 1): Top Zechstein to Top Rotliegend (Zechstein Group).....	32
Figure 23: Stratigraphic correlation of the seismic unit 1 (SU 1): Top Zechstein to Top Rotliegend (Zechstein Group).....	33
Figure 24: Time structural map of the Top Rotliegend with marked wells.....	36
Figure 25: Time structural map of the Top Rotliegend with marked four elevation zones. Zone 1 in black, zone 2 in orange, zone 3 in purple, zone 4 in red.	36
Figure 26: Time structural map of the Bottom Rotliegend.....	37
Figure 27: Time thickness map of seismic unit 2 (SU 2): Top Rotliegend to Bottom Rotliegend (Rotliegend Group).....	38
Figure 28: Well log response for 15/12-3 with interpreted lithology of the seismic unit 2 (SU 2): Top Rotliegend to Bottom Rotliegend (Rotliegend Group).	39

Figure 29: Well log response for 6/3-2 with interpreted lithology of the seismic unit 2 (SU 2): Top Rotliegend to Bottom Rotliegend (Rotliegend Group).	39
Figure 31: Well log response for 7/3-1 with interpreted lithology of the seismic unit 2 (SU 2): Top Rotliegend to Bottom Rotliegend (Rotliegend Group).	40
Figure 30: Well log response for 16/8-3S with interpreted lithology of the seismic unit 2 (SU 2): Top Rotliegend to Bottom Rotliegend (Rotliegend Group).	40
Figure 32: Well log response for 17/4-1 with interpreted lithology of the seismic unit 2 (SU 2): Top Rotliegend to Bottom Rotliegend (Rotliegend Group).	41
Figure 33: Well log response for 17/12-2 with interpreted lithology of the seismic unit 2 (SU 2): Top Rotliegend to Bottom Rotliegend (Rotliegend Group)	41
Figure 34: Structural correlation of the seismic unit 2 (SU 2): Top Rotliegend to Bottom Rotliegend (Rotliegend Group).....	42
Figure 35: Stratigraphic correlation of the seismic unit 2 (SU 2): Top Rotliegend to Bottom Rotliegend (Rotliegend Group).....	43
Figure 36: Interpreted cross section ST0611 xline 2950.	45
Figure 37: Interpreted cross section NH0201 xline 2600.	46
Figure 38: Interpreted cross section ST0611 inline 3860000.	47
Figure 39: Interpreted cross section NH0201 inline 1300.	48
Figure 40: Interpreted cross section ST0710 xline 4750.	49
Figure 41: Interpreted regional N-S cross section UGI98-224.....	50
Figure 42: Model of the tectonostratigraphic evolution of the study area.....	54

List of tables

Table 1: Amount of 2D lines and 3D volumes in each quality category after quality check scoring.....	18
Table 2: Average score of the different reflectors both in 2D lines and 3D volumes.	18
Table 3: Description of quality categories.....	19

1. Introduction

The Norwegian part of the North Sea is a mature petroleum province where petroleum exploration started in the 1960's and focused mostly on the Mesozoic and Cenozoic plays. However, in countries such as the United Kingdom, the Netherlands (both onshore and offshore), Germany and Poland the upper Paleozoic reservoirs (Devonian, Carboniferous, and Permian) were the main target of exploration (Monaghan et al., 2019). The countries are located in the area of the Southern Permian Basin, and therefore the upper Paleozoic reservoirs are the main contributors to the extracted hydrocarbon volumes (Evans et al., 2003). In the Norwegian sector the discoveries of the fields such as the Devonian Embla field prove that the upper Paleozoic prospects could be as well a successful exploration target in the Norwegian Continental Shelf (Ohm et al., 2012).

Furthermore, discoveries in the UK sector, located in the vicinity to the Norwegian sector, such as Auk and Argyll fields with reservoirs of the late Permian (Zechstein Group) and Sterling field with the reservoir located in the Devonian sandstone, give an insight of the prospectivity potential of the upper Paleozoic plays in the Norwegian sector. The above-mentioned prospects targeted reservoirs in the uplifted blocks or in the rotated fault-blocks (Trevin et al., 1991; Bifani et al., 1985).

1.1 Previous studies

The most recent complete study over the Sele high area was done by Jackson et al. (2016) Fossen et al. (2016) and Kalani et al. (2020).

Jackson et al. (2016) covers the supra- and sub-salt controls on the Permian salt deposition in the Sele High area. The study also questions whether the upper Paleozoic faulting occurred prior or during the salt deposition, as the timing of these processes would have an impact on the petroleum system creation. Moreover, it also includes the interpretation of the growing thicknesses of the Rotliegend group in vicinity of the bounding faults of the Sele High.

An alternative interpretation is given by Rodriguez (2021) where he covers the southwestern part of the Norwegian Continental Shelf. His report indicates that the Rotliegend strata was deposited in the tectonically stable environment and does not present the syn-sedimentary

growth. Additionally, he states that the Carboniferous and the Devonian strata was deposited in an already existing system of grabens and half-grabens. Skjoerestad (2021) comes to a similar conclusion that the Rotliegend group was faulted by the lower Permian to early Triassic rifting event. On the other hand, Kalani et. al (2020) suggests that the Carboniferous and Devonian strata was deposited while the faulting was active.

1.2 Knowledge gap

Since the Norwegian sector of the North Sea is thoroughly covered with the seismic, there are very few and sparsely drilled wells that penetrate the pre-Zechstein strata. Consequently, the Norwegian sector of the North Sea, does not have a settled lithostratigraphic division of the Devonian and Carboniferous rocks. The quality of the seismic reflectors of the Carboniferous and Devonian is also mostly vague and therefore its distribution is relatively known of, but not described in a detail.

On the other hand, the Top Rotliegend reflector is mostly of good quality and Rotliegend sediments are rather extensively distributed below the Zechstein Group. However, it is still uncertain what factors controls its lithological variability. Moreover, as mentioned in the paragraph above the timing of the tectonic activity is still uncertain. Authors suggest that the tectonic activity occurred during sedimentation of the Rotliegend Group while others suggest that this activity occurred posterior Rotliegend's deposition. Uncertientiy.

1.3 Aim and objective of the study

The aim of this study is to improve the understanding of the timing of the tectonic activity and its control over the distribution of the upper Paleozoic strata in the chosen study area.

The main objective of this study is to develop and evaluate tectonic framework, which will visualize the timing and the development of the upper Paleozoic tectonic processes and their control on the deposition of the Zechstein group, Rotliegend group and Devonian and Carboniferous rocks. In addition, after describing the lateral and vertical litho-stratigraphic variation of the Zechstein and Rotliegend groups and determining character of the sub-Rotliegend strata, a proposal of its stratigraphic evolution will be presented.

1.4 Location

The Sele High is located approximately 150 kilometers to the Southwest from Stavanger. The area of the study is confined to the 66 2D and 7 3D seismic lines along with 12 wells penetrating the Upper Paleozoic strata. It includes Sele High and the northernmost part of the Danish-Norwegian basin, northernmost part of Jæren High and the entire Southeastern bank of Ling Depression. The approximated study area is marked with the red rectangle in *Figure 1*.

Furthermore, the interpretation of the area is confined to the seismic quality of the horizons of interest (*Table 1*). Therefore, in the central, eastern, and distal parts of the study area and other parts where the seismic reflectors were of poorer quality and difficult to correlate to the well tops exhibited in the given wells, the interpretation contains less structural details than in the areas where the good quality 3D seismic cubes were present.

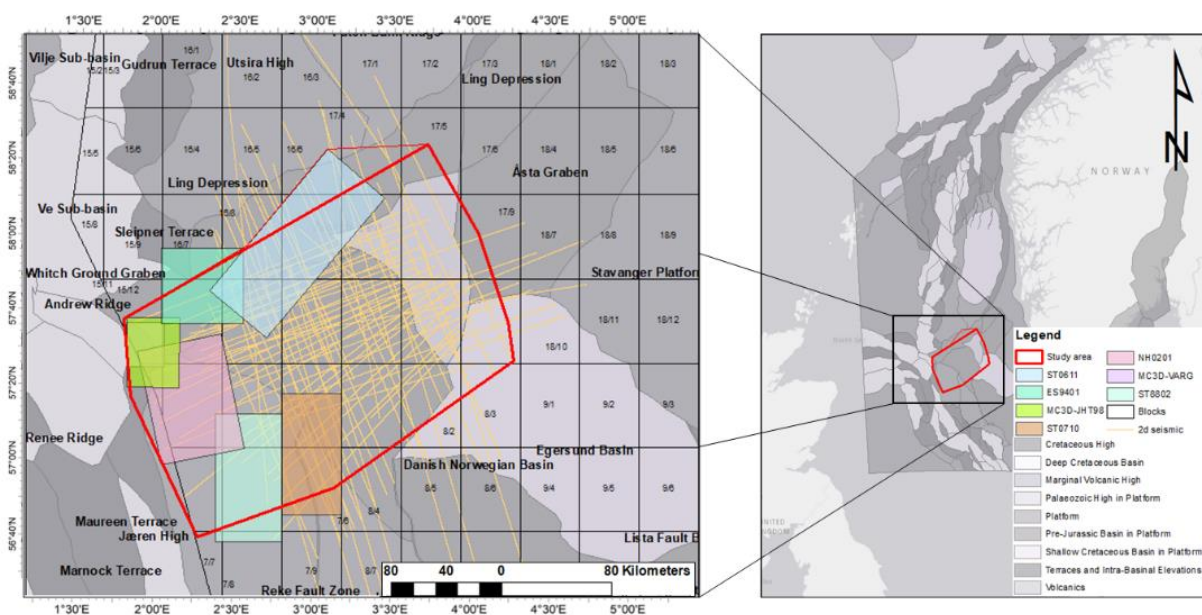


Figure 1: Location map of the Central North Sea with the study area marked in red – including the structural elements from the Norwegian sector, 3D seismic cubes and 2D seismic lines (NPD, 2021).

1.5 Geological setting

Present tectonic and sedimentary configuration of the North Sea is a consequence of about 460 million of years of geological evolution. As we read in Ziegler (1975) and Coward et al. (1989), the recognized tectonic outline of this area is a result of a few major events:

1. Lower Paleozoic Caledonian Orogeny,
2. Upper Paleozoic Variscan Orogeny,

3. Permian intracratonic stage,
4. Mesozoic rifting including Late Permian-Early Triassic rifting, Upper Jurassic-Early Cretaceous rifting and post rifting Cenozoic.

1.5.1 Tectonics

Lower Paleozoic Caledonian Orogeny

The Caledonian orogenic belt emerged during a three-way convergence between Laurentia, Baltica and Avalonia (Ziegler, 1975; Coward, 1990; Glennie, 1998). Before this collision, the Iapetus Sea was separating Laurentia from Baltica and Avalonia, and the Tornquist Sea separated Baltica from Avalonia. The first signs of closure are dated for Ordovician, but hundreds of kilometers of a crustal shortening continued until Early Devonian (Ziegler, 1975; Coward, 1990). It resulted in the creation of the main regional structure, such as the Iapetus Suture, which extends from Scotland towards the Norwegian Continental Shelf and Tornquist-Teisseyre suture, which extends from Poland through Denmark to the junction with Iapetus Suture placed in the vicinity of the Central North Sea. The north-eastern collision between Baltica and Laurentia were of a continent-continent character while the south-western collision between Laurentia and Avalonia had a continental-arc nature (Ziegler, 1975).

Upper Paleozoic Variscan Orogeny

The Variscan Orogeny was the outcome of a collision between Gondwana and Laurussia. The collision started in Carboniferous' Viséan, when both of those continents were moving northwards and the faster moving Gondwana reached Laurussia. This way, the Pangea Continent was formed (Ziegler, 1975; Coward, 1990; Glennie, 1998). Like in the Caledonian Orogeny, this collision also resulted in a compressional stress setting. Despite the overall compressional character, the Norwegian Continental Shelf was affected by the extensional forces caused by a gravitational collapse (Fazlikhani et al., 2017). Its culmination appeared to be in the Late Carboniferous (Ziegler 1975; Glennie 1998; Fazlikhani et al., 2017).

This resulted in the creation of a major West to East trending mountain belt ranging from north-western Spain, through Britain and central Germany to southern Poland and further (Ziegler, 1990). In the North Sea region those extensional forces reactivated the NW-SE trending faults inherited after the Iapetus Sea closure and the W-E trending faults inherited after the Tornquist Sea closure. This reactivation led to the formation of a series of rotated fault blocks and subsequently the creation of the Devonian mini sedimentary basins. Degradation and erosion

of the Caledonian Orogen began to provide the sediment supply for those basins (Ziegler, 1975; Coward, 1990; Fazlikhani et al., 2017).

Permian intracratonic stage

At the beginning of Early Permian when the Pangea continent was already consolidated, the differential uplift of the Variscides and the subsidence of the foreland basin led to reactivation of the faults inherited from Variscan Orogeny. This resulted in an extensive deposition of the volcanic rocks which are present along the Tornquist suture, along Polish, German, Danish and British regions. These volcanic types of rocks are found in the southwestern part of the Norwegian sector. The mentioned subsidence, combined with the rise of the eustatic sea level, established two major intracratonic basins: Southern and Northern Permian Basins (Ziegler, 1975; Coward, 1995; Glennie and Underhill, 1998).

Mesozoic rifting

During the Late Permian to the Early Triassic the extension forces led to the rifting in the North Sea region (Bell et al., 2014). This rifting stage took place in the W-E direction, causing a reactivation of the pre-Permian faults. Furthermore, it overprinted the area with a N-S and NE-SW trending fault system (Færseth, 1996; Zenella and Coward, 2003). In the Late Triassic to Early Jurassic, rifting caused a differential subsidence throughout a system of multidirectional grabens and half-grabens (Ziegler, 1982; Glennie et al., 2003).

Subsequently in Early to Mid-Jurassic another rifting pulse took place, known as the Mid-Cimmerian phase. Authors such as Underhill and Partington (1993), believe that this stage is a consequence of an uplift of a large rift dome located in the central part of the North Sea region. From the Middle to Late Jurassic, uplift of the rift dome ceased while the extension continued within the Viking graben. This rifting event led to a reactivation of the N-S and NE-SW trending faults in the northern part of the North Sea, and NW-SE trending faults in the Central North Sea (Underhill & Partington, 1993; Zenella and Coward, 2003; Bell et al., 2014). The period of the Late Jurassic-Early Cretaceous was marked with an increase in the rifting activity related to the Arctic-North Atlantic rift system, denominated the “Late Cimmerian” rifting pulse and produced a rapid subsidence in the rotational fault-blocks in the Viking Graben (Fazlikhani et al., 2017). The early to mid-Mesozoic rift tectonics events reactivated pre-

existing Paleozoic structures in the North Sea and developed new fault systems that led to new basin establishment such as Viking, Central Graben and Moray Firth basins (Ziegler, 1992).

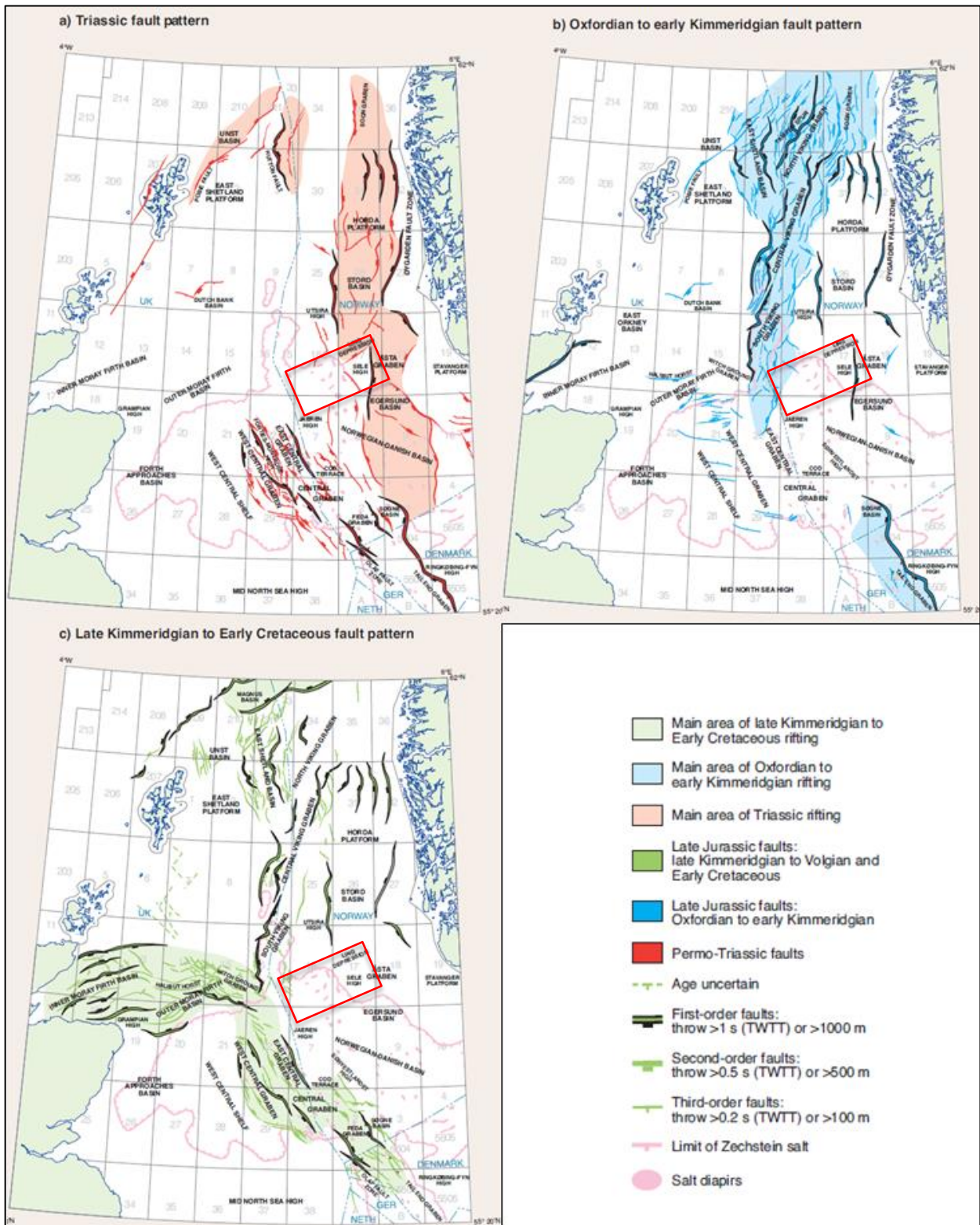


Figure 2: a) Triassic rift pattern of the North Sea with marked major first, second and third order faults. Evans et al., 2003. b) Middle to Late Jurassic pattern of the North Sea with marked major first, second and third order faults. Evans et al., 2003. c) Late Jurassic to Cretaceous rift pattern of the North Sea with marked major first, second and third order faults (Evans et al., 2003).

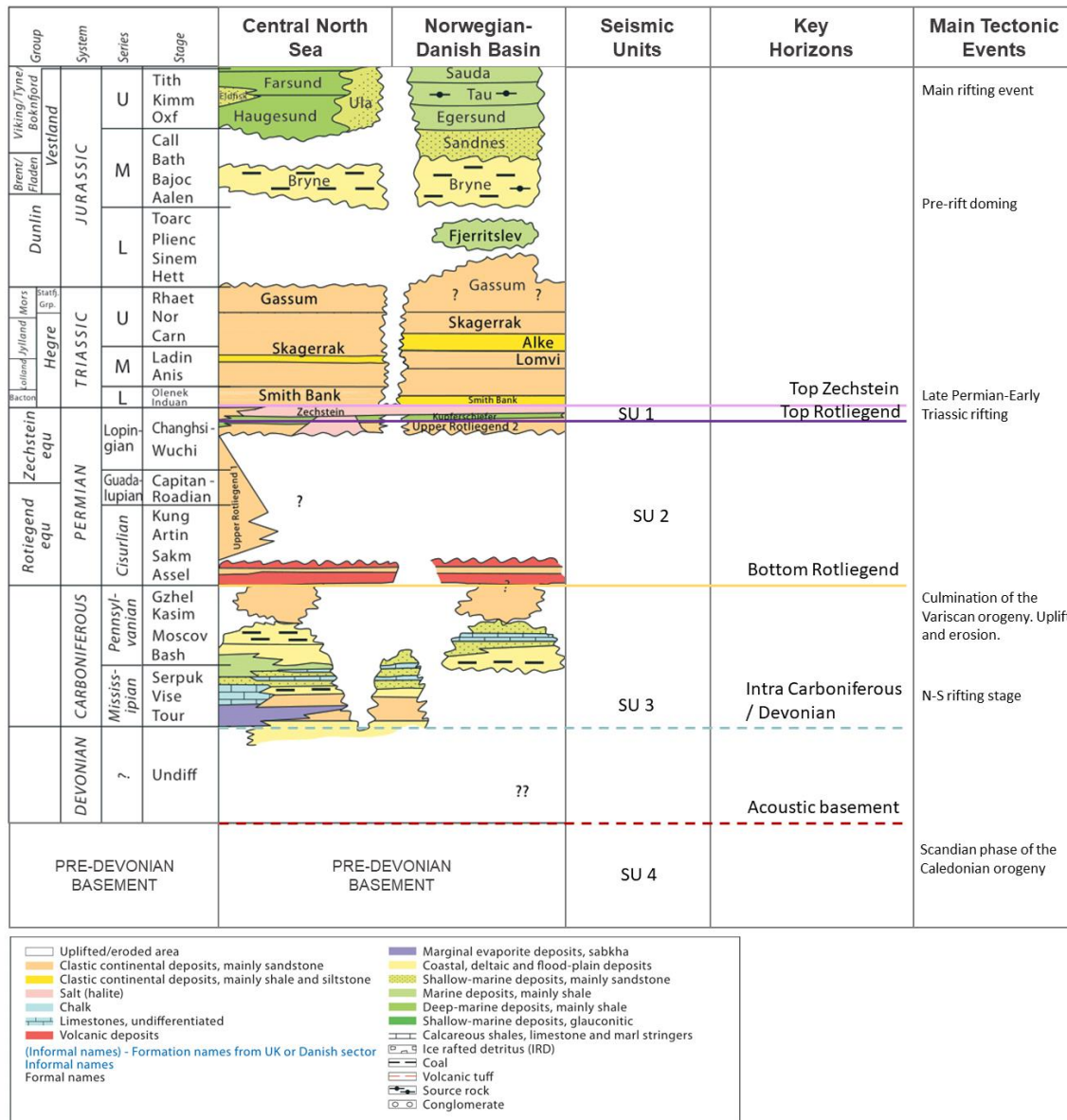


Figure 3: Lithostratigraphic graph with marked main well tops, seismic units and main tectonic events.

1.5.2 Paleogeography, depositional environment and stratigraphy

Pre-Devonian rocks

In the Scandinavian block of Baltica the crystalline crust was formed thanks to the magmatic-arc accretion during the Mid-Proterozoic, followed by Late Proterozoic reworking and plate accretion of the Sveconorwegian Terrane. The latter phase was associated with S-E directed overthrusting on the north trending mylonite belts. But the present-day crystalline basement of the North Sea largely formed during the Late Ordovician-Early Devonian Caledonian Orogeny (McKerrow et al., 1990). During the continent-continent collision between Laurentia and Baltica, allochthonous material was transported ESE onto the margin of Baltica along a basal

zone of mechanically weak Cambrian shales and phyllites overlain by a package of highly sheared rocks of the Baltican origin; collectively referred to as the basal decollement zone (McKerrow et al., 1990; Fossen, 1992). The Caledonian Deformation Front (CDF) represents the easternmost limit of the Caledonian allochthonous material. The in-situ CDF is preserved along the eastern Norway, whereas post Caledonian erosion across large parts of the southern Norway resulted in the westward translation of the CDF as observed today (Huuse, 2002; Japsen et al., 2002). CDF in that study is treated as an erosional boundary between Caledonian allochthonous material and Proterozoic autochthonous crystalline basement.

After a metamorphic process of reworking the Proterozoic rocks, the Silurian sediments started to be deposited on crystalline basement as they rest unconformable on crystalline gneissose/schistose basement. These nonmarine facies are confirmed to be of mid- to late Silurian age in all the wells that penetrate through the base of the Old Red Sandstone facies. The sedimentation of the Old Red Sandstone deposition is going to be explained in more detail in the next subchapter named 'Devonian'.

Devonian

Paleomagnetic data show that in Devonian, when the Old Red Continent, in other words Laurussia, was already formed - it was positioned around 15° to 30° S latitude where the climate was warm and characterized with arid to semi-arid conditions (*Figure 4*) (Marshall et al., 2003). In the North Sea region, the Devonian period is mainly restricted to the deposition of the Old Red Sandstone (ORS) Group, which includes Lower, Middle and Upper Old Red Sandstone. Since the ORS Group is barren of biostratigraphic correlative fossils, its division is mainly based on the regional scale unconformities which distinct Lower, Middle and Upper levels from each other (Seranne, 1992; Marshall et al., 2003). Its deposition is restricted to the Orcadian Basin which is a Devonian sub crop of the North Sea.

The sedimentation of the Lower ORS was a result of the erosion of the Caledonian Orogen when Baltica collided with Laurentia. The deposition started in Early Devonian with the emplacement of the fluvial conglomerates and sandstones as well as lacustrine mudstone (Marshall et al., 2003).

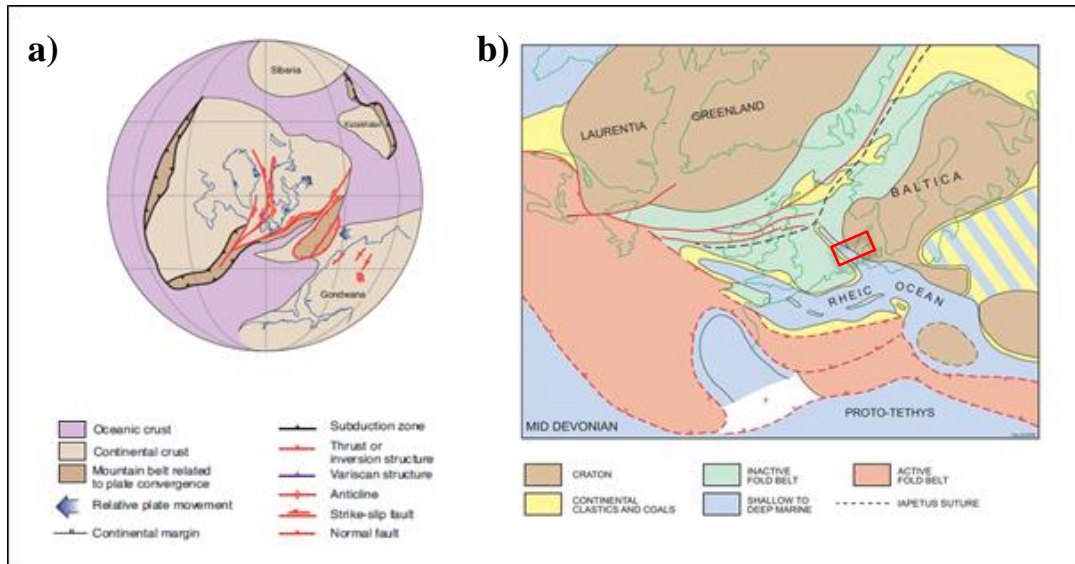


Figure 4: a) Palinspastic global map of the Devonian period (Evans et al., 2003)
 b) Simplified map of NW Europe and its Devonian tectonic and sedimentary setting with the study area marked with red rectangle (modified after K.W Glennie et al. 2005).

These sediments are deposited in a series of newly emerged half-graben sub basins. The boundary between Lower and Middle ORS marks the point at which most of those half-graben's footwalls became covered by sediment and resulted in establishment of one regional basin (Marshall et al., 2003). The Middle Old Red Group occurs either directly on the Lower Old Red Group or onlap onto the basement. The middle Old Red Group sediments occur as sandstones/conglomerate packages thickening towards major syn-depositional faults or basement highs (Vetti and Fossen, 2012). They are commonly interlapping both laterally and vertically, by lacustrine facies. The Upper Old Red Sandstone represents a succession of fluvial, well-sorted, monotonous sandstones, that were deposited in the system of sub-basins (Marshall et al., 2003). Locally it is present directly above the Lower Old Red Group from which it is separated by a significant unconformity. In some places its sedimentation lasted until Early Carboniferous (Kombrink et al., 2010).

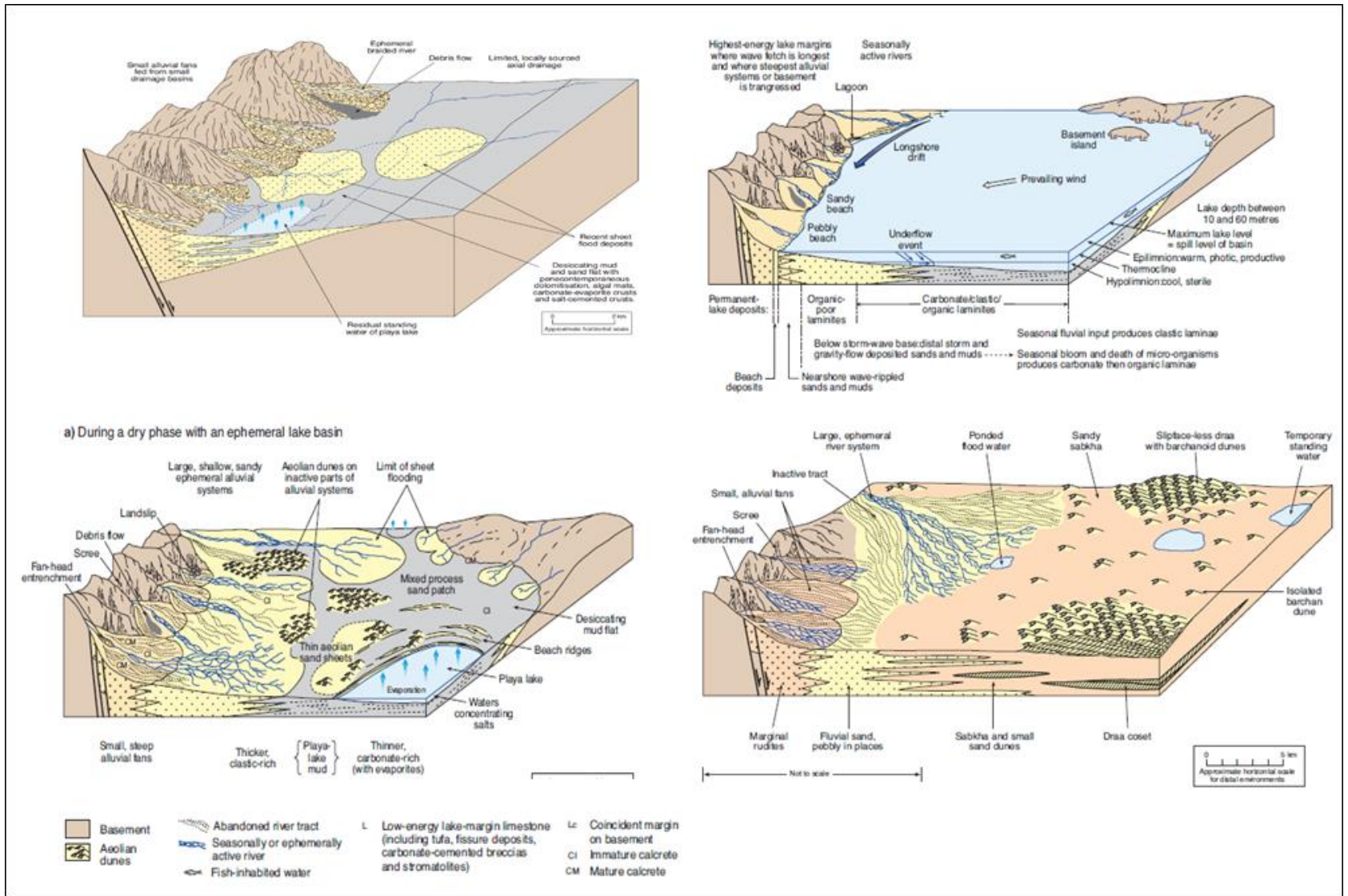


Figure 5: Depositional environment models for Lower Devonian, Middle Devonian with distinction between dry and wet periods and Upper Devonian of the Old Red Group with marked typical architectural elements for each period (Evans et al., 2003).

Carboniferous

Generally, the Carboniferous in the north-west Europe region is characterized by a change from the Devonian continental arid redbed depositional system to deposition under more varied conditions (Kombrink et al., 2010). In the northern part of the North Sea area, the oldest Carboniferous, red-bed sediments are hard to distinguish from the Devonian strata. However, since Early Carboniferous, the Old Red Continent was subjected to the continuous northward drift. Due to rising of the sea level and progressing subsidence (*Figure 6*), it started to be exposed to southern marine transgression and change to a more tropical and humid climate (Bruce et al., 2003). It had a major impact especially in the equatorial zone, leading to the deposition of shallow marine carbonate facies and deposition of coal sequences in the continental areas (Bruce et al., 2003).

In the earliest Carboniferous, the lateral distribution of sedimentary environments reflects the existence of the Boreal Ocean in the north of the study area and the Proto-Tethys Ocean to the south of it. In the southern part of the North Sea, the Carboniferous was a period of marginal marine, fluvial deltaic and alluvial deposits that were progressively filling up preexisting basins (Bruce et al., 2003). In the northern North Sea and Norwegian Sea, it resulted mainly in continental alluvial, fluvial and lacustrine environments showing reduced impact of humid and warm climate than in the southern part of the North Sea (Turner et al., 1993; Gautier, 2003).

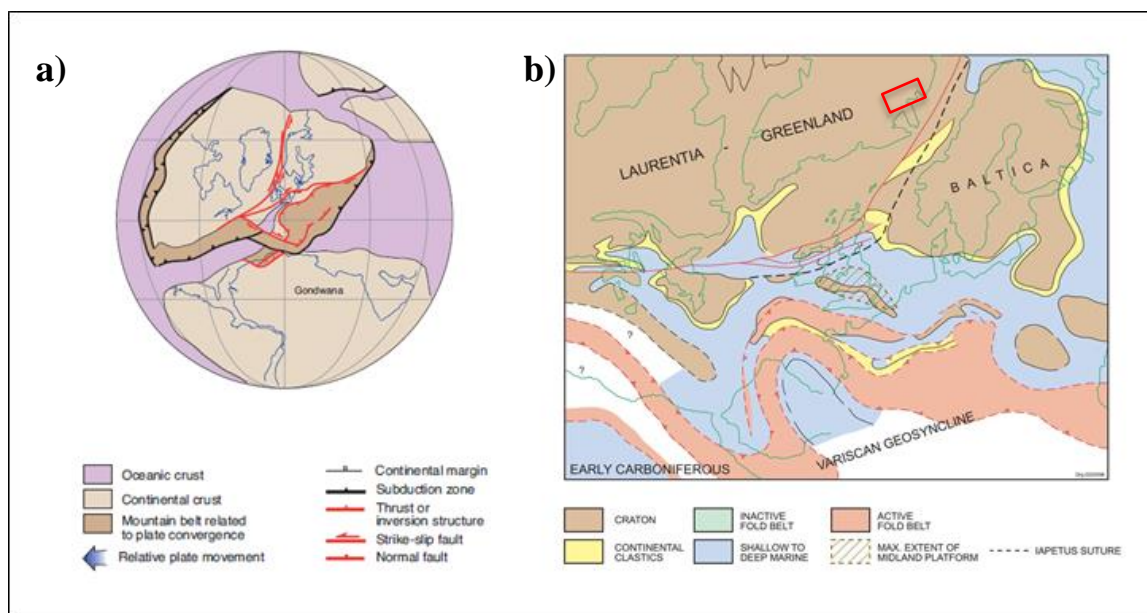


Figure 6: a) Palinspastic global map of the Early Carboniferous period (Evans et al., 2003). b) Simplified map of NW Europe and its Early Carboniferous tectonic and sedimentary setting with the study area marked with a red rectangle (modified after Glennie et al., 2005).

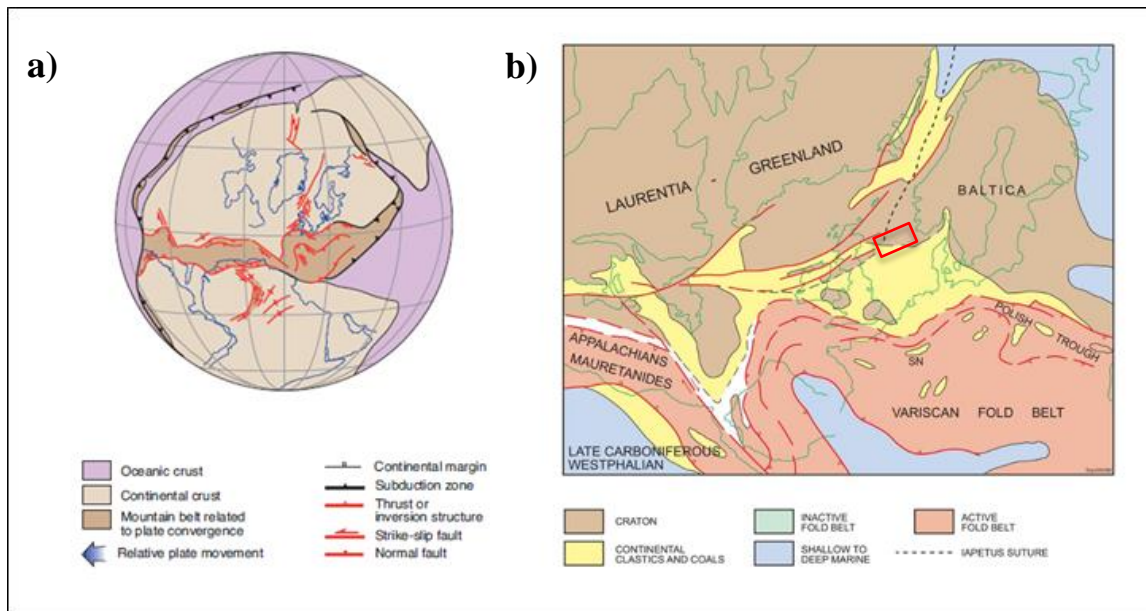


Figure 7: a) Palinspastic global map of the Late Carboniferous period (Evans et al., 2003). b) Simplified map of NW Europe and its Late Carboniferous tectonic and sedimentary setting with the study area marked with a red rectangle (modified after Glennie et al., 2005).

Permian

Rotliegend Group

During the Early Permian, the northward drift of the Pangea from the previous more equatorial humid areas to the northern tropic characterized by high temperatures and severe aridity, alongside with the uplift and erosion of the Variscan mountain range led to the accumulation of sediments in its northern foreland. It delivered sediments such as clays, silts, sand and conglomerates of pebbles and gobbles - characteristic for the continental deposition environments such as aeolian and fluvial (Lippman, 2012). Their accumulation resulted in thick series of red-bed type sediments and were classified as Rotliegend Group. However, in the lower and middle part of these sequences the volcanic rocks including tuffaceous sediments are present (Glennie et al., 2003). Over-mentioned clastic sediments are mainly red-colored, sometimes grey, and lacking diagnostic flora or fauna which results in fairly tough chronostratigraphic correlation. That type of clastic sedimentation in the northernmost region of NCS continued from Late Carboniferous and locally from Devonian until Late Permian (Gautier, 2003; Glennie et al., 2003; Lippman, 2012)

During that period the Variscan mountains extended from W to E of the continent, which caused a strong drapage effect affecting strength of the airflow and humidity flow from equatorial

zones onto northern parallels. Additionally, its location in the middle of the continent contributed to its extensive aridity. This type of setting led to a desert-like depositional environment with little rainfall, strong deflation and with the rate of subsidence exceeding the rate of sedimentation (Glennie et al., 2003).

In the Southern North Sea (Southern Permian Basin) Rotliegend is divided into Upper Rotliegend 1 (UR1) and Upper Rotliegend 2 (UR2). Normally the Rotliegend rests on the metamorphic basement or Devonian or Carboniferous strata. UR1 is described mainly based on German Rotliegend, its sedimentation started in Late Carboniferous and it is characteristic for the deposition of the aeolian sandstones (Stemmerik et al., 2000). In the German sector the bottom boundary of UR1 is marked with the Saalian Unconformity and its upper boundary is bounded with Altmark unconformity. Above Altmark unconformity lies the UR2 sedimentary sequence, which covered most of the Southern Permian Basin. However, due to insufficient data in the Norwegian sector no subdivision of the Rotliegend Group is made.

Zechstein Group

Soon after deposition of the Rotliegend, in middle Permian the global sea level arose that resulted with the widespread transgression of marine waters into previously established sedimentary basins (*Figure 8b and 9*). Lack of the clastic sediment delivery and fluctuations of the sea-level combined with high temperatures firstly led to deposition of Kupferschiefer formation which in the Norwegian sector is considered to be lowermost part of the Zechstein Group (Glennie et al., 2003; Peryt et al., 2010). It is a regional scale correlative formation. The Kupferschiefer formation is usually not thicker than a few meters it is often not recognized in the seismic. In well-logs it appears as a clear log break, since it was deposited as organic rich, radio-active and locally calcareous shale (Vaughan et al., 1989). Constantly continuing sea level rise and high temperatures led to deposition of cyclical evaporites and carbonate successions of the Zechstein Group. (*Figure 8b and 9*) The Zechstein sequence is the product of five major depositional cycles, each of which shows increasing salinity with time. However, in the Norwegian sector no subdivision of this group is made. Carbonate and anhydrite-rich successions were deposited in shallow water commonly encountered on the edge of the Zechstein Sea and/or in local structural highs (e.g., Sele, Utsira), whereas halite-rich sequences

precipitated at the basis (Vaughan et al., 1989; Glennie, 1997; Clark et al., 1998; Glennie et al., 2003).

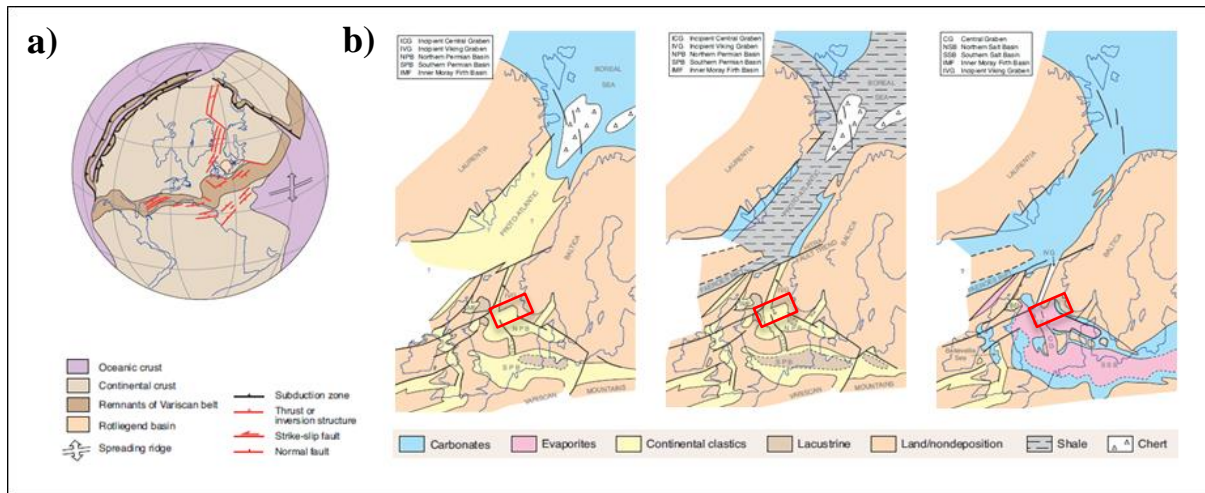


Figure 8: a) Palinspastic global map of the Permian period. (Evans et al., 2003). b) Simplified Permian tectonic setting map with marked variance of the depositional environments during I) Early Upper Rotliegend 2 deposition II) Late Upper Rotliegend 2 2 deposition III) Zechstein deposition – with the study area marked with a red rectangle (Glennie et al., 2003).

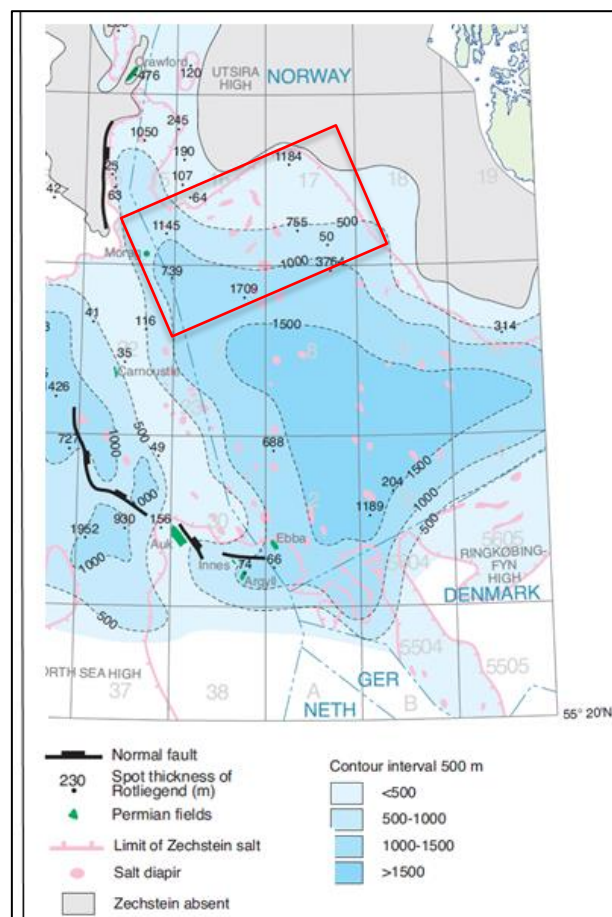


Figure 9: Map of the main Zechstein's structural elements with marked limits of Zechstein rocks and with averaged and restored initial thickness of all the Zechstein's facies (Glennie et al., 2003).

2. Dataset

Given data set compromise 12 wells. Half of them reached either the Rotliegend Group or Carboniferous or Devonian strata penetrating on the way Zechstein rocks. Wells 7/3-1 and 17/12-2 penetrates through Rotliegend bottom and terminates few meters into older units. 7/3-1 terminates in limestone most probably of the Carboniferous age, while 17/12-2 terminates in sandstones either Permian or Devonian age. The age of both is uncertain due to lack of the biostratigraphic record. Another 6 wells terminate in the Zechstein Group while the wells 15/12-2, 16/10-1, 16/10-4, and 16/11-2 reaches only 10 to 50 meters into the Zechstein Group, while most of its strata remains undrilled. Additionally, all the overmentioned wells include standard sets of the well logs (GR; DT; shallow, medium, deep resistivity, neutron, density and neutron logs) and five of them have core photos derived from Rotliegend and Zechstein Groups. All the wells contain interpreted chrono- or/and lithostratigraphic well-tops interpreted by operators or NPD representatives. The geochemical data was acquired, and it was presented in a table in *Appendix 5* (NPD, 2021).

All over mentioned wells were picked to provide depth and age control for the 66 seismic 2D lines and seven 3D seismic volumes. All the gathered 2D seismic lines present varied quality from poor to very good, while for some of the reflector's quality was not sufficient for reliable interpretation. The 3D seismic volumes present quality which varies from good to excellent.

Appendix 2

All the general well information, lithology, well tops, wireline logs, core and side cores samples, and cuttings were gathered from NPD database and available completion reports existing for each well. General well information such as: drilling depth, completion date placement, drilling objective and other relevant details are summarized in a table in *Appendix 1*.

This information and source of lithological data, lithology itself and sampled intervals are found in a table in *Appendix 3*. Only a few cored interval photos are available in the NPD database, and all of them are collected in *Appendix 4*. However, interpretations of those cores' lithologies are found in table 2. Additionally, core data was supplemented by side-wall cores and cuttings collected from drillings. and those supplementary rocks samples are summarized in table 2.

From each well, operation reports were completed and published to some extent. They have provided limited geochemical and palynological data and their values are presented in *Appendix 5*. The wells were picked carefully to convolve depth domain geophysical well logs to chosen seismic volumes. Therefore, all the wells, except 16/8-3S where drilling was finished in 2013 and the well details are still confidential, comprise individual sets of acquired geophysical well logs.

3. Methodology

3.1 Seismic well tie

Two seismic well ties were created to connect well tops expressed in depth domain to their respective key stratigraphic horizons, expressed in the time domain. The first well tie was created from the well tops from the 7/3-1 well and ST0710 seismic, the second was invoked from 17/4-1 and ST0611. The well tops used for correlation were Top Zechstein, Top Rotliegend and Bottom Rotliegend. The bottom of Rotliegend was presented only in 7/3-1 well. Additionally, for more consistent regional interpretation the well tops of Rogaland Group, Tor Formation and Cromer Knoll Group from 7/3-1 well were tied the seismic.

The objective was to create synthetic seismogram for 7/3-1 and 17/4-1 wells by using calibrated sonic log, density log and pre-defined Ricker wavelet of 30 Hz. All the synthetic seismogram needed small bulk shift adjustment to match well tops to their respective horizons.

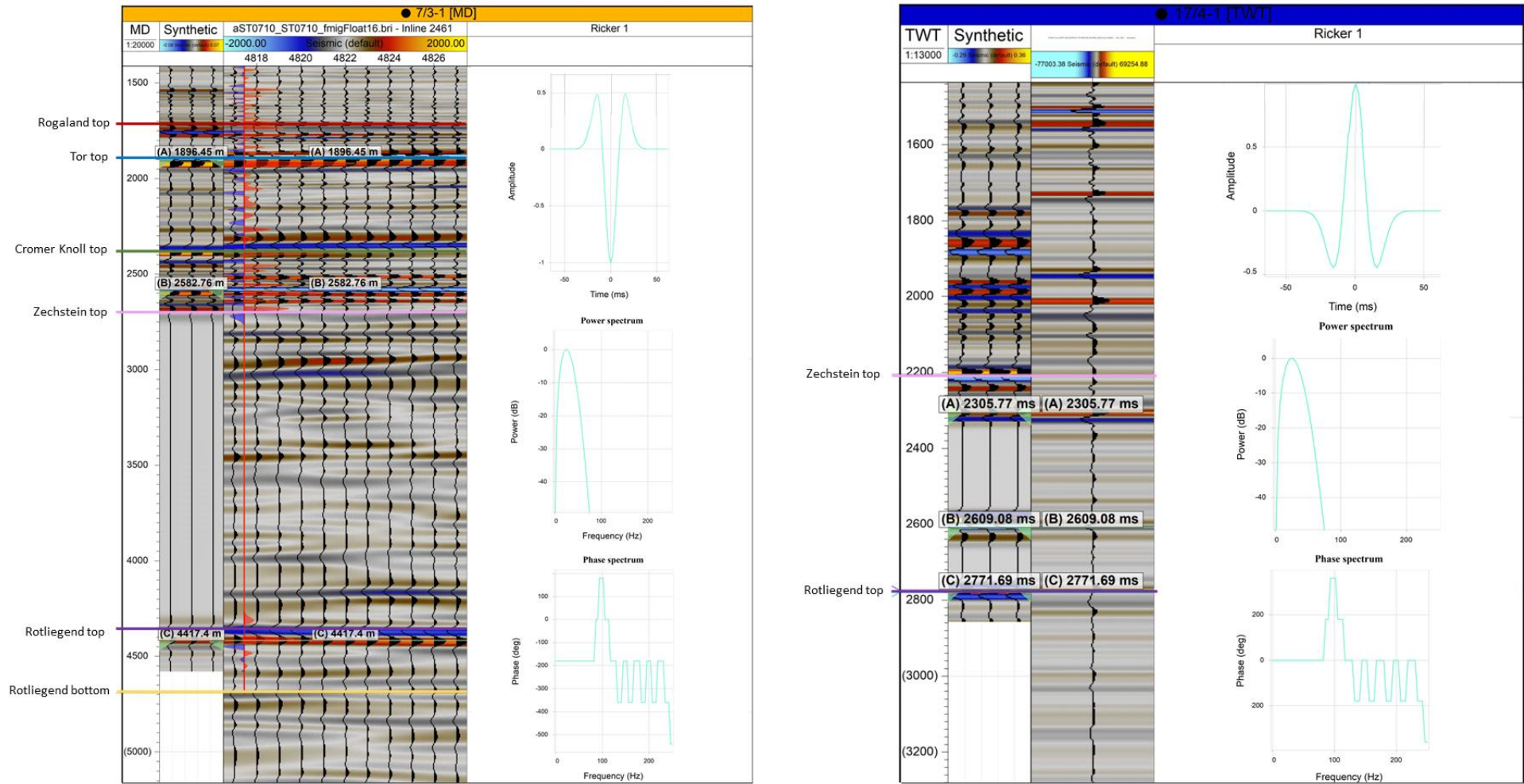


Figure 10: Synthetic well ties for 7/3-1 and 17/4-1 well with the predefined Ricker wavelet used for each seismic well tie.

3.2 Seismic interpretation

The quality of a seismic survey is dependent on the vertical and horizontal resolution, the amount of the noise and other artifacts such as ghost effects, multiples etc. The high level of attenuation of some reflectors and overall varying quality of the seismic volumes, led to extensive quality check of all the available 2D lines and 3D to pick horizons for the seismic interpretation (*Table 1 and 2*). Initially five relevant horizons were chosen for the quality check: The Top Zechstein, Top Rotliegend, Bottom Rotliegend, Intra Devonian/Carboniferous and Bottom of Carboniferous/Devonian (Acoustic basement) were chosen. All these horizons were scored from 1 to 5 points in all given seismic volumes and their score was based on the visual character, their continuity, and the strength of the reflector.

Quality score	Quality category	Number of 2D lines	Number of 3D volumes
15 equal or less	Poor	29	-
16-17.5	Decent	22	1
18-19.5	Good	12	4
20-21.5	Very good	3	2
22-25	Excellent	-	-

Table 1: Amount of 2D lines and 3D volumes in each quality category after quality check scoring.

	Average quality score of reflectors	
	2D lines	3D volumes
Top Rotliegend	4.3	4.8
Bottom Rotliegend	3.5	4.6
Top Zechstein	3.9	3.8
Acoustic basement	1.7	1.8
Intra Carboniferous Devonian	2.2	2.6

Table 2: Average score of the different reflectors both in 2D lines and 3D volumes.

Summed points	Quality category	Category description
15 equal or less	Poor	Very attenuated and weak reflectors, chaotic discontinuous, sedimentary features invisible, impossible to interpret
16-17.5	Decent	Locally distinguishable reflectors, mostly weak, mostly attenuated and impossible for consistent interpretation
18-19.5	Good	Rather strong or at least distinguishable reflectors, locally attenuated, locally discontinuous, locally attenuated and very difficult to interpret
20-21.5	Very Good	Strong reflectors, locally attenuated but allows for further interpretation, visible outline of the chaotic reflectors, possible to interpret sedimentary features
22-25	Excellent	Very strong reflectors, continuous, possible to interpret sedimentary features, very good visibility in the entire volume

Table 3: Description of quality categories.

The quality check resulted with the pick of three trustworthy seismic horizons for the interpretation: Top Zechstein, Top Rotliegend, Bottom of Rotliegend. The time surface map of each of that horizon was created and the time thickness map of the Zechstein Group and Rotliegend group was created as well. Since the intra Carboniferous-Devonian reflector, and Acoustic basement they obtained average value of 1.7 and 2.2 points from all the seismic sections they were excluded from proceeding horizon interpretation which would lead to the creation of reliable time surface maps. Intra Devonian/Carboniferous and Acoustic basement were interpreted only in the presented cross sections. The only 2D and 3D seismic volumes which had score equal or higher than 3.5 were covered with the interpretation.

3.3 Seismic attributes

To improve the reliability of the Top of Zechstein, Bottom of Rotliegend and Intra Devonian-Carboniferous the cosine phase attribute was used. This seismic attribute enhances the continuity of the reflectors while disregards amplitude variations (Rojo et al., 2016). This allowed to reveal syn-sedimentary growth of strata, unconformities and improved visibility of the weak but continuous reflectors.

4. Results

A seismic interpretation was carried out in vicinity of the Sele high. It resulted with the identification of three seismic units representing effects of the upper Paleozoic evolution in study area. The seismic units are bounded by 4 main horizons:

- Top Zechstein,
- Top Rotliegend,
- Bottom Rotliegend,
- Acoustic Basement.

Additionally, 'Intra Carboniferous/Devonian' was interpreted in the representative cross-sections. The resultant seismic units are, as following:

- Seismic unit 1(SU 1), Top Zechstein to Top Rotliegend,
- Seismic unit 2(SU 2), Top Rotliegend to Bottom Rotliegend,
- Seismic unit 3(SU 3), Bottom Rotliegend to Acoustic Basement

Top Zechstein, top Rotliegend and Bottom of Rotliegend horizons are presented as structural time surfaces maps and they are interpreted in representative cross sections while the quality of seismic allowed only the interpretation of the Intra Carboniferous/Devonian and Acoustic basement in some of the representative cross-sections. For the SU 1, SU2 the time thickness maps were created. These units cover entire study area and all of them have depth control derived from the wells. The SU1 is frilled by all the 12 wells picked for this study, SU2 have control derived from six wells and SU3 have depth control in 2 wells.

4.1 Fault families

The fault interpretation resulted with interpretation of the 16 main faults, which based on their strikes, were divided into three main groups. Near the main faults other minor fault were recognized and are illustrated in the cross sections.

- FG1 (N-S, SSE-NNW),
- FG2 (SW-NE),
- FG3 (E-W).

4.2 Seismic unit description

4.2.1 Seismic unit 1 (SU 1): Top Zechstein to Top Rotliegend (Zechstein Group)

Seismic observations

The time structural map of the Top Zechstein was interpreted with the medium to high confidence level. The map shows huge variations of the burial depth where the highest points are located at -1200ms two-way-time (TWT) and the lowest are found around at -4700ms. The general burial depth is decreasing towards the South of the study area, but other lower located areas are found in the northwest and east section of the area. The thickness map of the SU1 is presented in the figure. The SU1 thickness varies dramatically throughout the entire study area, and it ranges from 0ms, where Zechstein salt is absent to 2000ms in the southern and central part of the area. The sections where SU 1 is absent are vastly spread all over study area. The increasing thickness points are coincided with the highest located points on the time structural map suggesting existence of salt mobilized structures. These structures are approximately 700-1500ms thick and are present in the entire area.

Seismic interpretation suggests that the SU 1 formed structures typical for salt mobilization. In the Eastern area which coincidence with the interpreted Top of Rotliegend Sele High, the Zechstein Group present homogenous thickness over the major of the central part of the plateau. Apart from this plateau, in the entire area we can find structures resembling salt diapirs, salt walls and salt pillows as marked in *Figure 13*. The salt structure distribution seems to be depended on the morphology of the Top Rotliegend. Therefore, the salt diapirs are mostly present in the central part and south-eastern part of the study area, where Rotliegend Top exhibit a large depocenter which depth is increasing towards the south (*Figure 25*).

The Southern part of this depocenter is ranging from -3750ms to -4800ms, while its central part burial depth ranges from -3400ms to -3750. In the central part of the depocenter the salt diapirs thickness oscillates from 800 to 1500 ms, with one diapir reaching 2500 ms TWT of thickness. However, in the southern part of this depocenter salt diapirs seem to be more massive since their base cover larger area than the diapirs in the central part of the depocenter.

These massive diapirs reaches around 2300 ms TWT of thickness. Subsequently the salt walls are present on the elevated footwall of the faults belonging to the fault group 1 and fault group 3 and their elongated shape coincide with the strike of those faults. The average thickness of

the salt walls is similar to the thickness of salt diapirs from central part of the depocenter. The salt pillows are more commonly present on the structural highs which surrounds central depocenter. The depth of this structural highs rank between -2900ms to -2400 ms and are mostly surrounded by the salt welds (*Figure 13*). The salt absence coincides with the most elevated Rotliegend highs.

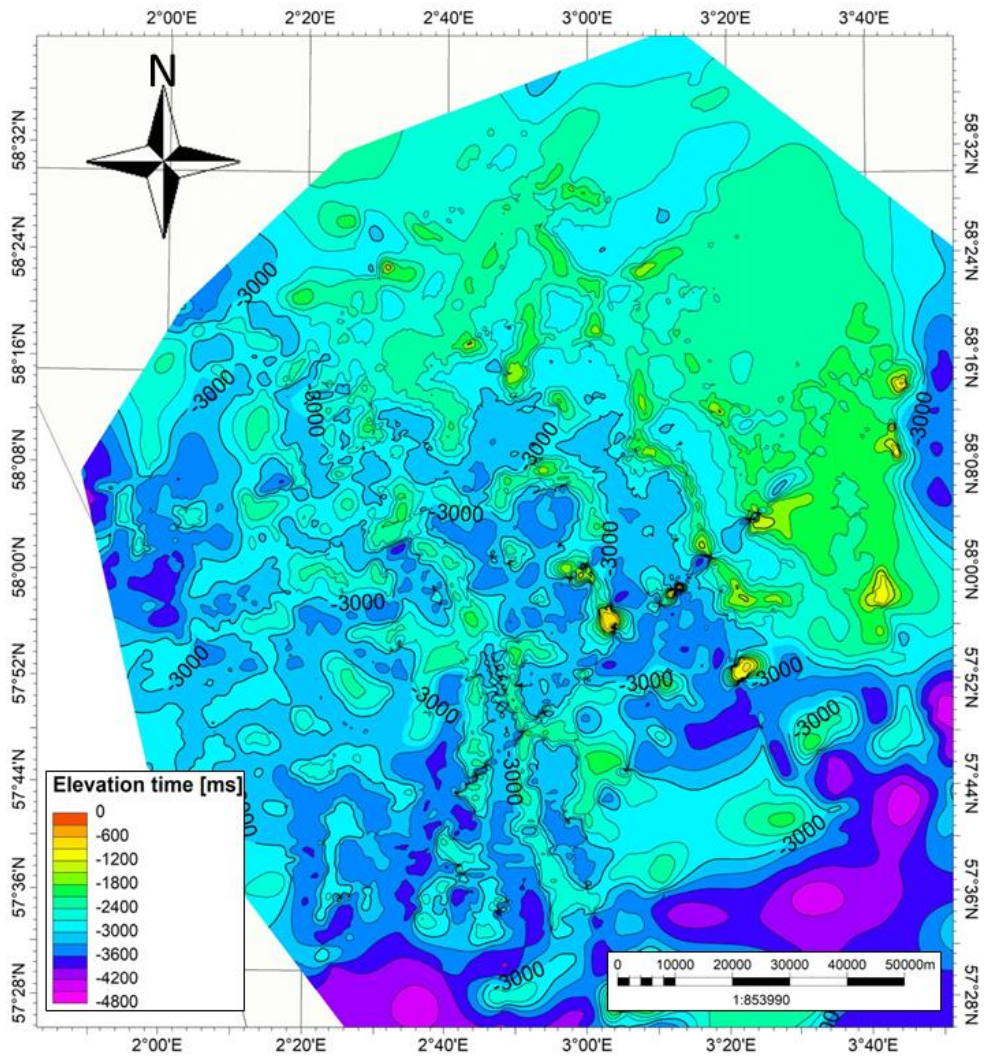


Figure 11: Time structural map of the Top Zechstein.

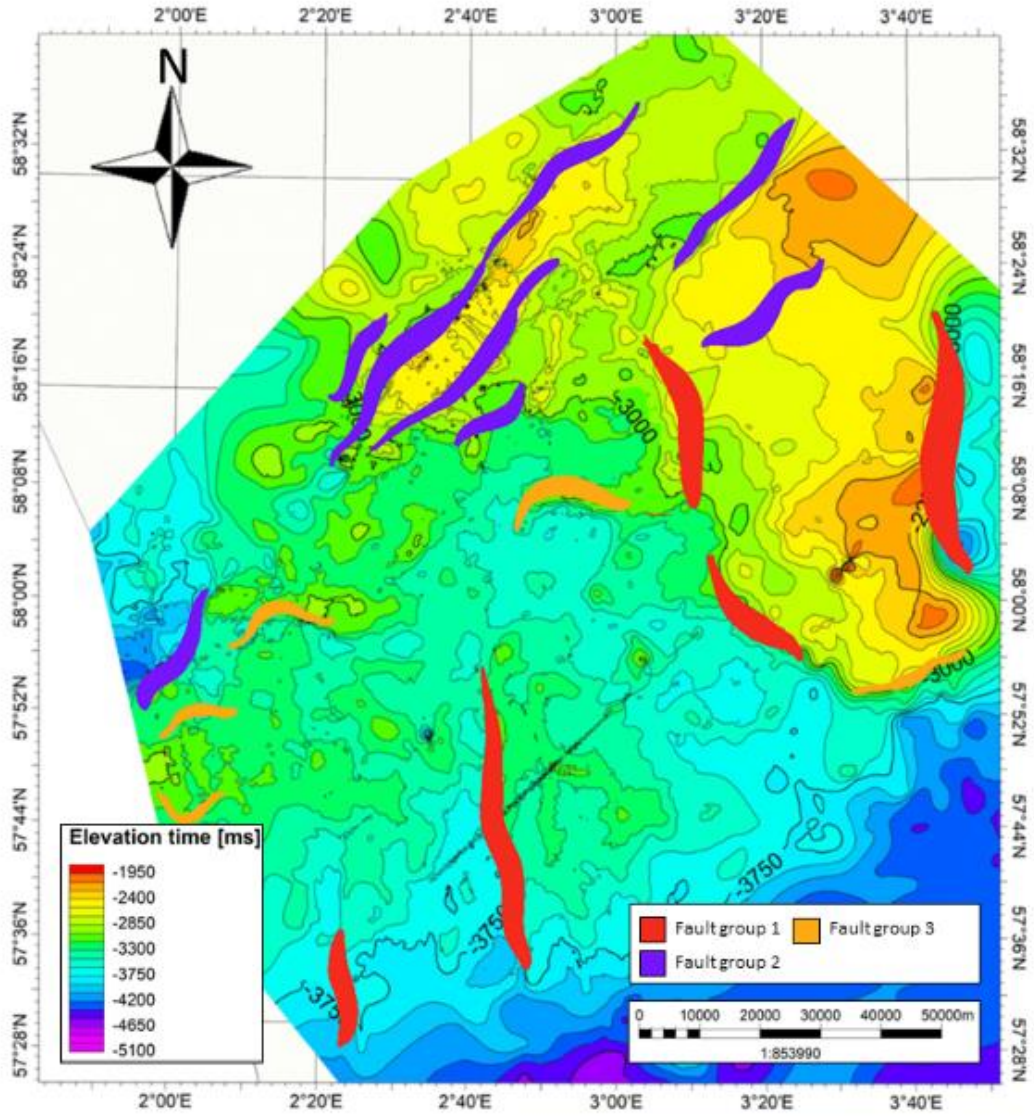


Figure 12: Top Rotliegend with marked fault groups.

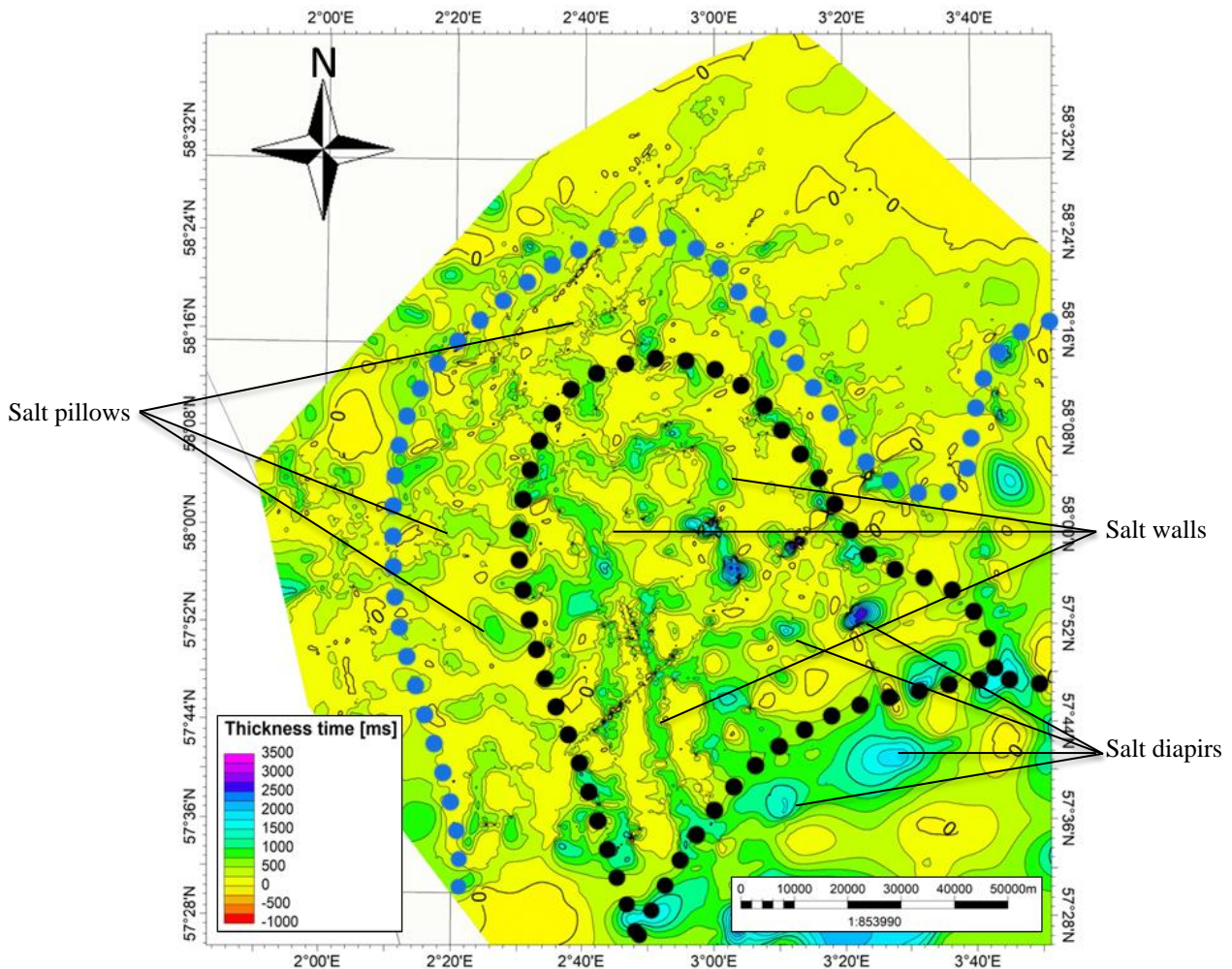


Figure 13: Time thickness map of seismic1 (SU 1), Top Zechstein to Top Rotliegend (Zechstein Group with marked Northern and Southern depocenter (black) and structurally elevated high (blue)).

Composition of the SU1 well logs, cores and cuttings observations

The proposed lithology in Figures 14-21 is based on the interpretation of the well logs, cores and cuttings descriptions from the well completion reports available in NPD.

All of the wells shown in the structural and stratigraphic correlation (Figure 22 and 23) except 17/11-1 well were drilled throughout the entire section of Zechstein Group and terminates in older rocks.

Wells 15/12-2, 16/10-1, 16/10-4 and 16/11-2 were not included into stratigraphic and structural correlation therefore they are marked with the black dots in the location map in the well log responses (Figure 14-21). These four wells penetrate averagely 50 m into Zechstein strata. Only 16/11-2 well penetrates around 100 meters of Zechstein strata. However, as the NPD's

completion reports states, in all of these wells the upper part of succession consists of grey to pale grey, blocky, amorphous anhydrite. In the 16/10-4 and 16/10-1 wells this anhydrite section is followed by red to brown subfissile shale and in the well 16//11-2.

Looking at stratigraphic correlation we can see greatly varying thickness of drilled sections. The thickness variation of given sections depends mainly on the type of the salt structure that was penetrated in this well. The well 15/12-3 and 6/3-2 (*Figure 14 and 15*) show similar GR, sonic and density log response. The 15/12-3 well presents 1200 meters of the Zechstein Gp deposition, while 6/3-2 presents around 700 meters of thickness. Description of the cuttings from both wells suggest that despite the varying thickness of the drilled sections, both of them present similar sedimentary succession - starting with the anhydrite interlapped with thin shale laminas in the upper part, followed by halite deposition with thin carnallite in central part, and anhydrite richly interlapped with halite and siliciclastic rocks in the basal part. The relatively higher values in the central part of succession represent carnallite and shale inserts. In both wells the lowermost section consists of anhydrite interlapped with halite and silicoclastic rocks.

In both wells the upper section is around 50 m thick. In the well 15/12-3 the central part of halite succession is almost 800m thick while 650 m thick in 6/3-2. Moreover, the basal section in 6/3-2 is around 50 m thick while 370 m thick in 15/12-3. 16/8-3S well is located in a structural high (*Figure 11*). The Zechstein Group in this well is around 230m thick and consists mainly of silicoclastic rocks in the central part and a thin layer of carbonates in its basal part, while its upper 70 meters of the successions is abundant in anhydrite of the same composition as it is in 15/12-2 and 6/3-2 wells.

Well, 7/3-1 and 8/3-1 present similarly low GR and DT responses throughout almost entire Zechstein succession length (*Figure 17 and 21*). The main difference in the lithology between these wells is visible in the upper part of Zechstein Gp in 8/3-1 well, showing around 50 m thick section of the mixed anhydrite with silicoclastic rocks and limestone, while in 7/3-1 this section is 10m thick and was not distinguished in *Figure 17*.

The 17/4-1 and 17/11-1 present almost the same Zechstein succession, which is confirmed by the GR, DT, density, NPHI well log responses and cuttings descriptions (*Figure 18 and 19*). 17/11-1 Zechstein succession is 700m thick while in 17/4-1 it is 1150m thick. In both wells the Zechstein succession from the top starts with the section of mixed anhydrite silicoclastic rocks

and limestones, and in both wells this section is around 200m thick, however, in 17/11-1 this section developed two thicker homogenous anhydritic intervals.

The 17/12-2 well has approximately 60m thick Zechstein succession which consist mainly of carbonates (*Figure 20*).

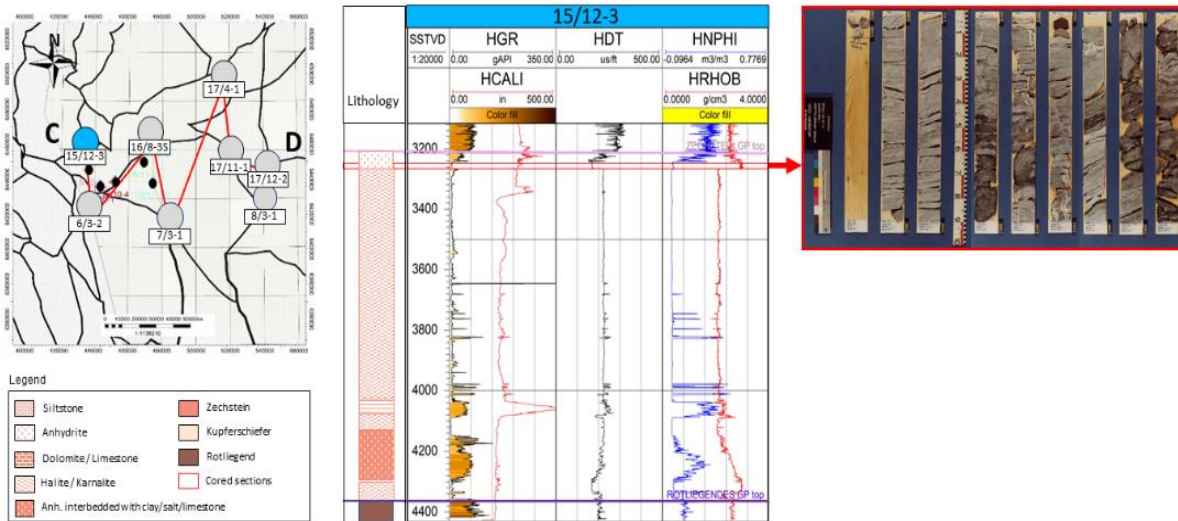


Figure 15: Well log response for 15/12-3 with interpreted lithology of the seismic unit 1 (SU 1): Top Zechstein to Top Rotliegend (Zechstein Group).

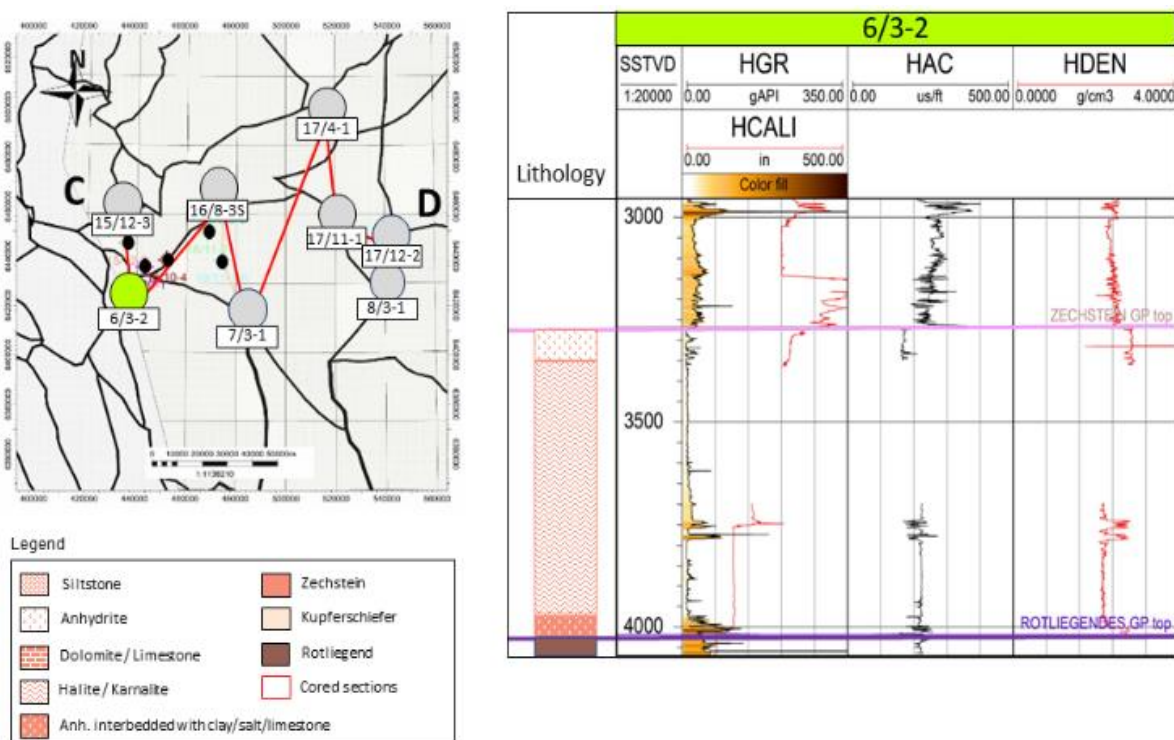


Figure 14: Well log response for 6/3-2 with interpreted lithology of the seismic unit 1 (SU 1): Top Zechstein to Top Rotliegend (Zechstein Group).

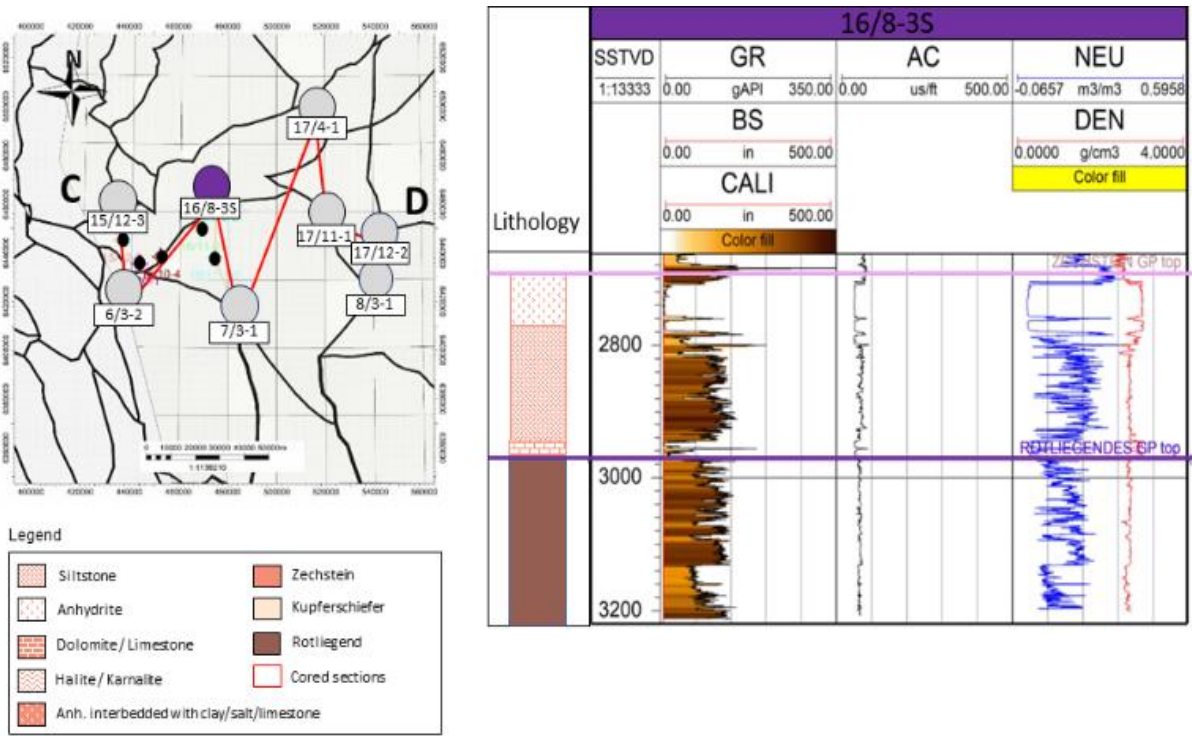


Figure 16: Well log response for 16/8-3S with interpreted lithology of the seismic unit 1 (SU 1): Top Zechstein to Top Rotliegend (Zechstein Group).

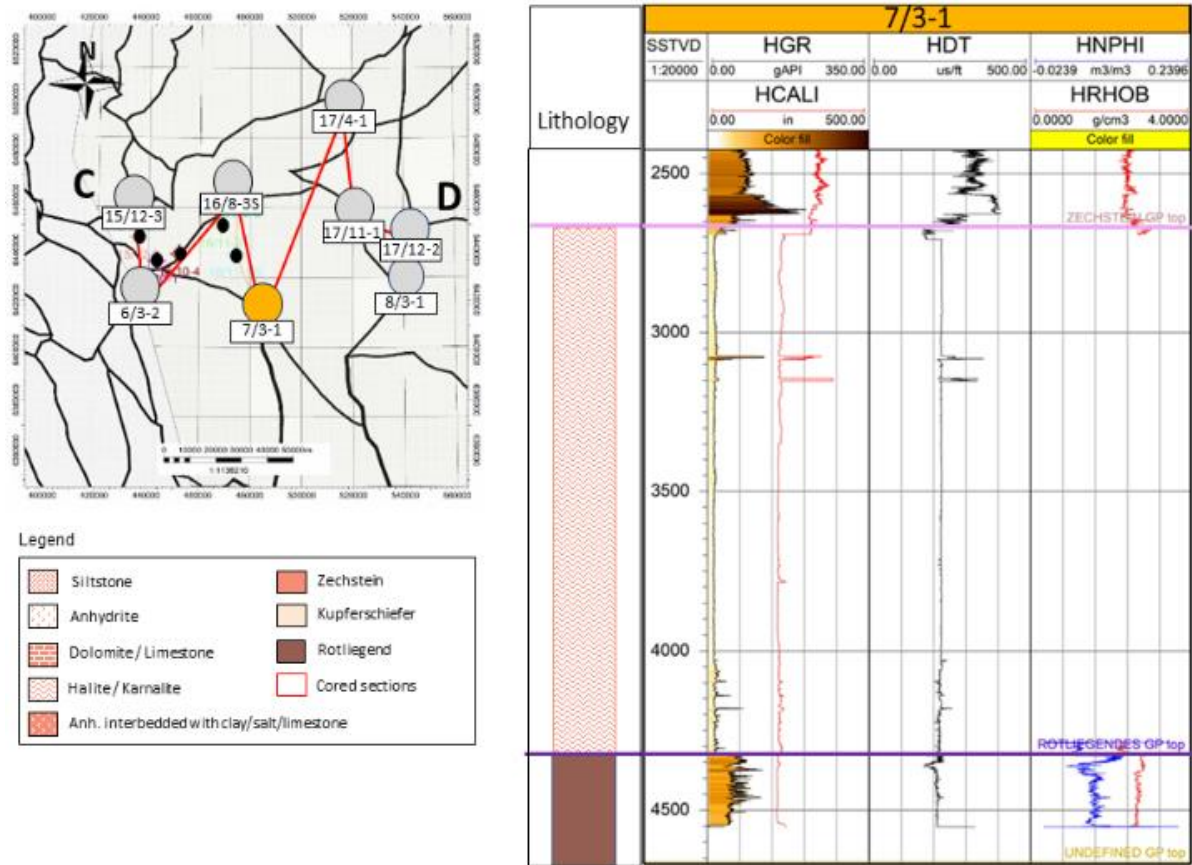


Figure 17: Well log response for 7/3-1 with interpreted lithology of the seismic unit 1 (SU 1): Top Zechstein to Top Rotliegend (Zechstein Group).

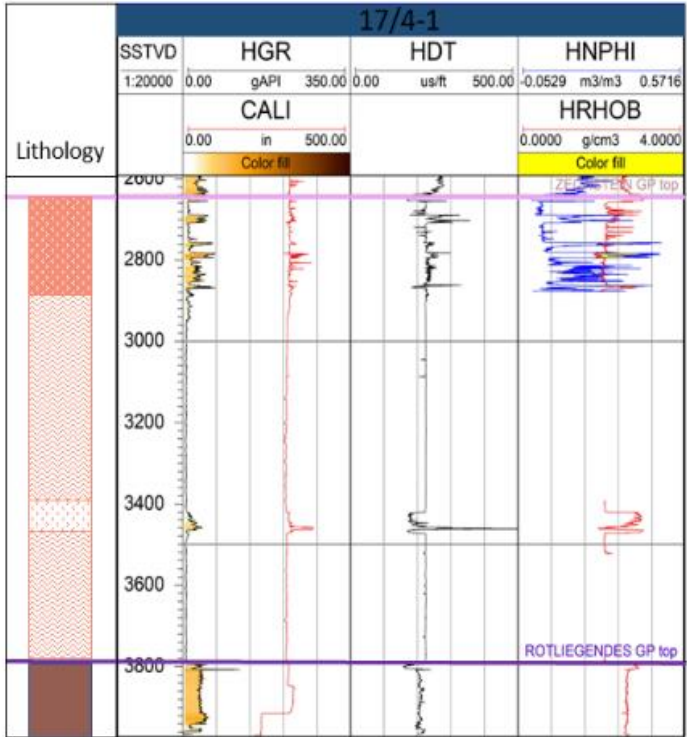
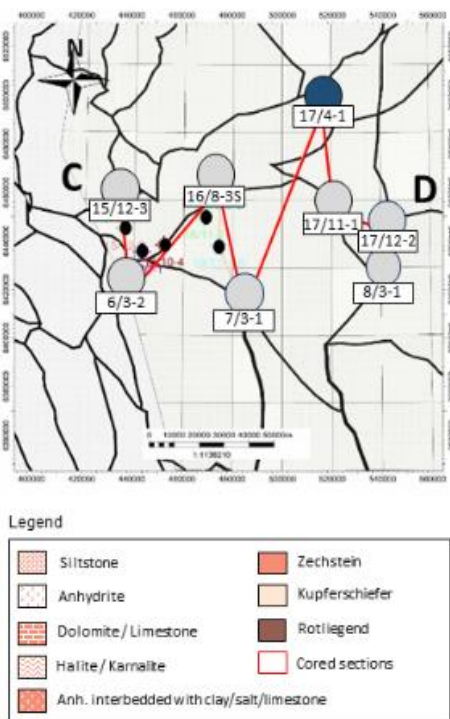


Figure 18: Well log response for 17/4-1 with interpreted lithology of the seismic unit 1 (SU 1): Top Zechstein to Top Rotliegend (Zechstein Group).

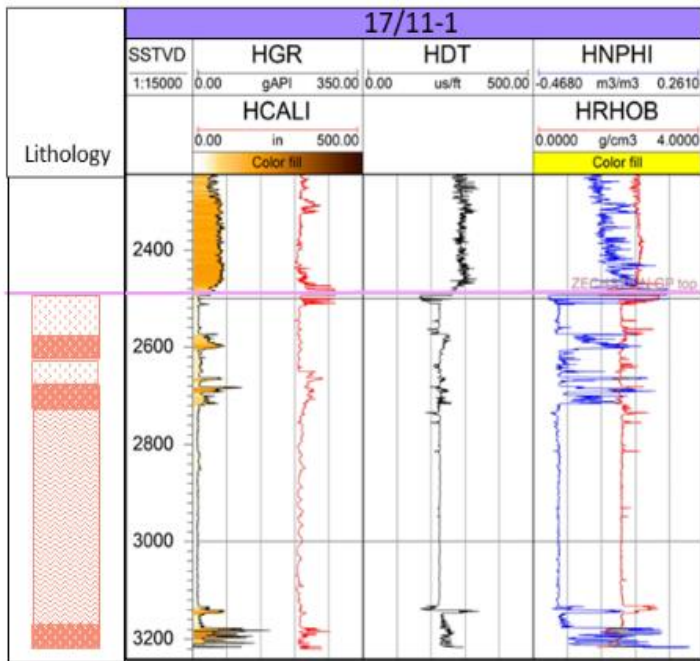
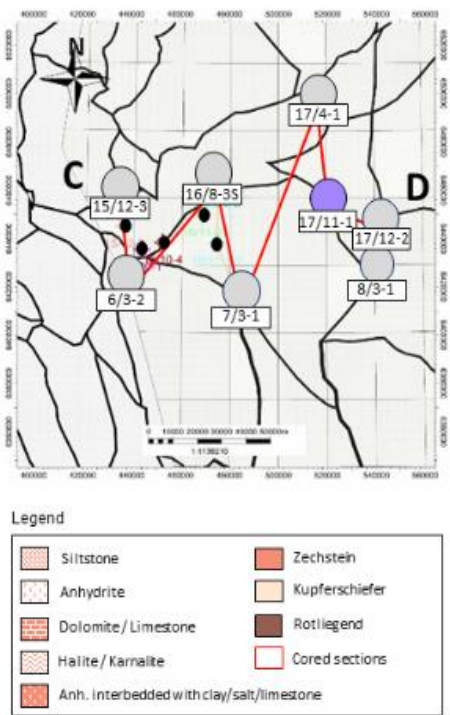


Figure 19: Well log response for 17/11-1 with interpreted lithology of the seismic unit 1 (SU 1): Top Zechstein to Top Rotliegend (Zechstein Group).

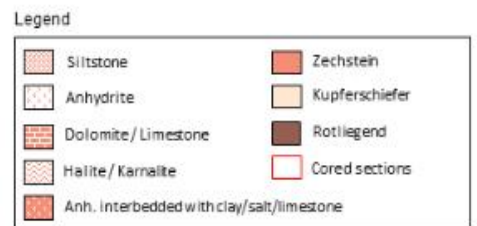
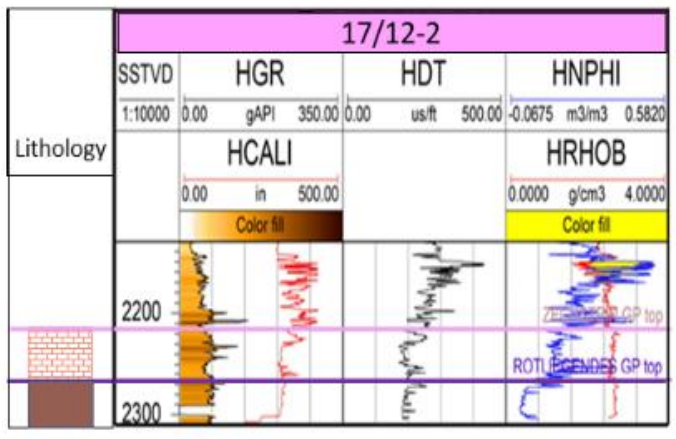
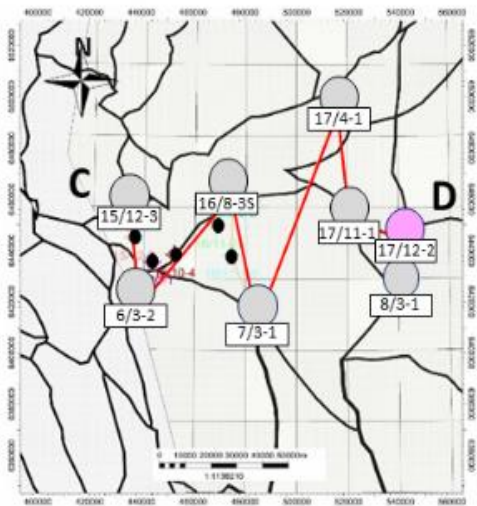


Figure 20: Well log response for 17/12-2 with interpreted lithology of the seismic unit 1 (SU 1): Top Zechstein to Top Rotliegend (Zechstein Group).

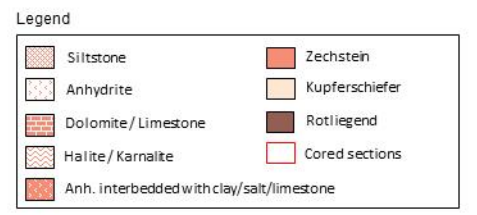
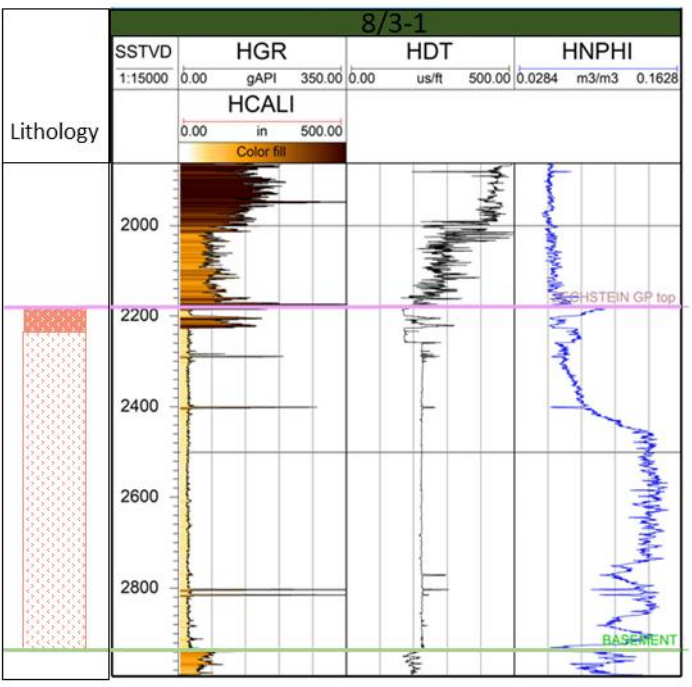
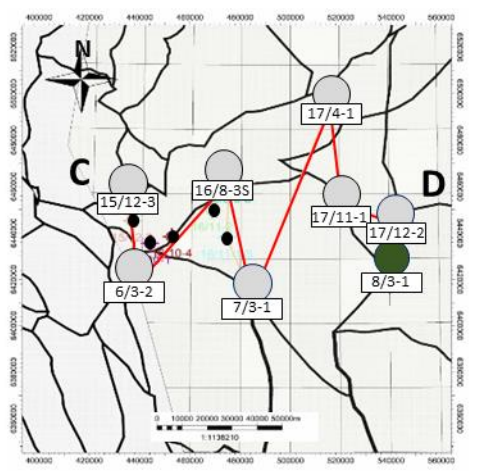


Figure 21: Well log response for 8/3-1 with interpreted lithology of the seismic unit 1 (SU 1): Top Zechstein to Top Rotliegend (Zechstein Group).

Structural and stratigraphic correlation

As it is presented in *Figure 22*, wells in which the bottom of Zechstein succession (Top of Rotliegend) is structurally elevated the general composition of the Zechstein become more siliciclastic and carbonates dominated. With an extreme example of the 17/12-2 well which is almost entirely composed of siliciclastic rocks and 16/8-3S which is almost entirely composed of dolomites.

In all the wells including 15/12-2, 16/10-1, 16/10-4, 16/11-2 the upper part of Zechstein is mainly composed of anhydrite. Furthermore, in wells 15/12-3, 6/3-2 16/8-3S, 17/11-1 the upper part of the Zechstein is almost solely characterized by grey, bulky anhydrite, while in the wells 17/4-1 and 8/3-1 the anhydrite sections are not thick enough to distinguish them separately in the proposed lithology and are mostly interlapped with shales and carbonates. In *Figure 23*, it is visible that the thicker the entire Zechstein succession is, the more halite dominated is its composition.

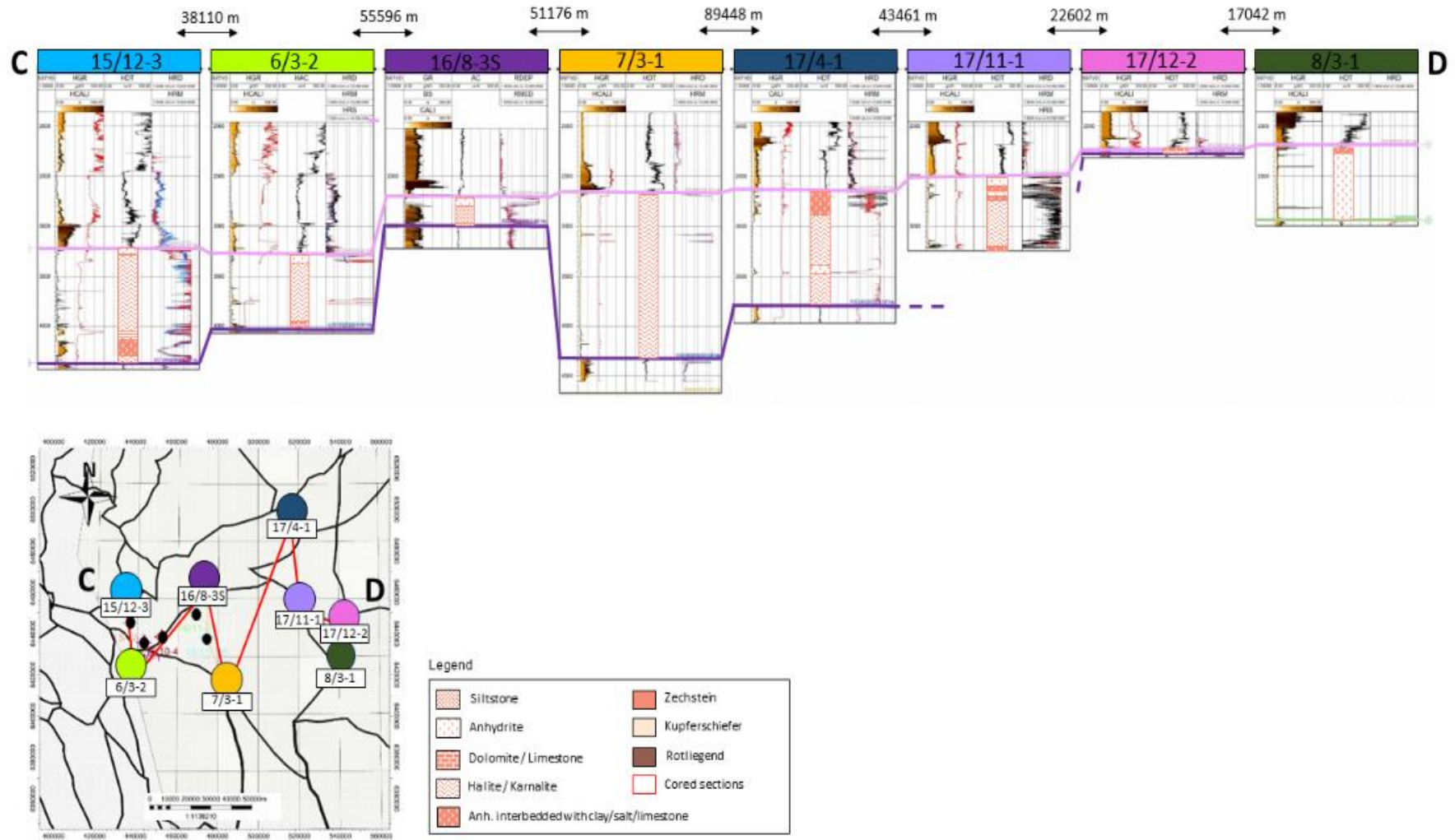


Figure 22: Structural correlation of the seismic unit 1 (SU 1): Top Zechstein to Top Rotliegend (Zechstein Group).

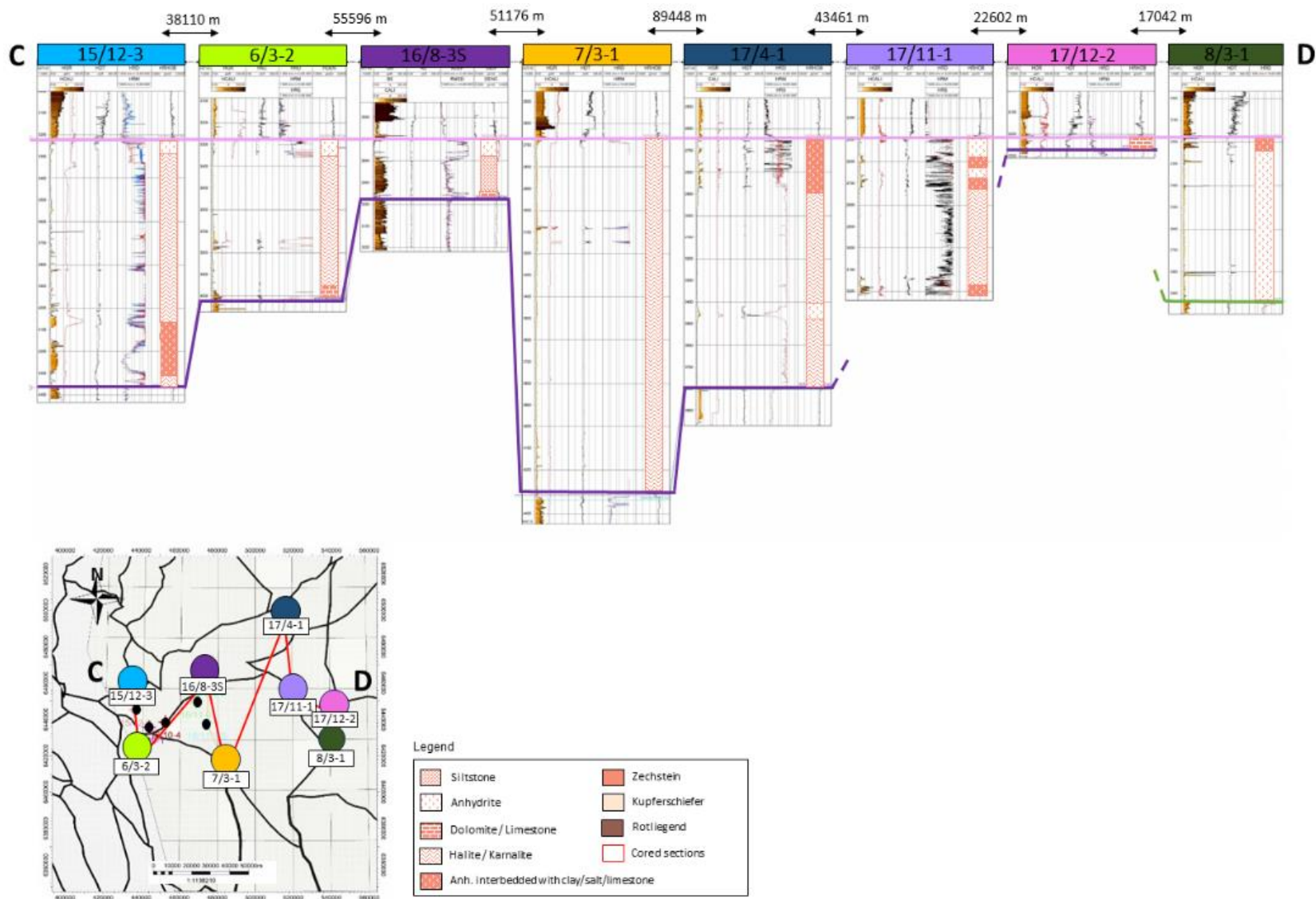


Figure 23: Stratigraphic correlation of the seismic unit 1 (SU 1): Top Zechstein to Top Rotliegend (Zechstein Group).

4.2.2 Seismic unit 2 (SU 2): Top Rotliegend to Bottom Rotliegend (Rotliegend Group)

Seismic observations

Top of the Rotliegend was described with very high confidence since it appears as strong, continuous, and relatively horizontal reflector. The resultant time surface map was created based on Top Rotliegend interpreted horizon and it is shown in *Figure 24*. The Bottom Rotliegend is mostly parallel to the Top Rotliegend and appears as strong to medium strong reflector, but very often attenuated. The Bottom of Rotliegend horizon was interpreted with low confidence in the areas of poor seismic quality and medium confidence in the areas covered with 3D seismic cubes and good quality 2D seismic lines. Based on the interpretation of this horizon the time structural map of the Bottom Rotliegend was summoned (*Figure 26*).

As it is presented in *Figure 26*, the general thickness of the Rotliegend Gp is uniform in the central and eastern part of the study area. The time thickness map present multiple areas where the thickness of Rotliegend Gp reaches 0ms TWT. However, these zero thickness areas are the pitfalls of the Petrel software interpolation of the low confidence interpretation of the bottom of Rotliegend reflector. In multiple cross section as well as in the general observation the bottom of the Rotliegend does not truncate towards its top and it presents itself in the entire study area. Despite the fact that the time thickness map does not show the isopaches between 0ms and 200ms, the cross-sections intersecting the Sele High indicate lower strata thicknesses on this elevated structural high. The time thickness map shows that the thickness of the central and eastern part of the study area varies on average between 50 to 200 ms seconds. However, Rotliegend thickness is bigger in the Southern part of the area and reaches values that range between 400 to almost 800ms. Another part of the area where thickness growth is spotted is the North-western section. In this part the values of thickness vary from 200 to 400 ms TWT.

The growing thicknesses are coinciding with the structural lows of the bottom of the Rotliegend (*Figure 26 and 27*). The burial depth of the time structural map of the Bottom of the Rotliegend ranges from -4800ms TWT in the southernmost and easternmost part to -2100ms TWT in the Northern and north-eastern part. Generally, the geomorphological features of the Bottom of Rotliegend can be divided into 4 zones as presented in *Figure 25*. First zone is the depocenter placed in the central part of the study area where its burial depth is ranging from -4000ms to 3500ms. The main fault of the FG1 seems to crosscut this zone creating local structural high ranging from 3500ms to -3100ms. Second zone are the structural lows located in the east west

and south of the area. Eastern and Western structural lows seem to be hanging walls of respectively FG 3. and FG 2. While the southern structural low seems to have slope character possibility inherited from pre-Permian faults. The third zone are the structural highs found in the west and the northwest of the study area. Their elevation ranges from -3500ms to -3000ms. The fourth zone are the structural high elevated in the north and east of the study area and their elevation spans from -3000ms to -2100ms. The northern elevations of this zone exhibit horst structures and system of a half grabens which is bounded by the FG2 while the eastern elevation - Sele High is bounded by the fault of all recognised fault groups. The interpreted Top Rotliegend exhibit the same morphological features as the Bottom Rotliegend, yet the Top of Rotliegend is interpreted in greater details.

Composition of the SU2 well logs, cores and cuttings observations

From all the 6 wells penetrating Rotliegend Group (*Figures 28-33*) only 7/3-1 and 17/12-2 wells reaches its bottom. All the wells penetrating Rotliegend have GR, DT, resistivity, and density logs. However, the well 7/3-1 has log data record reaching until the half of penetrated Rotliegend strata. The well 15/12-3 wells and 6/3-2 wells terminate after 100 meters with the Rotliegend Group. 16/8-3S, 7/3-1, 17/4-1 and 17/12-12 are penetrating into Rotliegend strata 225m, 325m, 200m, 170m and 45m respectively. All of the wells are characterized with the siliciclastic rocks. Mainly sandstone, siltstones and locally shales (*Appendix 4*).

In *Figure 24 and 25* we can see that 15/12-3, 6/3-2 wells are located in the third zone which is on the structural highs. Well 7/3-1 is located on the footwall of the main fault of the FG1, which is located in the zone 1. The 17/4-1 and the 17/12-12 wells are located in the zone 4 and represent rocks Rotliegend sequence located on the highest structural highs. The well 17/4-1 is located on the elevated horst in the northern part of zone 4. Graben while well 17/12-2 is located on the Sele High

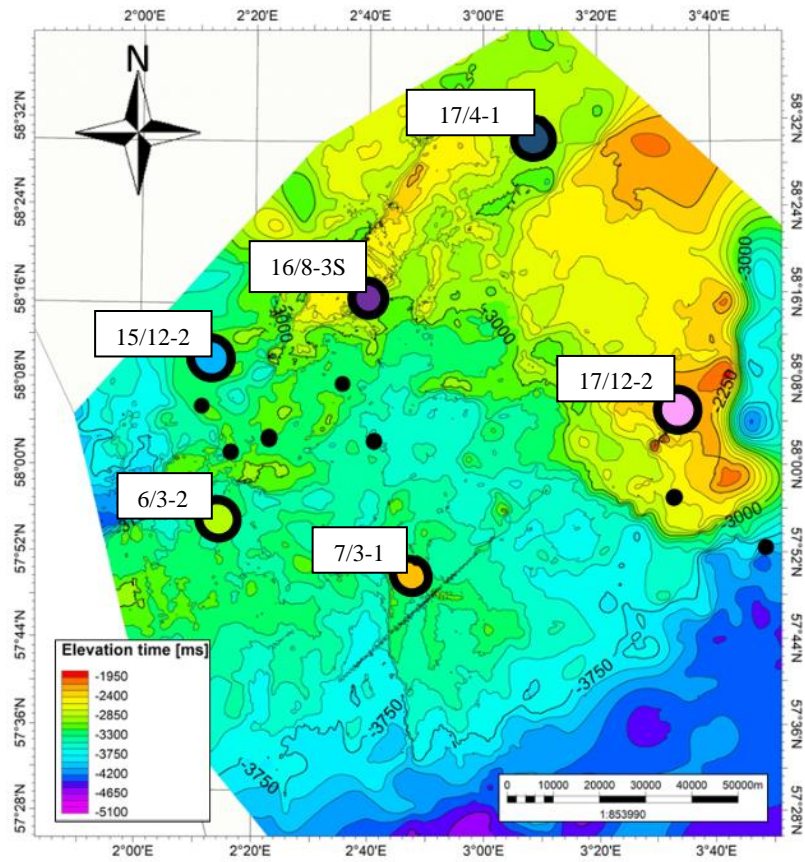


Figure 24: Time structural map of the Top Rotliegend with marked wells.

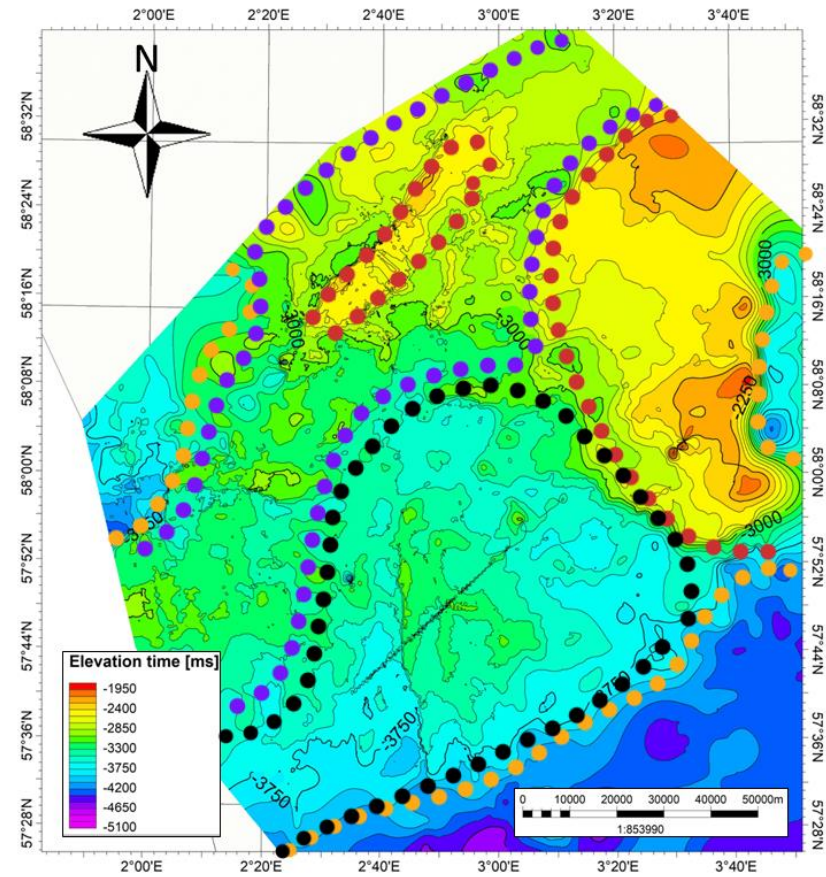


Figure 25: Time structural map of the Top Rotliegend with marked four elevation zones. Zone 1 in black, zone 2 in orange, zone 3 in purple, zone 4 in red.

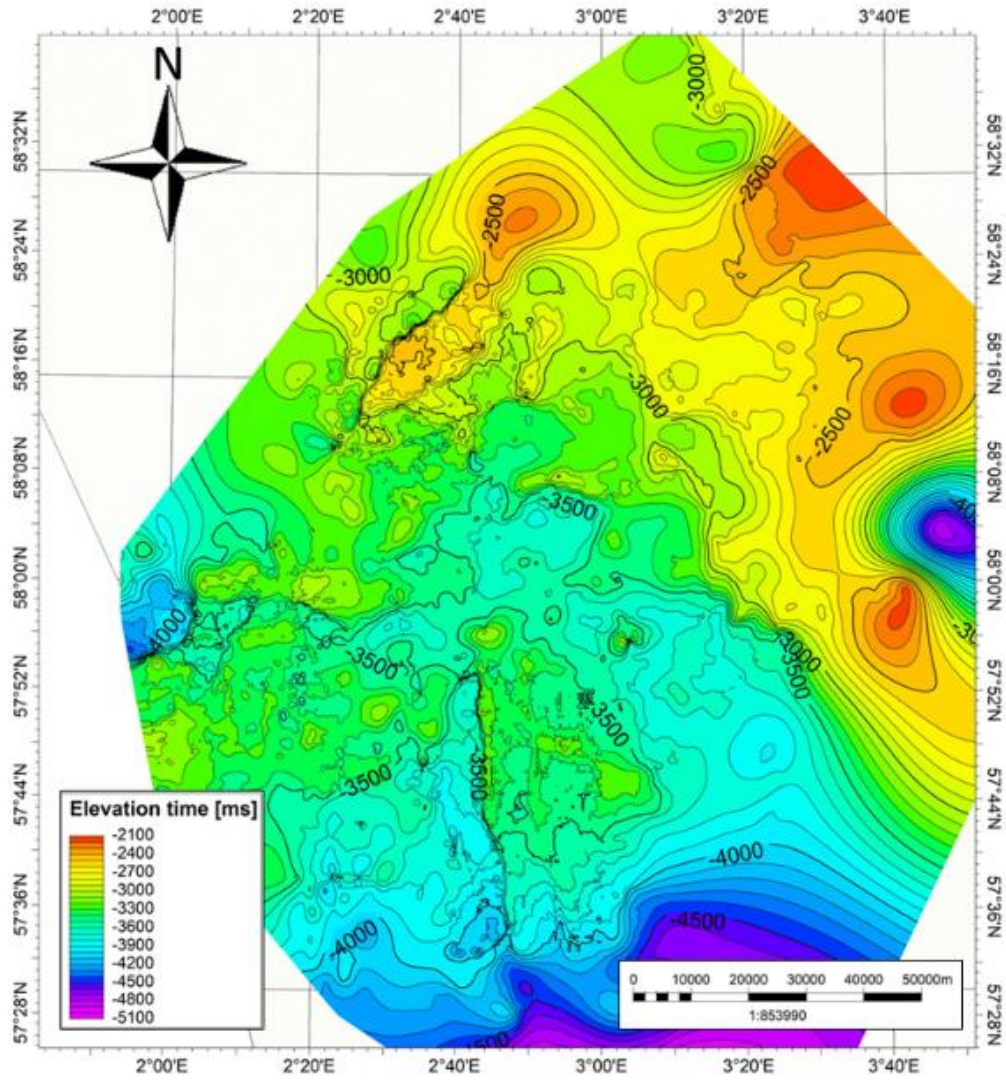


Figure 26: Time structural map of the Bottom Rotliegendes.

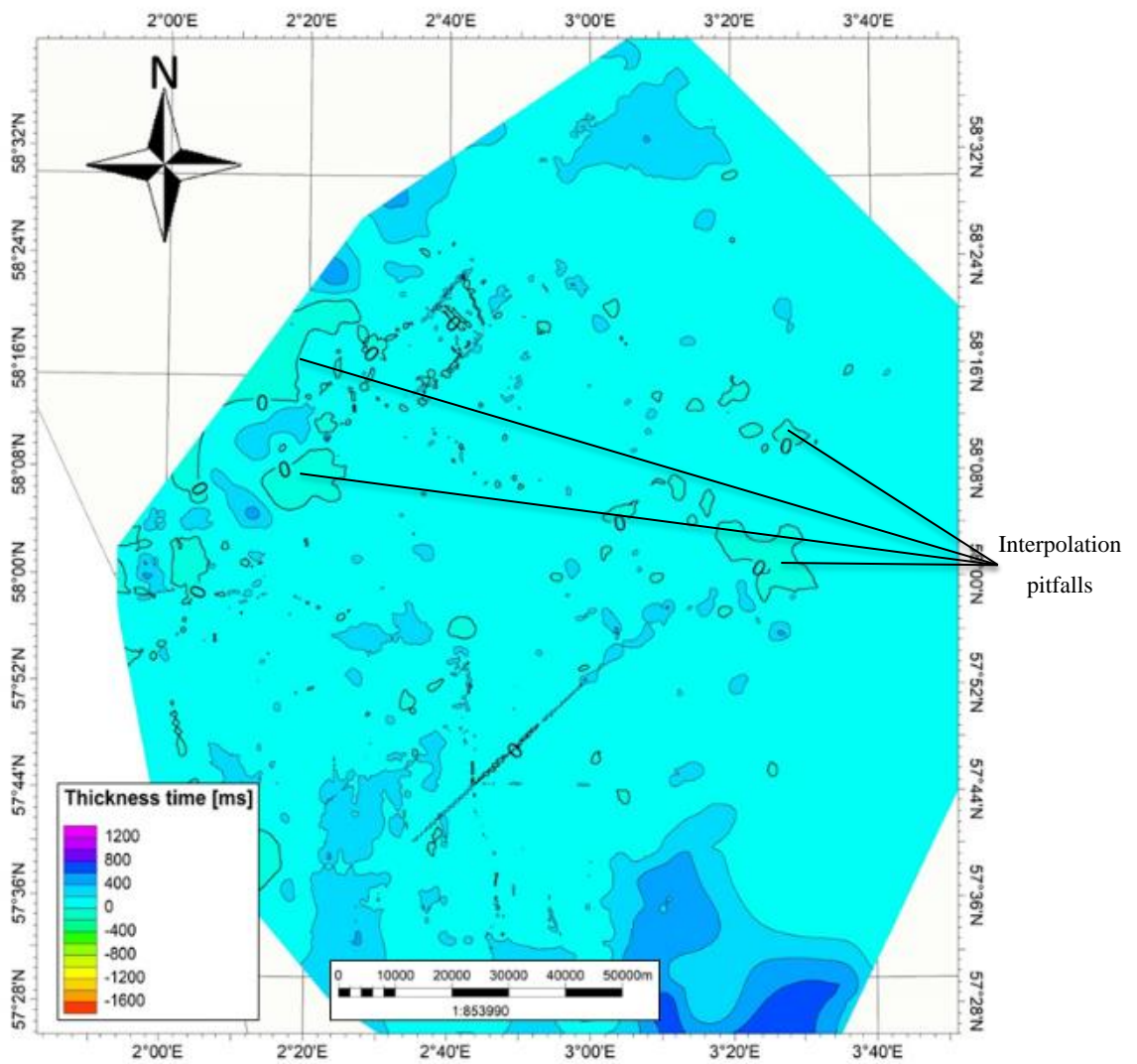


Figure 27: Time thickness map of seismic unit 2 (SU 2): Top Rotliegend to Bottom Rotliegend (Rotliegend Group).

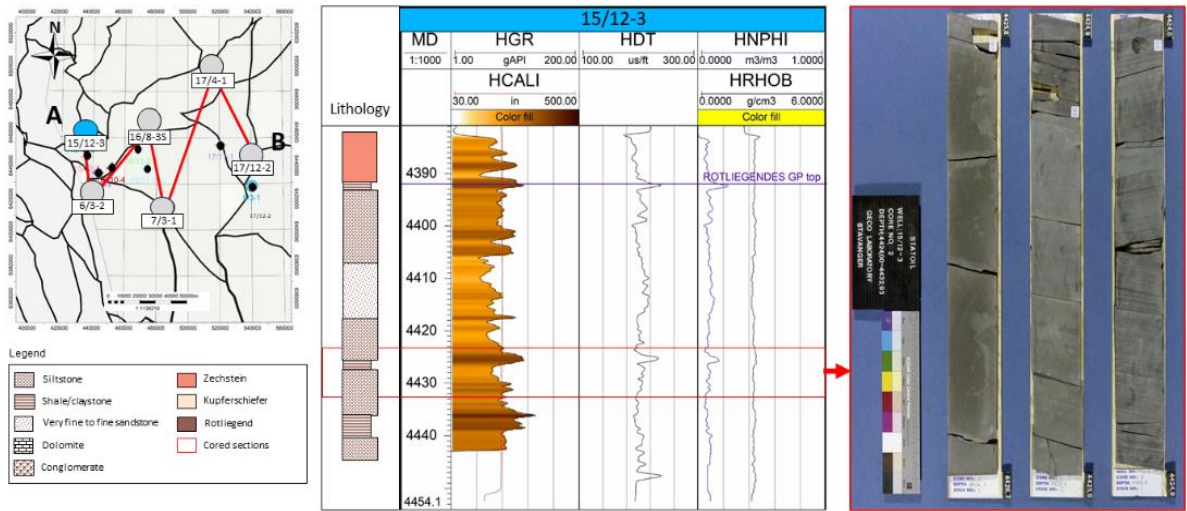


Figure 28: Well log response for 15/12-3 with interpreted lithology of the seismic unit 2 (SU 2): Top Rotliegend to Bottom Rotliegend (Rotliegend Group).

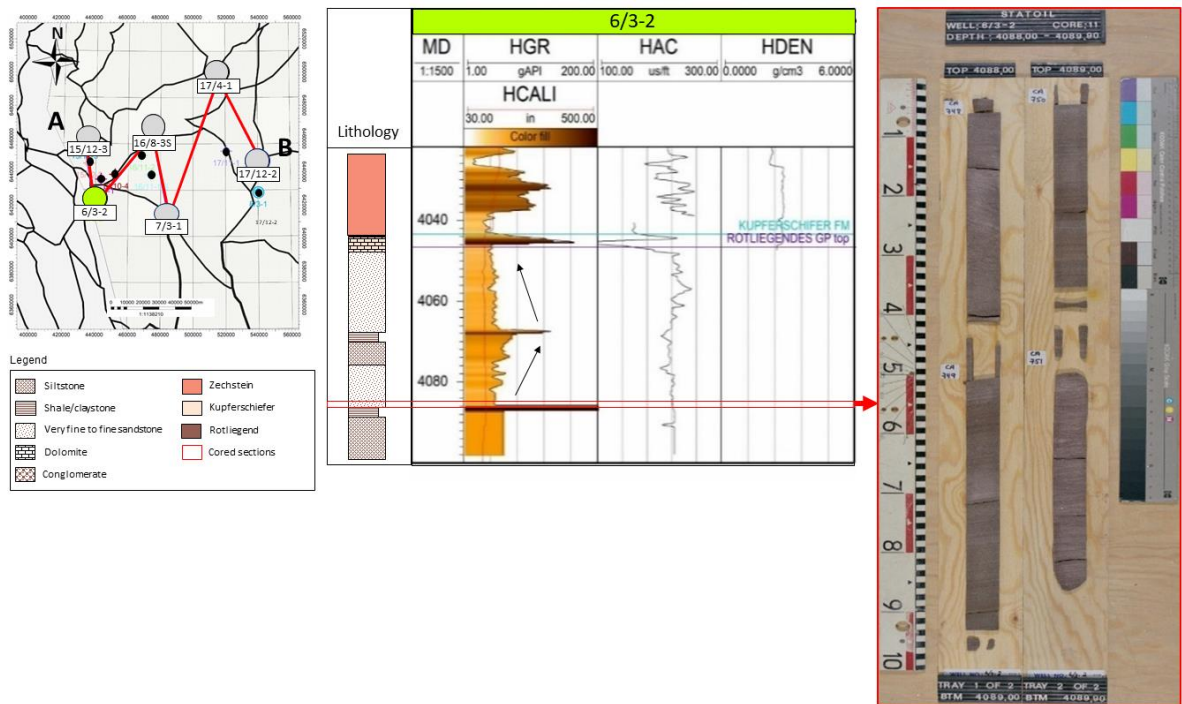


Figure 29: Well log response for 6/3-2 with interpreted lithology of the seismic unit 2 (SU 2): Top Rotliegend to Bottom Rotliegend (Rotliegend Group).

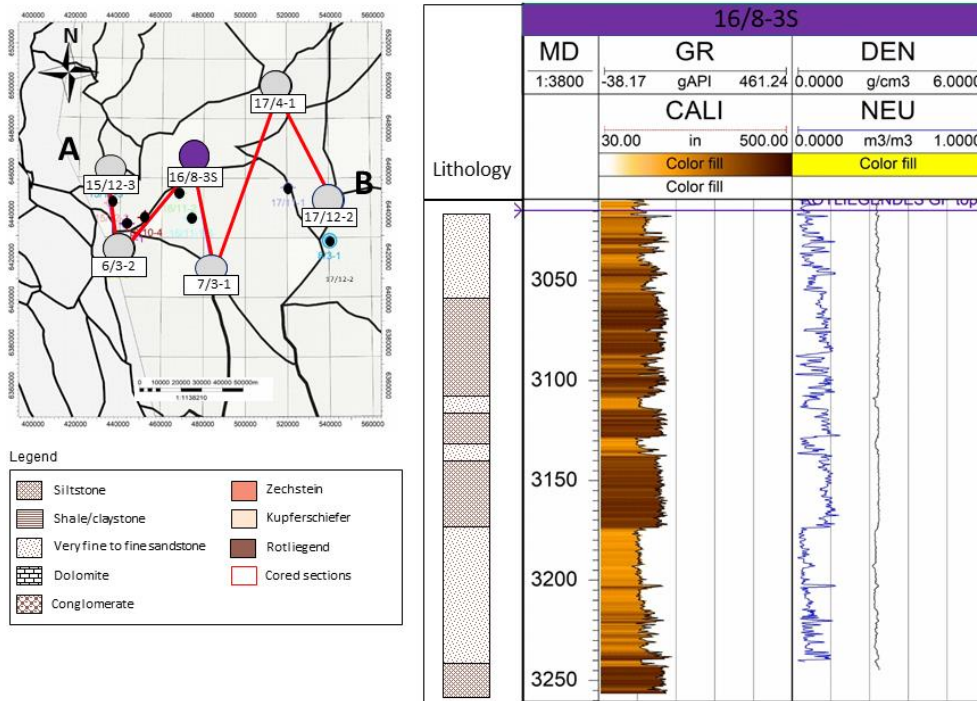


Figure 31: Well log response for 16/8-3S with interpreted lithology of the seismic unit 2 (SU 2): Top Rotliegend to Bottom Rotliegend (Rotliegend Group).

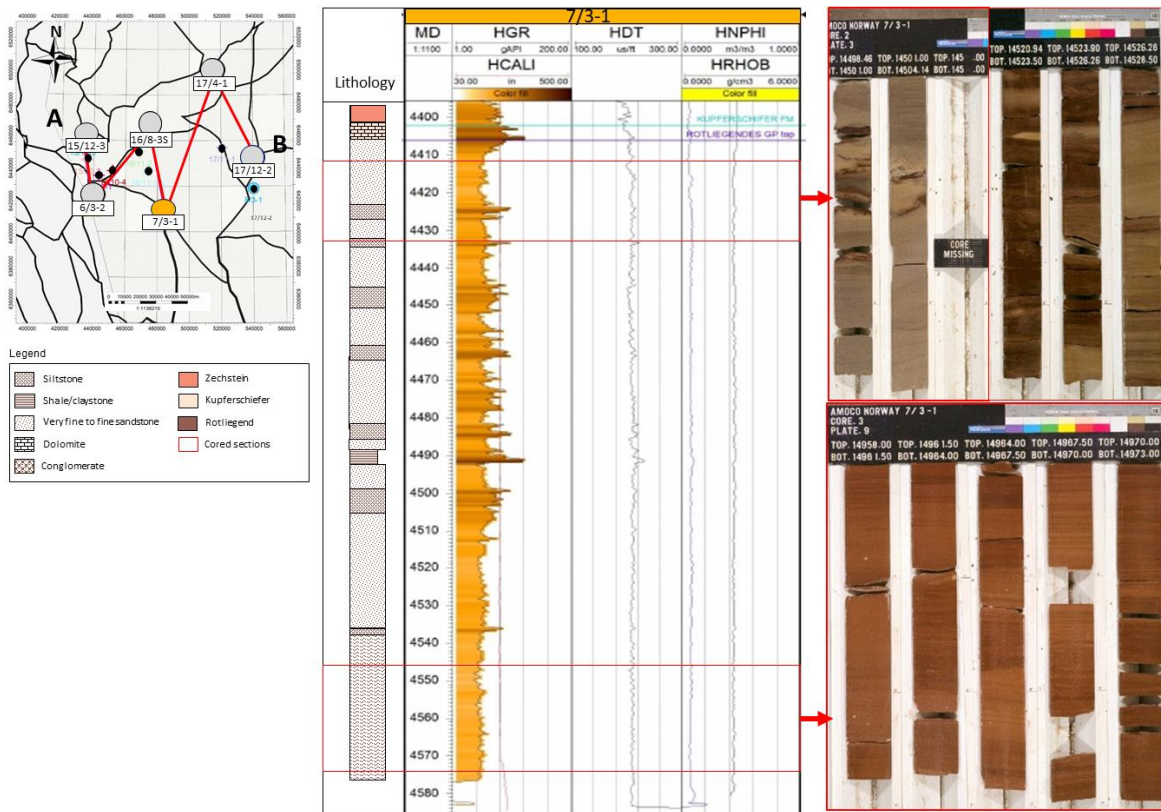


Figure 30: Well log response for 7/3-1 with interpreted lithology of the seismic unit 2 (SU 2): Top Rotliegend to Bottom Rotliegend (Rotliegend Group).

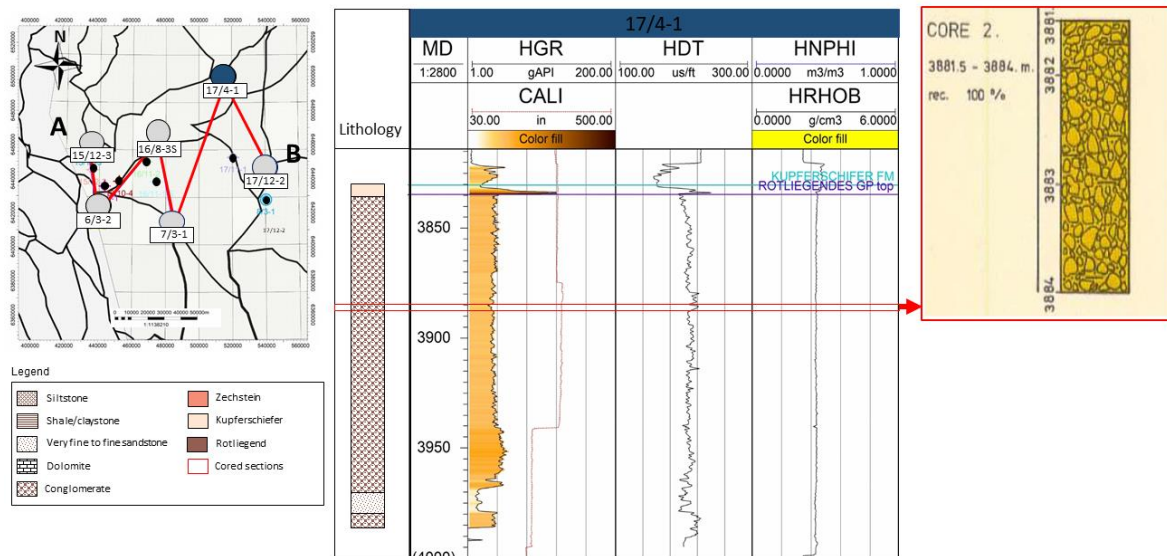


Figure 32: Well log response for 17/4-1 with interpreted lithology of the seismic unit 2 (SU 2): Top Rotliegend to Bottom Rotliegend (Rotliegend Group).

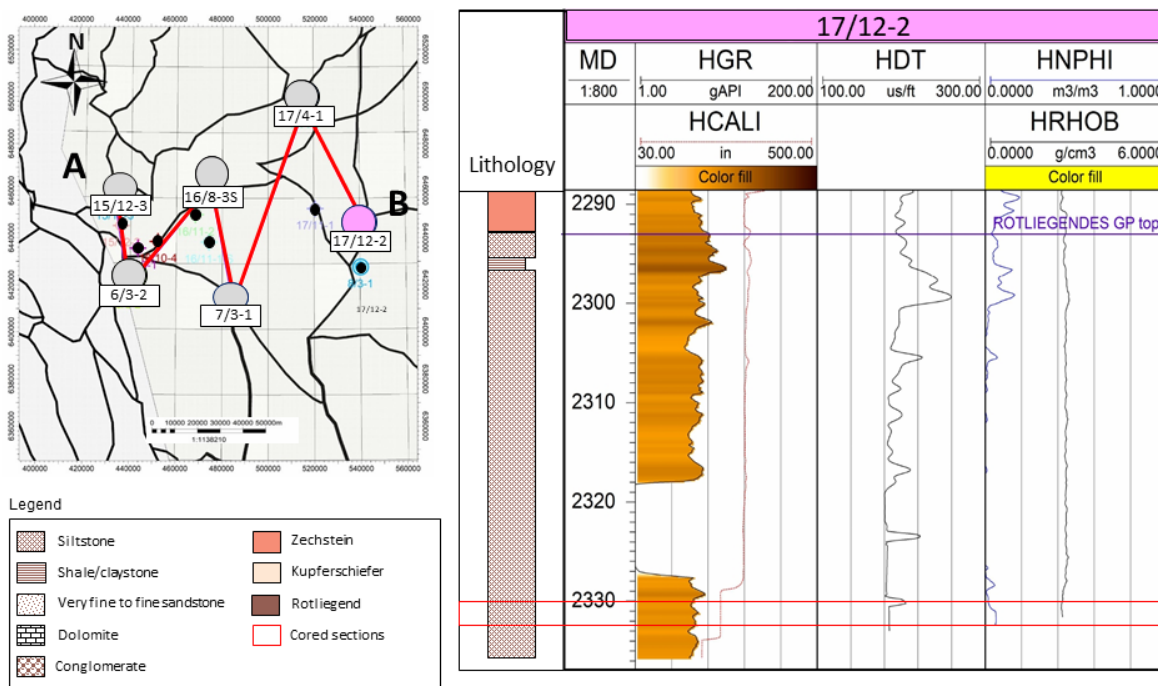


Figure 33: Well log response for 17/12-2 with interpreted lithology of the seismic unit 2 (SU 2): Top Rotliegend to Bottom Rotliegend (Rotliegend Group)

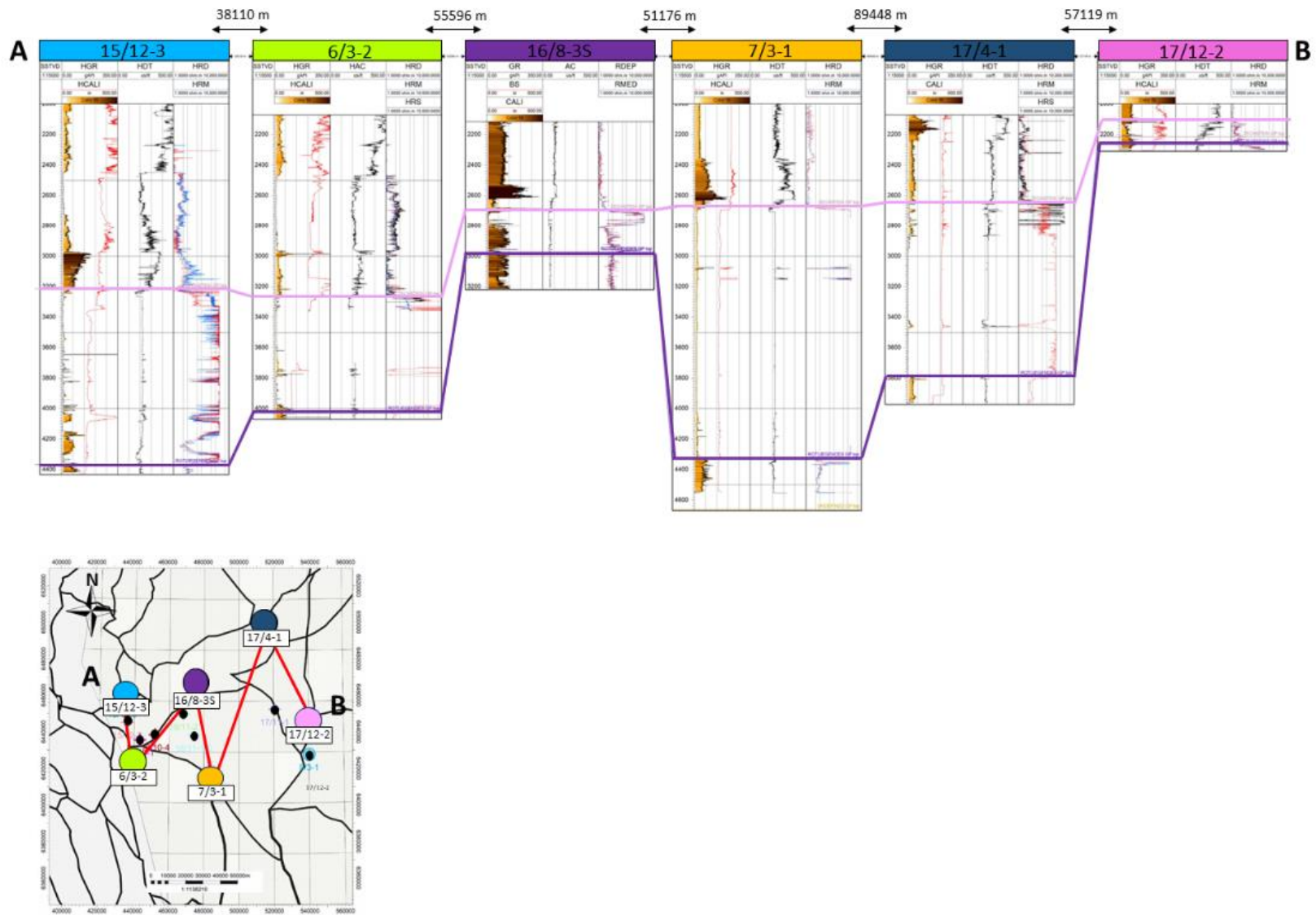


Figure 34: Structural correlation of the seismic unit 2 (SU 2): Top Rotliegend to Bottom Rotliegend (Rotliegend Group).

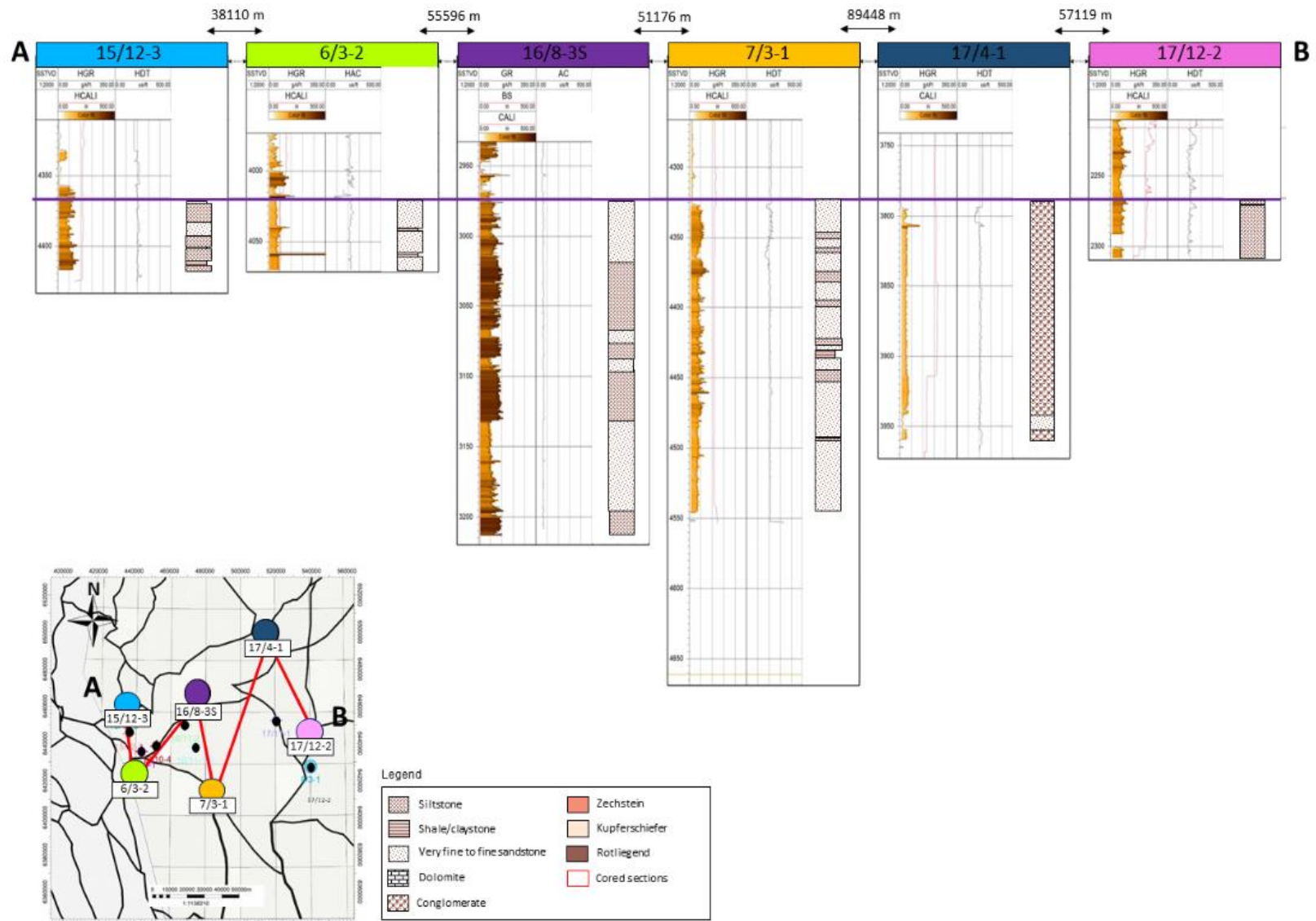


Figure 35: Stratigraphic correlation of the seismic unit 2 (SU 2): Top Rotliegend to Bottom Rotliegend (Rotliegend Group).

4.2.3 Seismic unit 3 (SU 3): Bottom Rotliegend to Bottom Devonian or Carboniferous

Visualization of stratal basal termination of SU3 was not possible due to low quality of the seismic images (*Table 2*). The lithological control is only present in the 7/3-1 well for the Carboniferous and 17/12-2 well for the Devonian. The distinction between Carboniferous and Devonian was proceeded based on the differences in seismic reflectors character and truncation of the Devonian reflectors towards the Carboniferous. Both Carboniferous and Devonian sections are intersected by all of the interpreted fault groups. The growth of strata is identified only along a hanging wall of the faults belonging to the fault group 3 and it is constrained to the Devonian and lower part of the Carboniferous deposition (*Figure 38*). In the figure 38 there is evidence for the pre-Rotliegend faulting which intersects only SU3. This fault has the same strikes as the fault group 3 (E-W) and presents growth of SU3 strata in the vicinity of its hanging wall.

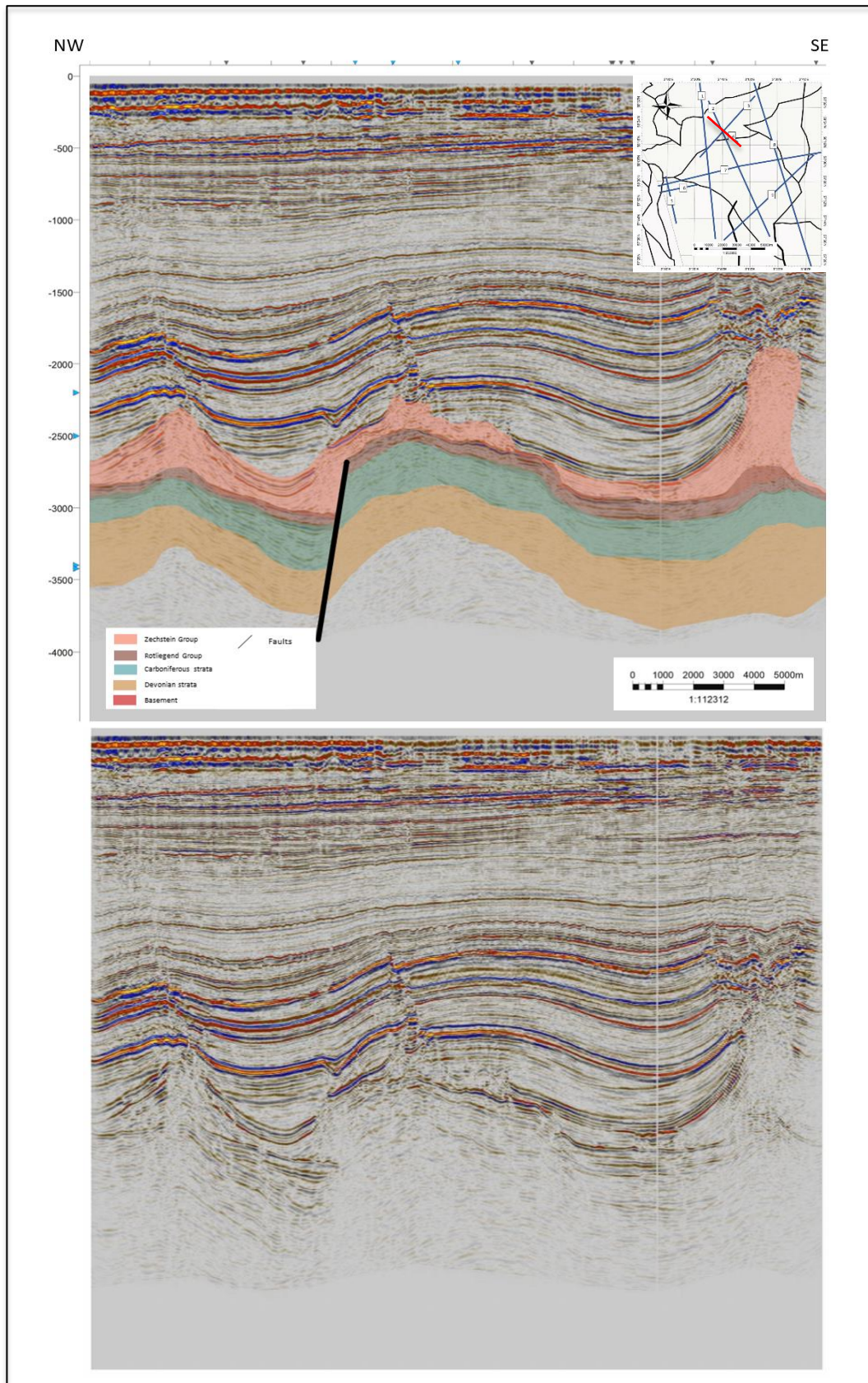


Figure 36: Interpreted cross section ST0611 xline 2950.

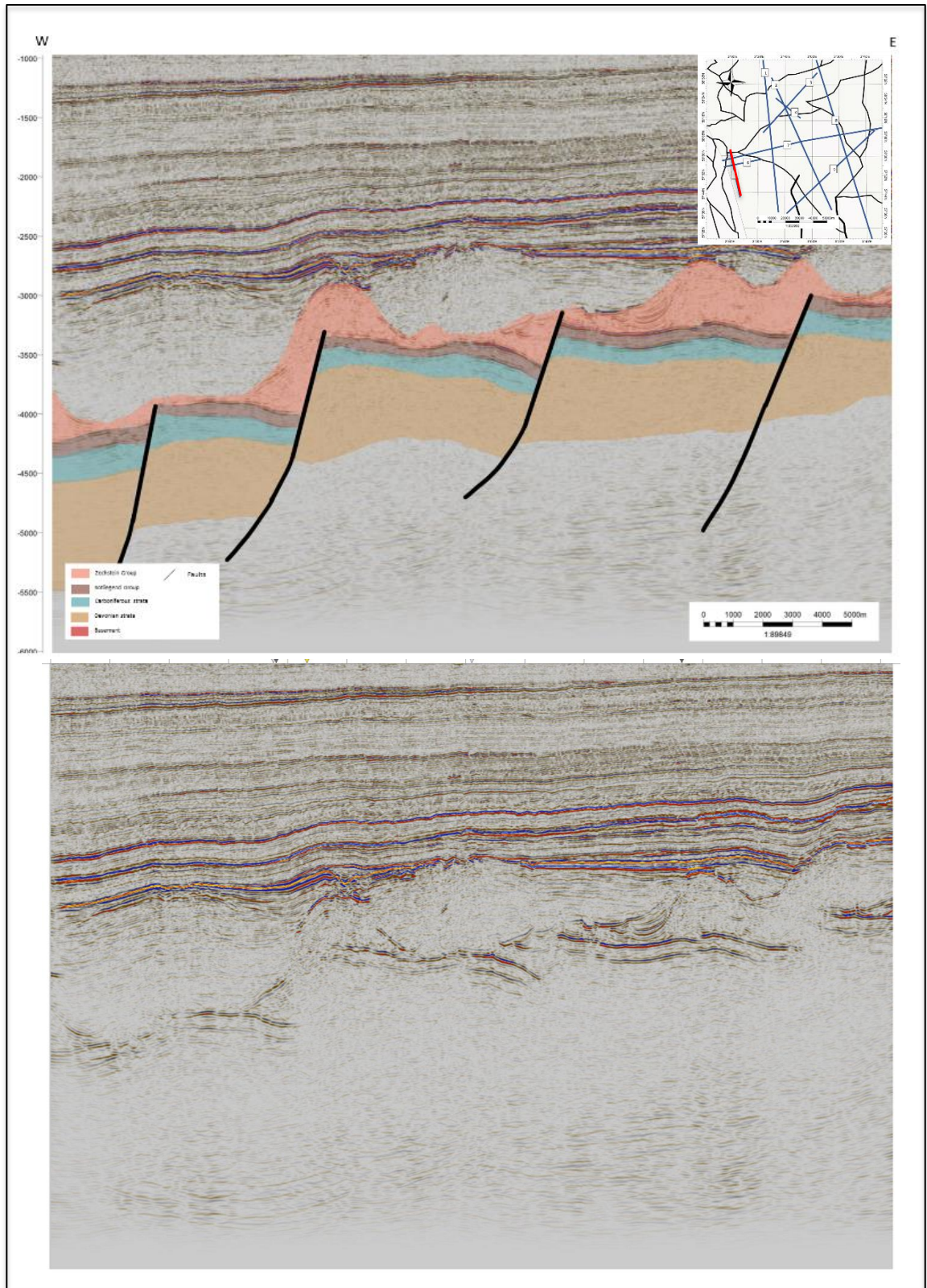


Figure 37: Interpreted cross section NH0201 xline 2600.

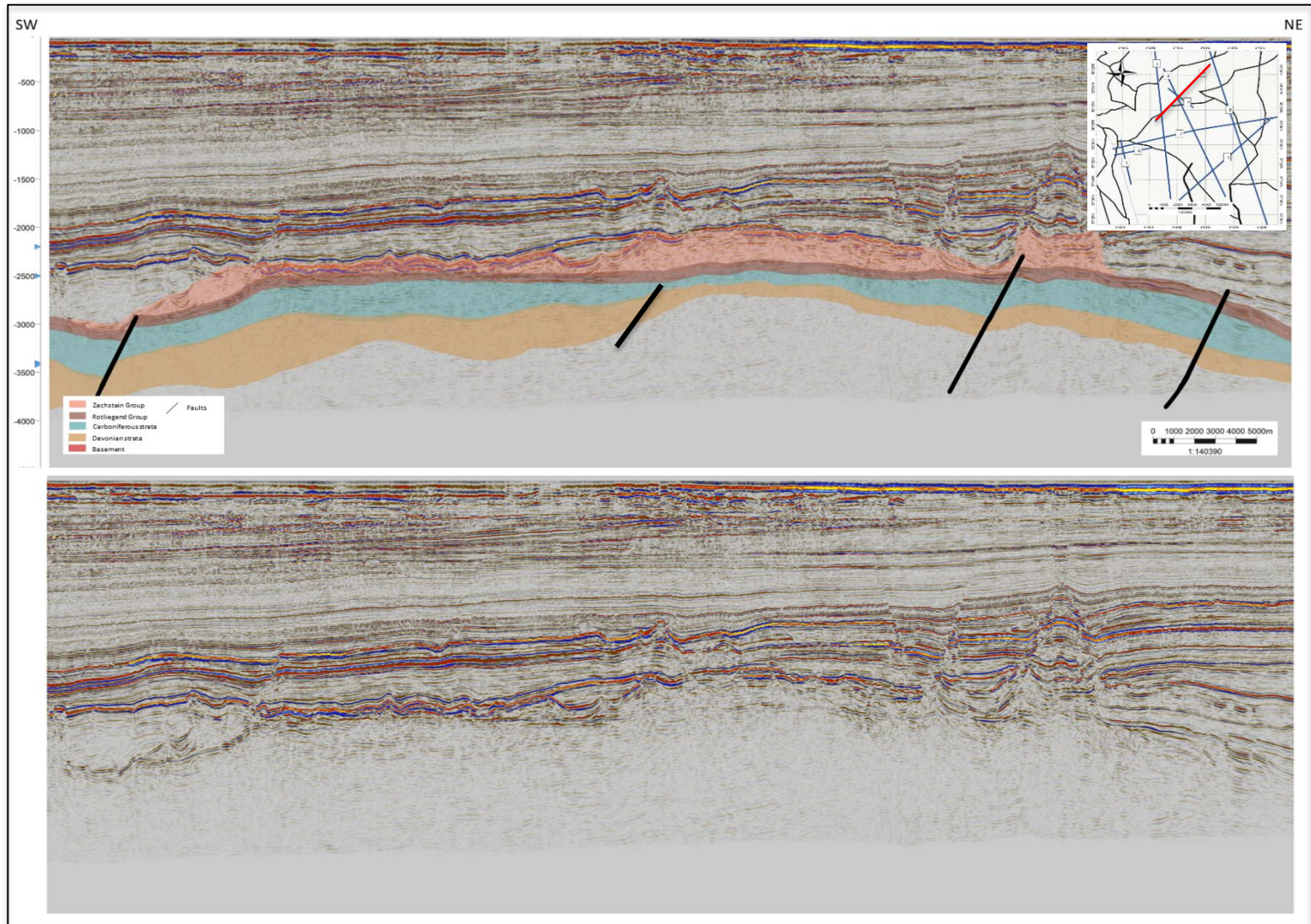


Figure 38: Interpreted cross section ST0611 inline 3860000.

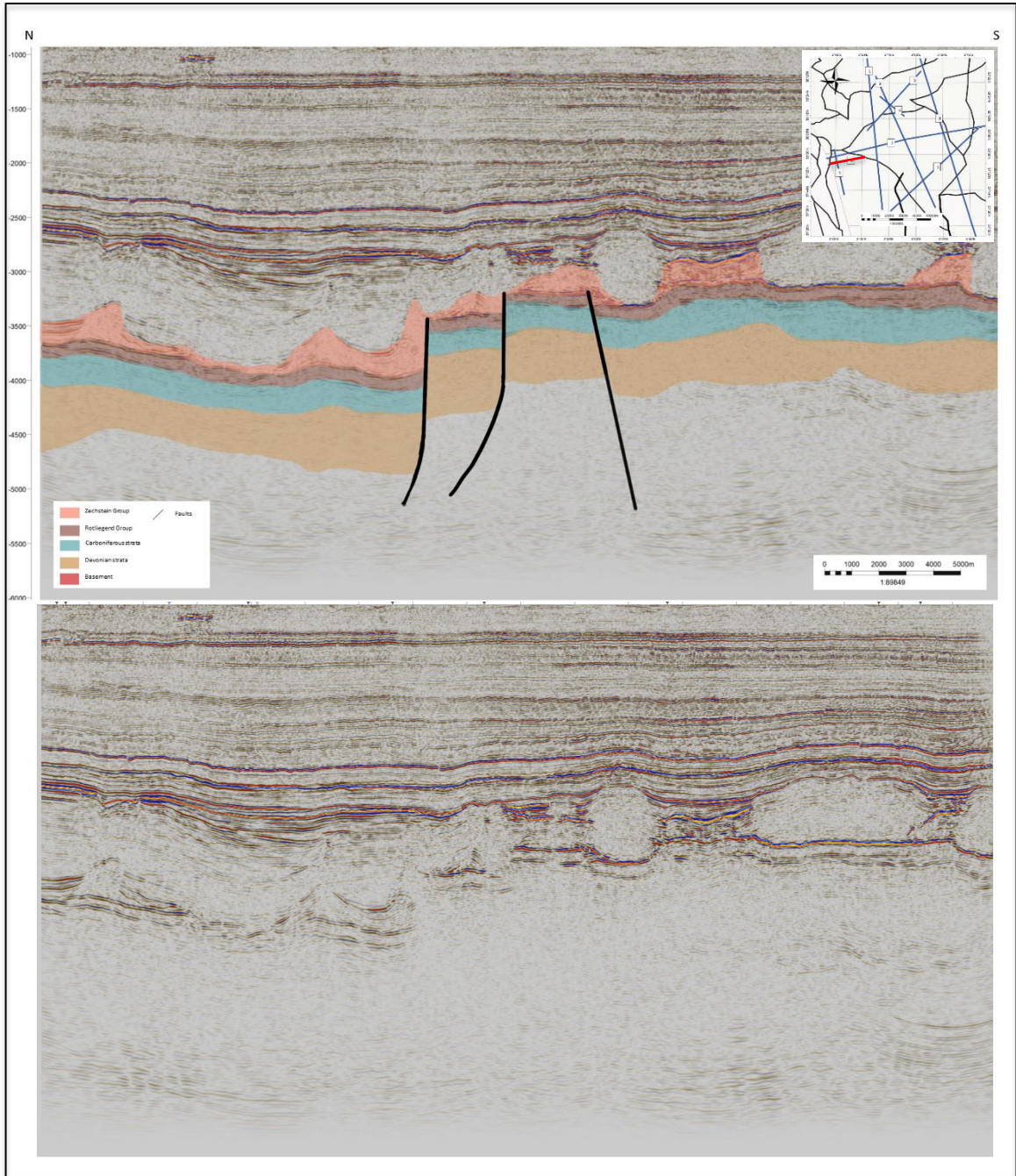


Figure 39: Interpreted cross section NH0201 inline 1300.

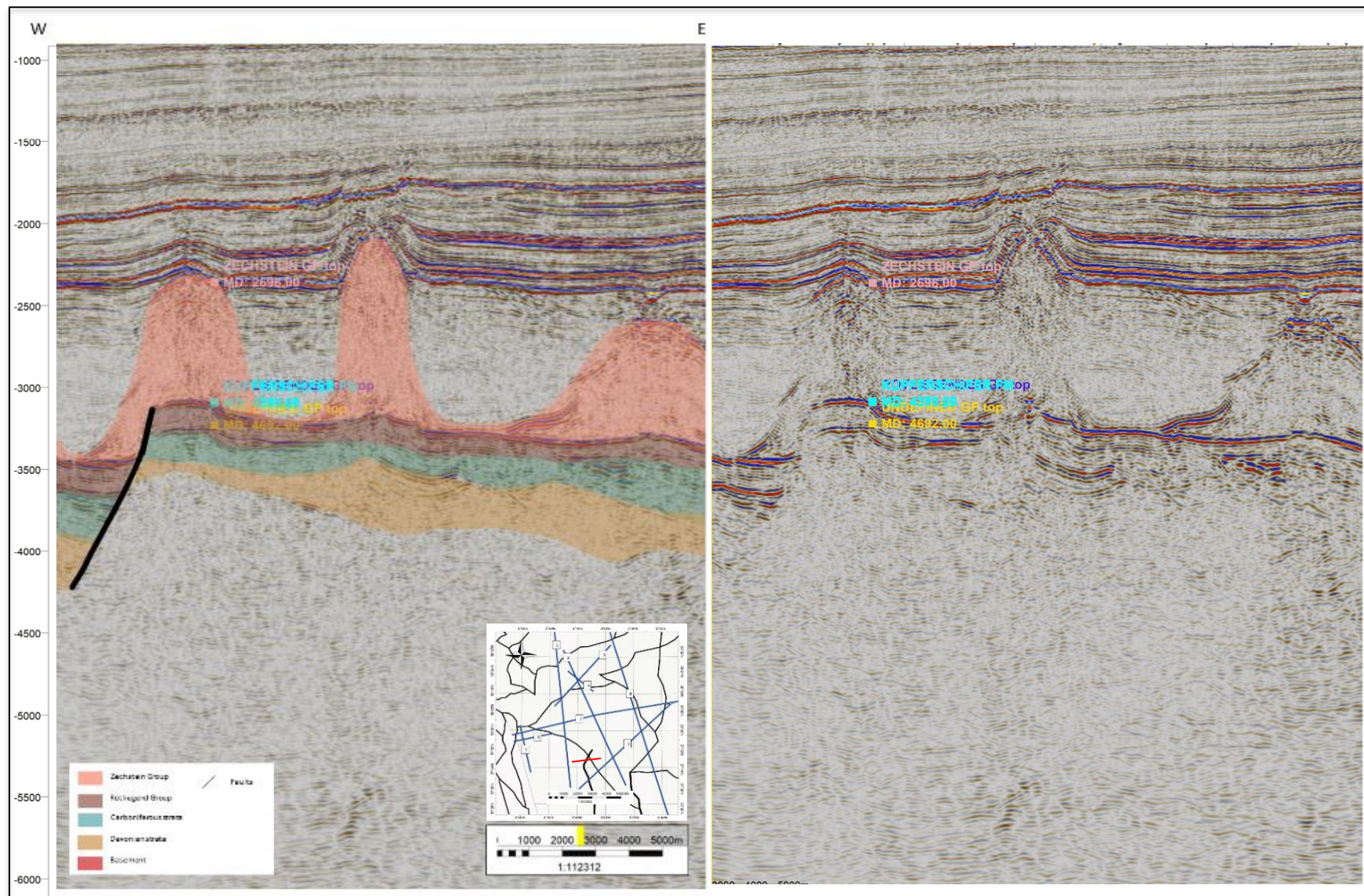


Figure 40: Interpreted cross section ST0710 xline 4750.

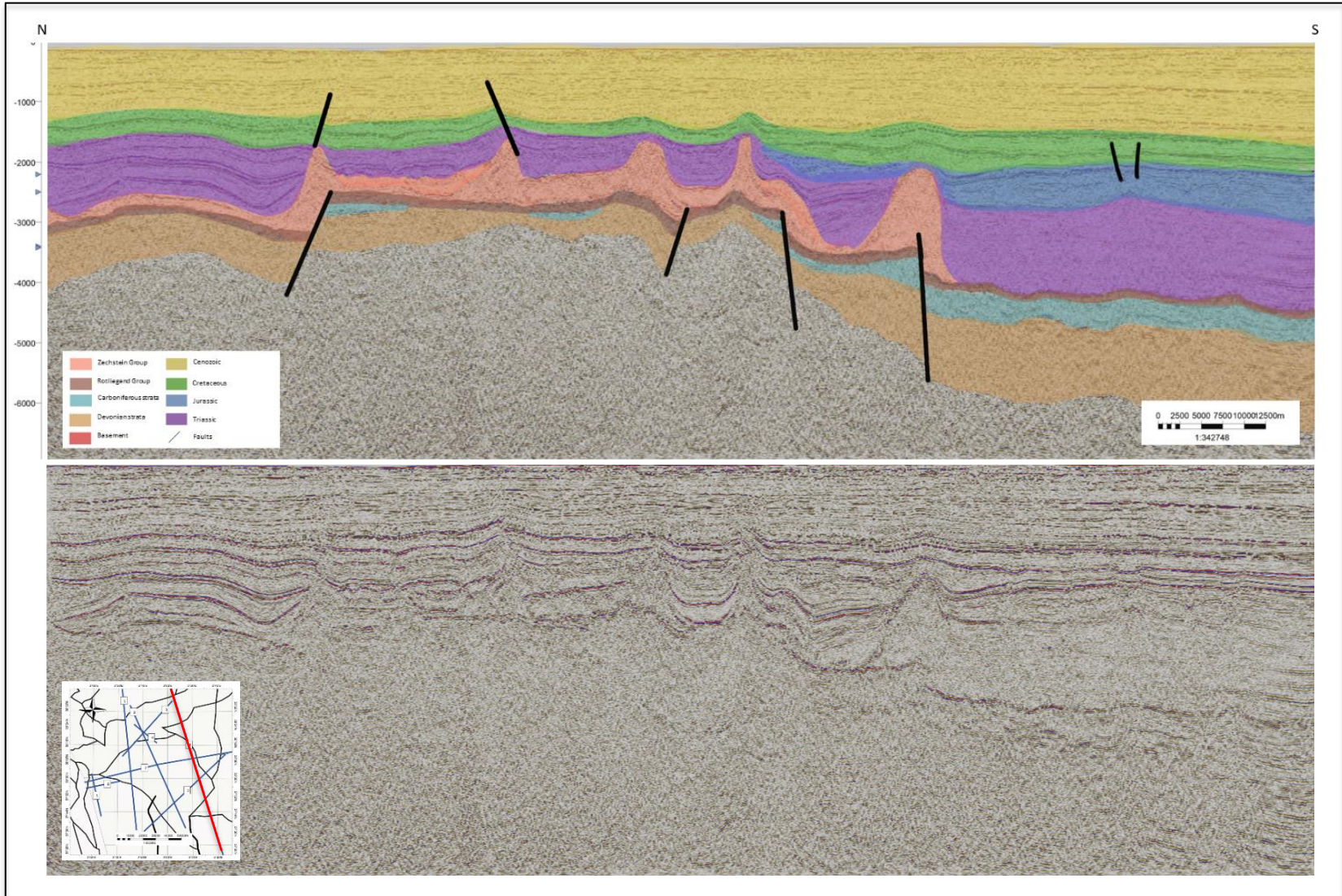


Figure 41: Interpreted regional N-S cross section UGI98-224.

5. Discussion

5.1 Tectonostratigraphic evolution of SU 1

5.2 Tectonostratigraphic evolution of SU 2

The SU2 is widely distributed in the given study area. It covers Sele High, the northernmost part of the Danish-Norwegian basin, northernmost part of Jæren High and the entire Southeastern bank of Ling Depression. It appears that during the time of deposition of this group only Sele High acted as local significant paleoelevation resulting in a reduced accommodation space than in the other parts of the study area. The Rotliegend Gp is intersected by all three interpreted fault groups and no evidence of the syntectonic fault- or fold-related deformation has been found. This suggests that the faulting occurred posterior to the deposition of Rotliegend Gp. Additionally, the significant southernward growth of strata might suggest that the region, which is found to the south, behaved as the regional depocenter where the accommodation space for Rotliegend Gp sedimentation was significantly greater than the accommodation space found in the central part of the study area (*Figure 36*). Interpretation of the southward growth of strata correlates with Skjoerestad (2021) and Rodriguez (2021) interpretation.

Since the SU 3 is truncating (*Figure 38*) towards the bottom of the SU 2, it is considered as unconformity. This interpretation is consistent with Ziegler (1990), Glennie et al. (1998) and NPD (2021). Therefore the erosional base of the SU 2 can be correlated to the Saalian Unconformity. Although some sections of the SU 3 seem to lay comfortably with the SU 2, the entire bottom of Rotliegend reflector can be treated as a part of the regional Saalian Unconformity.

5.3 Tectonostratigraphic evolution of SU 3

Visualization of the stratal basal termination of SU3 was not possible due to low quality of the seismic images (*Table 1 and 2*). The SU 3 was described as the section consisting of both Carboniferous and Devonian strata. Since in the entire study area there is only one well reaching the bottom of Rotliegend, the Devonian section of the SU3 is interpreted solely based on the change in character of the seismic reflectors. The Carboniferous part of the SU3 is drilled

in the 7/3-1 well (*Figure 31*) and it was distinguished by the change in the lithology from siliciclastic rocks of the Rotliegend Gp to the undated limestones. The distinction in the interpretation of the Carboniferous and Devonian strata of the SU3 is based on the difference in the seismic reflector character. Therefore, the lower boundary of the SU3 is interpreted with extremely low confidence, while the boundary which separates both sections is interpreted with low to medium-low confidence.

SU3 is intersected by all the interpreted fault groups. However, most of these faults become difficult to interpret at greater depths. Additionally, *Figure 38* shows evidence of the faulting that occurred prior to the SU 2 deposition. The most likely it is related to the extensional period of the Variscan orogeny. These extensional faulting resulted in creation of the series of a half graben basin. The Devonian and Carboniferous sediments are deposited in the hanging wall of overmentioned faults. (*Figure 37*). Nevertheless, in vicinity of the fault group 1 and fault group 2 we can spot evidence for the syn-sedimentary growth of thickness of the Devonian part of the SU3, which indicates that the extensional regime was active during the Late Devonian - Early Carboniferous times in the earliest stages of SU3 deposition and later were reactivated by late-Permian-Early Triassic rifting. These observations are consistent with the observations of Kalani et al. (2020) and Rodriguez (2020). According to Marshall et al. (2003), Kalani et al. (2020), Faleide et al. (2010) and *Figure 38* it is assumed that the Devonian rocks are deposited uncomfortably in the basins created by grabens and half-grabens basins of Caledonian basement. In some areas of the interpretation the reflectors of Devonian and Carboniferous sections of the SU3 are comfortable (*Figure 36*). This interpretation is consistent with Rodriguez (2021) and Kelani et al. (2020). The Carboniferous part of SU3 most likely consist of the strata typical for fluvial and lacustrine environment which by that time governed deposition in Central and Southern part of the North Sea (Marshall et al. 2003). Based on the regional geology, lithology content, Carboniferous part of the SU3 can be time equivalent with the Scremerston or Yordale Formations found in the UK sector. The absence of Carboniferous rock on the Sele High is an evidence that during Carboniferous, Sele high was existing as a structural high or that Saalian erosion removed Carboniferous sediments from the highest elevated structures. The unconformity marked at the top of the unit suggest that the ling graben area was relative uplifted and exposed to erosion. According to Kombrik et al. (2010) the uplift of the area could occur after Namurian times.

5.4 Tectonostratigraphic evolution of SU 4

The Central part of the North Sea rests on the merged basement rocks of the Caledonian Orogeny, where three continental plates collided with each other in Ordovician to Silurian times. The compressional stress regime produced thrusting of smaller scale terranes onto Scandinavian plate. The general rock composition of the basements are gneisses, schist and granites. However, in the study area only the 8/3-1 well which is located in the eastern flank of the Sele High provided depth and lithological control. During the drilling basal section of this well, the metamorphic schists were encountered. The K/Ar dating indicates that these rocks are Devonian age; Myhre, 1975). In most of the seismic lines and volumes SU4 top could not be interpreted due to the low seismic quality (*Table 2*). Furthermore, the vertical displacement of the SU 3 suggests the relative structural outline of the basement rocks (*Figure 41*).

Based on the examples given by Fazlikhani et al. (2017). The SU4 is possibly a result of the Caledonian Orogeny. It is supposedly present under the entire study area comprising a series of mini basins which were created under Variscan extensional regime which affected the central part of the North Sea. Subsequently, these basins became a depocentres for the Devonian and Carboniferous age sediments coming from erosion of over mentioned Caledonian rocks. Most probably due to the gravitational collapse proposed by Fossen et al. (2017) the faults presented in the study area are the result of the reactivation of the Caledonian thrust faults and creating a tectonic framework for the deposition of post-Devonian strata.

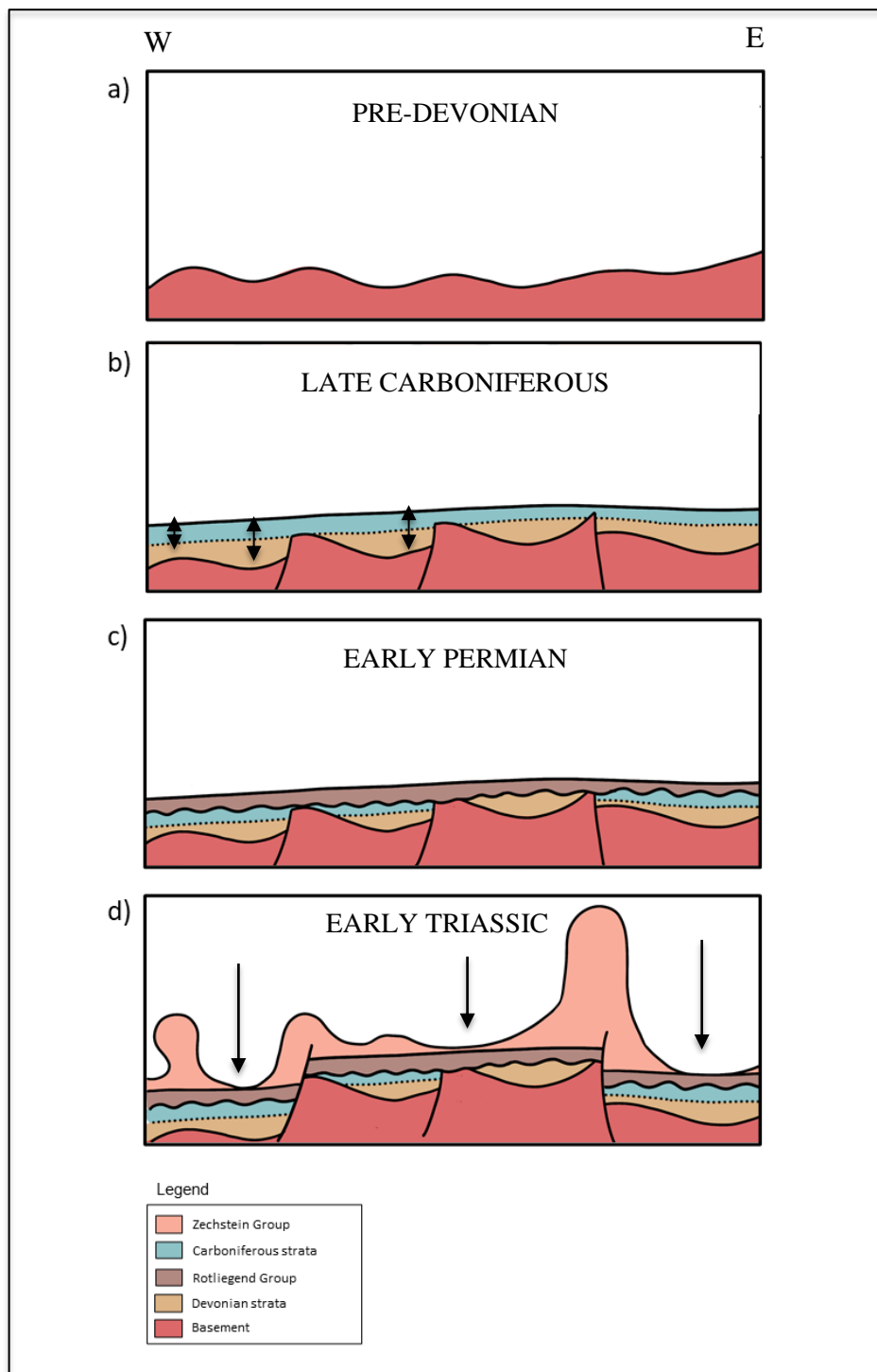


Figure 42: Model of the tectonostratigraphic evolution of the study area

6. Conclusions

Three fault families have been identified affecting the study area. Fault group 1 with N-S strike and fault group 2 with main strike NW-SE and Fault group 3, with the main strike E-W. Fault group 1 and fault group 2 created series of depocenters for the Devonian and Carboniferous rocks (SU3). Fault group 3, with the main strike E-W is considered to be active during Upper Permian-Early Triassic deposition of the Zechstein Group (SU1). Therefore, the configuration and tectonic outline of the study area is the result of multistage deformation where direction of extension has been gradually changing. The Sele high was a structural high since the pre-Carboniferous period. The SU2' horst with its series of half grabens most probably was formed as a result of Late Permian- Early Triassic extensional period. The SU3 were deposited in a series of grabens and half grabens basins. The basal part of SU3 of assumed Devonian age was deposited when the faulting was still active.

The upper part of the SU3 of the Carboniferous age strata was partially deposited during faulting activity and partially during post faulting. SU2 was deposited under tectonically stable conditions and appear to coincide with the regional thermal subsidence period, where the depocenters location and facies distribution were controlled by structural lows inherited from the Pre-Permian geomorphology. Its lateral and vertical lithological variation is a result of the heterogeneity of the braided- fluvial and aeolian depositional system. SU1 evaporites were deposited during early stages of the late Permian-Early Triassic rift phase which affected a wider part of the central and northern North Sea. Its lithological composition presents cyclicity and is controlled by the structural outline of the top of the SU1, the depth of the basin and the proximity to the basin's boundary.

References

- Bell, R. E., Jackson, C. A.-L., Whipp, P. S., & Clements, B. (2014). Strain migration during multiphase extension: Observations from the northern North Sea. *Tectonics*, 33(10), 1936-1963. doi:<https://doi.org/10.1002/2014TC003551>
- Bifani, R., and C. A. Smith, 1985, The Argyll Field After A Decade Of Production, Offshore Europe, Aberdeen, United Kingdom, Society of Petroleum Engineers, p. 32.
- Bruce, D. R. S., & Stemmerik, L. (2003). Carboniferous. In D. Evans, C. Graham, A. Armour, & P. Bathurst (Eds.), *The Millennium Atlas: petroleum geology of the central and northern North Sea* (pp. 83-89). London: The Geological Society of London.
- Clark, J. A., Stewart, S. A., & Cartwright, J. A. (1998). Evolution of the NW margin of the North Permian Basin, UK North Sea. *Journal of the Geological Society*, 155(4), 663-676.
- Coward, M. P., 1990, The Precambrian, Caledonian and Variscan framework to NW Europe: J Geological Society, London, Special Publications, v. 55, p. 1-34.
- Coward, M. P., 1995, Structural and tectonic setting of the Permo-Triassic basins of northwest Europe: Geological Society, London, Special Publications, v. 91, p. 7.
- Coward, M. P., M. A. Enfield, and M. W. Fischer, 1989, Devonian basins of Northern Scotland: extension and inversion related to Late Caledonian — Variscan tectonics: J Geological Society, London, Special Publications, v. 44, p. 275-308.
- Evans, D., C. Graham, A. Armour, and P. Bathurst, 2003. The Millennium Atlas: Petroleum Geology of the Central and Northern North Sea. Geological Society of London, 125-256.
- Evans, D., G. S. o. London, N. petroleumforening, and D. o. G. g. undersøgelse, 2003b, The Millennium Atlas: Petroleum Geology of the Central and Northern North Sea, Geological Society of London.
- Færseth, R. B. (1996). Interaction of Permo-Triassic and Jurassic extensional fault-blocks during the development of the northern North Sea. *Journal of the Geological Society*, 153(6), 931-944. doi:10.1144/gsjgs.153.6.0931
- Faleide, J. I., K. Bjørlykke, and R. H. Gabrielsen, 2010, Geology of the Norwegian Continental Shelf, Petroleum Geoscience: From Sedimentary Environments to Rock Physics: Berlin, Heidelberg, Springer Berlin Heidelberg, p. 467-499.
- Fazlikhani, H., Fossen, H., Gawthorpe, R. L., Faleide, J. I., & Bell, R. E. (2017). Basement structure and its influence on the structural configuration of the northern North Sea rift. *Tectonics*, 36(6), 1151-1177. doi:<https://doi.org/10.1002/2017TC004514>
- Fazlikhani, H., H. Fossen, R. L. Gawthorpe, J. I. Faleide, and R. E. Bell, 2017, Basement structure and its influence on the structural configuration of the northern North Sea rift, v. 36, p. 1151-1177.
- Fossen, H., Khani, H. F., Faleide, J. I., Ksienzyk, A. K., & Dunlap, W. J. (2016). Post-caledonian extension in the West Norway–Northern North Sea Region: The role of structural inheritance. *Geological Society, London, Special Publications*, 439(1), 465–486. <https://doi.org/10.1144/sp439.6>
- Fossen, H., 2010, Extensional tectonics in the North Atlantic Caledonides: a regional view: J Geological Society, London, Special Publications, v. 335, p. 767-793.
- Fossen, H., and E. Rykkelid, 1992, Postcollisional extension of the Caledonide orogen in Scandinavia: Structural expressions and tectonic significance: *Geology*, v. 20, p. 737-740.
- Gautier, D. L. (2003). Carboniferous-Rotliegend total petroleum system description and assessment results summary. *US Geological Survey, Bulletin 2211*, 24 pp.

- Glennie 2005 [Carboniferous hydrocarbon resources: the southern North Sea and surrounding onshore areas](#)
- Glennie, K. W. (1997). Recent advances in understanding the southern North Sea Basin: a summary. *Geological Society, London, Special Publications*, 123(1), 17-29.
doi:10.1144/gsl.Sp.1997.123.01.03
- Glennie, K. W., and Underhill, J. R., 1998, Origin, Development and Evolution of Structural Styles, v. IV, p. 42 - 84 in *Petroleum Geology of the North Sea - Basic concepts and recent advances*. Glennie, K. W. .
- Glennie, K. W., Higham, J., and Stemmerik, L., 2003, Permian: The Geological Society of London, p. 91 - 103 In: *The Millennium Atlas: petroleum of the central and northern North Sea*. Evans, D., Graham, C., Armour, A., and Bathurst, P. (editors and co-ordinators).
- Jackson, C. A.-L., & Lewis, M. M. 2016. Structural style and evolution of a salt-influenced rift basin margin; the impact of variations in salt composition and the role of polyphase extension. *Basin Research*, 28(1), 81–102.
- Kalani, M., J. I. Faleide, and R. H. Gabrielsen, 2020, Paleozoic-Mesozoic tectono-sedimentary evolution and magmatism of the Egersund Basin area, Norwegian central North Sea: *Marine and Petroleum Geology*, v. 122, p. 104642.
- Kombrink, H., and S. Patruno, 2020, The integration of public domain lithostratigraphic data into a series of cross-border North Sea well penetration maps: *J Geological Society, London, Special Publications*, v. 494, p. SP494-2020-25.
- Kombrink, H., Besly, B.M., Collinson, J.D., Den Hartog Jager, D.G., Drozdowski, G., Dusar, M., Hoth, P., Pagnier, H.J.M., Stemmerik, L., Waksmundzka, M.I. & Wrede, V., 2010, Carboniferous: EAGE Publications b.v. (Houten), p. 81-99 In: Doornenbal, J.C. and Stevenson, A.G. (editors): *Petroleum Geological Atlas of the Southern Permian Basin Area*.
- Lippmann, R. (2012). Diagenesis in Rotliegend, Triassic and Jurassic clastic hydrocarbon reservoirs of the Central Graben, North Sea : inorganic diagenetic processes and interactions with organic maturation products.
- Marshall, J. E. A. a. H., A. J., 2003, Devonian: EAGE Publications b.v. (Houten), p. 65 - 81 In: *The Millennium Atlas: petroleum geology of the central and northern North sea*. Evans, D., Graham, C., Armour, A., and Bathurst, P. (editors and co-ordinators).
- McKerrow, W. S., J. Dewey, and C. Scotese, 1990, The Ordovician and Silurian Development of the Iapetus Ocean, v. 44.
- Monaghan, A. A., J. R. Underhill, A. J. Hewett, and J. A. E. Marshall, 2019. Paleozoic Plays of NW Europe, Geological Society, 1-120. NPD Fact Maps, 2021. Fact Maps.npd.no (Accessed November 2021)
- NPD. (2021). Norwegian Petroleum Directorate. Retrieved from <https://factpages.npd.no/no>
- Ohm, S. E., D. A. Karlsen, N. T. Phan, T. Strand, and G. Iversen, 2012, Present Jurassic petroleum charge facing Paleozoic biodegraded oil: Geochemical challenges and potential upsides, Embla field, North Sea: *AAPG Bulletin*, v. 96, p. 1523-1552.
- Peryt, T. M., Geluk, M.C., Mathiesen, A., Paul, J. & Smith, K., 2010, Zechstein: EAGE Publications b.v. (Houten), p. 123 - 147 In: Doornenbal, J.C. and Stevenson, A.G.(editors): *Petroleum Geological Atlas of the Southern Permian Basin Area*.
- Rodriguez, D., 2021. Upper Paleozoic basin evolution in the Feda Graben and the Steinbit Terrace area, Northern Central Graben, Norway. Master's thesis, University of Stavanger, Stavanger, Norway, 136 p
- Rojo, L. A., Escalona, A., & Schulte, L. (2016). The use of seismic attributes to enhance imaging of salt structures in the Barents Sea. *First Break*, 34(11).
doi:<https://doi.org/10.3997/1365-2397.2016014>

- Scandinavian Caledonides. *Geology*, 40, 571-574. doi:10.1130/g32512.1
- Séranne, M., 1992, Orcadian basin Devonian extensional tectonics versus Carboniferous inversion in the northern: *Journal of the Geological Society*, v. 149.
- Skjoerestad, H., 2021. Halokinesis influence on the Triassic deposition and the evolution of minibasins in the Central North Sea. Master's thesis, University of Stavanger, Stavanger, Norway, 91 p
- Stemmerik et al 2000 Stratigraphy of the Rotliegend Group in the Danish part of the Northern Permian Basin, North Sea
- Trewin, N. H., and M. G. Bramwell, 1991, The Auk Field, Block 30/16, UK North Sea: Geological Society, London, Memoirs, v. 14, p. 227.
- Turner, B. R., Younger, P. L., & Fordham, C. E. (1993). Fell Sandstone lithostratigraphy south-west of Berwick-upon-Tweed: implications for the regional development of the Fell Sandstone. *Proceedings of the Yorkshire Geological Society*, 49(4), 269-281.
- Underhill, J. R., and M. A. Partington, 1993, Jurassic thermal doming and deflation in the North Sea: implications of the sequence stratigraphic evidence: Geological Society, London, Petroleum Geology Conference series, v. 4, p. 337.
- Vaughan, D. J., Sweeney, M. A., Friedrich, G., Diedel, R., & Haranczyk, C. (1989). The Kupferschiefer; an overview with an appraisal of the different types of mineralization. *Economic Geology*, 84(5), 1003-1027. doi:10.2113/gsecongeo.84.5.1003
- Vetti, V., & Fossen, H. (2012). Origin of contrasting Devonian supradetachment basin types in the
- Zenella, E., & Coward, M. P. (2003). Structural Framework. In D. Evans, C. Graham, A. Armour, & P. Bathurst (Eds.), *The Millennium Atlas: petroleum geology of the central and northern North Sea* (pp. 45-59). London: The Geological Society of London.
- Ziegler, P. A. (1982). Triassic rifts and facies patterns in Western and Central Europe. *Geologische Rundschau*, 71(3), 747-772. doi:10.1007/BF01821101
- Ziegler, P. A., 1975, The geological evolution of the North Sea area in the tectonic framework of North Western Europe.
- Ziegler, P. A., 1990, Geological atlas of western and central Europe.
- Ziegler, P. A., 1992, North Sea rift system: *Tectonophysics*, v. 208, p. 55-75.

Appendices

Appendix 1: Table of wells

Table of wells							
1	2	3	4	5	6	7	8
Well name	MD/TVD [m]	Completion date	Oldest Penetrated Age	Paleozoic formations from youngest to the oldest penetrated [m]	Bottom hole temperature [°C]	Discovery, HC age, reservoir formation and age	Well placement and objectives
6/3-2	4091/4085	10.03.1986	Early Permian	3229 Zechstein Gp 4043 Kupferschiefer Fm 4045 Rotliegend Gp	154	Oil shows in Cretaceous section	Well 6/3-2 was drilled on the gamma structure on an early Permian formed fault block, 1.4 km from the Norwegian/UK median line. The primary objective was to test Jurassic/Triassic sandstones at different levels for possible hydrocarbon accumulations. Secondary objectives were to test Cretaceous porous/fractured limestone/chalk and Rotliegend sandstone.
7/3-1	4700/4700	10.06.1969	Devonian/ Carboniferous?	2696 Zechstein Gp 4402 Kupferschiefer Fm 4406 Rotliegend Gp 4692 Undefined Gp	131	none	Exploration well 7/3-1 was drilled on the Sørvestlandet High close to the Western part of the Danish Norwegian Basin objectives were to test all horizons down to Permian Rotliegend.
15/12-2,	2924/2922	27.02.1976	Late Permian	2888 Zechstein Gp	81	none	Well 15/12-2 was drilled to evaluate Jurassic formations on a seismic structure located in the eastern part of block 15/12. The principal objective of the 15/12-2 well was to test the Dogger (Hugin Formation) sandstone, where oil shows had been encountered in the 15/12-1 well. A secondary object was a possible sand in the Paleocene.

15/12-3	4450/4449	22.12.1980	Devonian/ Carboniferous?	3238 Zechstein Gp 4382 Kupferschiefer Fm 4392 Rotliegend Gp	136	none	Well 15/12-3 is located in the South Viking Graben in the North Sea, south of the Sleipner Øst Field. The primary objective of the well was to test possible hydrocarbons in late Jurassic sand. Secondary objectives were Danian and Rotliegend sands.
16/8-3 S	3261/3243	01.05.2013	Early Permian	2734 Zechstein Gp 3015 Rotliegend Gp	109	none	The 16/8-3 S Lupin well was drilled in the Ling depression in the North Sea. The Lupin prospect was defined by a tilted horst block with several small internal rotated fault blocks of Permian age. The objective was to prove a commercial accumulation of hydrocarbons in Permian Rotliegend sandstones.
16/10-4	2580/2580	10.08.1998	Late Permian	2550 Zechstein Gp	109	none	Well 16/10-4 was drilled on the Trond prospect located in the northeast part of PL 101, which is southeast of the existing Sleipner field. The prospect was a north-south elongated salt-induced structure with dip closure in all directions. The main purpose was to test the hydrocarbon potential within the upper Jurassic (Hugin) formation in the prospect and to obtain representative cores of that sand package.
16/10-1	3151/3151	14.07.1986	Late Permian	3116 Zechstein Gp	none	none	Among the various structures defined within block 16/10, the one called "Alpha", located in the southwestern area. The purpose of the well was to explore all main reservoirs down to Triassic. The primary targets were the Jurassic and Triassic sandstone units, expected at 2850 m and 2980 m, respectively.
16/11-1S	3050/3020	31.10.1967	Late Permian	2255 Zechstein Gp	100	none	Well 16/11-1 S is located in the Danish Norwegian Basin. The objective of the well was to test the hydrocarbon potential of the Tertiary, Mesozoic and Permian sediments. Specifically, Tertiary sandstones, Cretaceous sandstones and limestones, Jurassic and Triassic sandstones, Permian carbonates and Permian Rotligend sandstone were considered to be prospective.
16/11-2	2378/2372	23.07.1973	Late Permian	2269 Zechstein Gp	none	none	The Anchovy (16/11-2) well was drilled on a semi-domal structure, about 5 miles long and 4 miles wide situated in the Danish-Norwegian Basin. The principal objective horizons were the Jurassic and Paleocene sands.

17/4-1	3997	26.08.1968	Early Permian	2665 Zechstein Gp 3829 Kupferschiefer Fm 3834 Rotliegend Gp	98	none	Well 17/4-1 was drilled on a NNE-SSW trending monocline in the Ling Depression between the Sele High and the Utsira High /Patch Bank ridge. The objective was to investigate the sedimentary section down to the pre-Permian, and particularly to test the hydrocarbon potential of the Mesozoic sands and Zechstein dolomites. Furthermore, Early Permian and/or pre-Permian reservoirs were to be evaluated if present.
17/12-2	2334	09.10.1973	Devonian/ Carboniferous?	2243 Zechstein Gp 2293 Rotliegend Gp 2300 Undefined Gp	none	Oil shows in middle Jurassic (Sandnes Fm.)	Well 17/12-2 is located on the north-western margin of the Egersund Basin in the North Sea, ca 14 km southwest of the 17/12-1R Discovery. The primary objective was to test Middle Jurassic and/or Triassic sands.
17/11-1	3269/3269	30.06.1968	Late Permian	2517 Zechstein Gp	83	none	Well 17/11-1 was drilled close to the western edge of the Sele High in the North Sea, in the anticlinal/flank feature. The original objective to test the Tertiary and Mesozoic sequences, was extended to penetrate the Zechstein salt and investigate the underlying formations.

Appendix 2: Table of seismic quality

	Name of seismic line	Top Rotliegend reflector	Bottom Rotliegend reflector	Top of Zechstein reflector	Acoustic basement reflector	Intra Carboniferous Devonian reflectors	Sum of quality points
1	UG97-101_mig320001	5	3	4	1	2	15
2	UG97-102_mig320001	4	3	5	1	2	15
3	UG97-103_mig320001	5	3	3	4	3	18
4	UG97-205_mig320001	5	4	3	2	4	18
5	UG97-207_mig320001	5	4	4	2	4	19
6	UG97-208_mig320001	5	3	4	1	3	16
7	UG97-212_mig320001	4	2	4	1	2	13
8	UGI98-118_mig320001	3	1	3	1	2	10
9	UGI98-119_mig320001	4	3	4	1	2	14
10	UGI98-120_mig320001	5	4	5	3	3	20
11	UGI98-121_mig320001	4	3	5	1	1	14
12	UGI98-122_mig320001	5	4	4	1	2	16
13	UGI98-123_mig320001	5	5	4	1	2	17
14	UGI98-125_mig320001	5	4	5	1	2	17
15	UGI98-126_mig320001	5	3	5	1	2	16
16	UGI98-127_mig320001	3	2	4	1	2	12
17	UGI98-214_mig320001	5	3	4	2	4	18
18	UGI98-217_mig320001	5	3	5	1.5	3	17.5
19	UGI98-222_mig320001	4	3	4	2	3	16
20	UGI98-224_mig320001	5	3	4	1	2	15
21	UGI98-229_mig320001	3	2	3	1	2	11
22	SHDE98-106_mig320001	4	4	3	2.5	1	14.5
23	SHDE98-107_mig320001	4	3	3	1	1	12
24	SHDE98-108_mig320001	3	3	4	1	2	13
25	SHDE98-109_mig320001	3	3	4	2	2	14
26	SHDE98-110_mig320001	5	4	4	1	2	16
27	SHDE98-111_mig320001	5	5	5	1	2	18
28	SHDE98-113_mig320001	4	4	4	2.5	2	16.5
29	SHDE98-114_mig320001	5	5	4	1.5	2	17.5
30	SHDE98-115_mig320001	5	5	4	2	3	19
31	SHDE98-116_mig320001	5	3	5	2.5	3	18.5
32	SHDE98-117_mig320001	5	4	3	1	2	15
33	SHDE98-202_mig320001	5	5	3	3	2.5	18.5
34	SHDE98-204_mig320001	5	4	3	2	2	16
35	SHDE98-205_mig320001	5	4	4	1	2.5	16.5
36	SHDE98-208_mig320001	3	2	3	1	2.5	11.5
37	SHDE98-210_mig320001	3.5	2.5	3	2	2	13
38	SHDE98-211_mig320001	5	4	4	1.5	2	16.5
39	SHDE98-213_mig320001	3	3	4	1	2	13
40	SHDE98-214_mig320001	3	2.5	3	1	2.5	12
41	SHDE98-215_mig320001	5	5	5	3	2.5	20.5

42	SHDEI98-105_mig320001	2.5	1.5	2.5	1	1.5	9
43	SHDEI98-106_mig320001	5	4	4	3	3	19
44	SHDEI98-107_mig320001	3	3	4	2	3	15
45	SHDEI98-109_mig320001	4	4	5	2	3	18
46	SHDEI98-110_mig320001	5	5	5	1	2	18
47	SHDEI98-114_mig320001	5	3	3	3	2	16
48	SHDEI98-116_mig320001	4	4	4	1	2	15
49	SHDEI98-118_mig320001	4	5	4	2	1	16
50	SHDEI98-206_mig320001	5	5	4	2	2	18
51	SHDEI98-207_mig320001	4	3	3	1	2	13
52	SHDEI98-208_mig320001	5	3	3	2	3	16
53	SHDEI98-209_mig320001	4	4	4	1	2	15
54	ES9501-35_mig320001	5	4	3	2	2	16
55	GLD-92-202_mig320001	5	4	4	2	1	16
56	GLD-92-205_mig320001	4	4	4	1	2	15
57	GLD-92-401_mig320001	4	3	3	2	2	14
58	GLDI-92-201_mig320001	5	5	4	1	2	17
59	GLDI-92-202_mig320001	4	5	4	2	3	18
60	GLDI-92-205_mig320001	5	4	4	2	2	17
61	GLDI-92-401_mig320001	4	3	5	1	2	15
62	GLDI-92-402_mig320001	4	3	4	2	2	15
63	GNSR-91-011_mig320001	4	4	4	1	1	14
64	GNSR-91-012-A_mig320001	4	2	2.5	3	3	14.5
65	GNSR-91-014_mig320001	4	3	3	2	1	13
66	ST8107WE-440_mig320001	4	3	4	3	2	16
Average reflector quality score		4.3	3.5	3.9	1.7	2.2	

	Name of seismic volume	Top Rotliegend reflector	Bottom Rotliegend reflector	Top of Zechstein reflector	Acoustic basement reflector	Intra Carboniferous Devonian reflectors	Sum of quality points
1	MC3D-JHT98_MC3D-JHT98_fmigFloat32	5	4.5	4	2	2.5	18
2	MC3D-VARG2002_MC3D-VARG2002-PSDM-TIME_fmigFloat16	4.5	3.5	3.5	1	2.5	15
3	NH0201_NH0201-FULL-OFF_fmigFloat32	5	5	5	1	1.5	17.5
4	ST0710_ST0710_fmigFloat16.bri	5	5	4	2.5	3	19.5
5	ST8802_ST8802_fmigFloat16.bri	4.5	4.5	2.5	1.5	2.5	15.5
6	ES9401_ES9401-AGC_fmigFloat32	4.5	4.5	4	1.5	2.5	17
7	ST0611-FULL-DEPTH-MIG-STRETCH-TO-TIME.MIG_FIN.POST_STACK.3D.JS-029412	5	5	4	3	4	21
Average reflector quality score		4.8	4.6	3.8	1.8	2.6	

Points	Quality category	
1	Very poor	Very attenuated and weak reflectors, chaotic discontinuous, sedimentary features invisible, impossible to interpret
2	Poor	Locally distinguishable reflectors, mostly weak, vastly attenuated and impossible for consistent interpretation
3	Good	Rather strong or at least distinguishable reflectors, locally attenuated, locally discontinuous, locally attenuated and very difficult to interpret
4	Very Good	Strong reflectors, locally attenuated but allows for further interpretation, visible outline of the chaotic reflectors, possible to interpret sedimentary features
5	Excellent	Very strong reflectors, continuous, possible to interpret sedimentary features, very good visibility in the entire volume

Summed points	Quality category	
15 equal or less	Poor	
16-17.5	Decent	
18-19.5	Good	
20-21.5	Very Good	
22-25	Excellent	

Appendix 3: Table of lithology

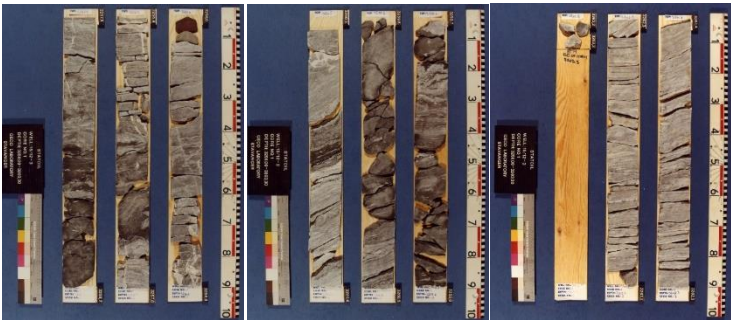
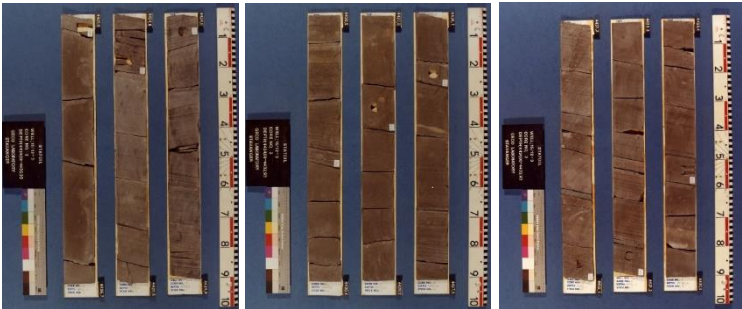

Well information				Conventional cores	
Well name	Formation well top [m](MD)	Lithology	Lithology based on NPD reports	Cored Paleozoic interval [m](MD)	Total core sample length [m]
6/3-2	3229 Zechstein Gp	The top is marked based on log break and is supported by appearance of white to pale gray anhydrite, occ. Pink, soft to firm, amorphous, occ. Crystalline. It is interbedded with thin medium to dark grey firm blocky, subfissile, slightly silty, micro micaceous, non to slightly calcareous shale. Trace amounts of dolomite occurs throughout entire section. From 3385m, clear to translucent, occasionally opaque white, firm to moderate hard, brittle and crystalline halite is dominating. From 4025m to 4045m it is interbedded with shale and very dark grey to grey dolomite dominate.	cuttings, logs, side-wall cored		
	4043 Kupferschiefer Fm	Red-brown, occ. medium to dark grey, moderate hard, blocky, and slightly dolomitic shale. Picked based on very high gamma response.	cuttings, logs		
	4045 Rotliegend Gp	Red-brown sandstone, very fine to fine to, moderate to well sorted, moderate hard, none to calcareous and silica cemented, slightly argillaceous and silty, angular to subangular, with some feldspar and mica. Brown to reddish brown to occ. black shale occur, soft to hard, occ. silty and non calc.	cuttings, logs, cores, side-wall cores	4098-4091	3m
7/3-1	2696 Zechstein Gp	Predominantly evaporites such as clear halite with some anhydrite and potassium salt with beds of dolomites and shale. The last 45m consists mainly of dark shale interbedded with dolomite.	cuttings, logs, cores	4380-4385	5m
	4402 Kupferschiefer Fm	Thick black radioactive shale.	cuttings, logs		
	4406 Rotliegend Gp	Red sequence of sandstone, shales and siltstones. In the upper part light grey slowly grading into red color. Fine to medium grained with dolomitic cement	cuttings, logs, cores	4415-4434; 4548-4575	46m
	4692 Undefined Gp (Devonian/Carboniferous?)	Dark brownish grey hard dolomite.	cuttings, logs		
15/12-2,	2888 Zechstein	The well bottoms in anhydrite section. It has sacroscopic to amorphous texture, grey-white and mostly soft. Minor amounts of siltstones are interbedded.	cuttings, logs		
15/12-3	3238 Zechstein	This group consist dominantly of halite interbedded with some K and Mg salt, shale and anhydrite. The halite is clear to light, buff occ. Pink, translucent, opaque, hard, brittle and crystalline. The K and Mg salt is pink to dark red, clear translucent brittle, crystalline and often interbedded with shale. the anhydrite is grey to white, massive and soft. The shale is brown, dark grey to black, hard, dense.	cuttings, logs, cores	3256-3263	7m
	4382 Kupferschiefer	Dark grey, moderately hard, dolomitic shale.	cuttings, logs		

	4392 Rotliegend	Red to red grey, very fine to fine, fair sorted, subangular, hard to very hard, dolomite cemented, argillaceous in places, slightly micaceous sandstone interbedded with red to red grey, moderate to hard, non-silty to silty, slightly calc./dolomitic shale.	cuttings, logs, cores	4424-4433	9m
16/8-3 S	2734 Zechstein Gp		cuttings, logs		
	3015 Rotliegend Gp		cuttings, logs		
16/10-4	2550 Zechstein Gp	The white to very light grey to grey, soft to firm amorphous to blocky anhydrite interbedded with red brown to medium dark grey, soft to firm, subfissile, non calc. Claystone.	cuttings, logs		
16/10-1	3116 Zechstein Gp	The sequence is composed of anhydrite and gypsum interbedded with shale, olive grey to dark greenish grey, hard, blocky. At 3113 a change of lithology to halite is inferred by a slight change in the gamma and resistivity log responses and a fall in sonic velocity.	cuttings, logs		
16/11-1S	2255 Zechstein Gp	Top 5 to 6 meters consist of anhydrite which is white and clear and consist of 3 or 4 layers which are underlain by 40m of anhydrite before clear colourless to pink rock salt reached at 2300m	cuttings, logs		
16/11-2	2269 Zechstein Gp	Anhydrite white, soft to firm interbedded with light to dark grey soft anhydritic shale. Below there is halite section.	cuttings, logs		
17/4-1	2665 Zechstein Gp		cuttings, logs		
	3829 Kupferschiefer fm	Dark grey shale and dolomite and anhydrites.	cuttings, logs		
	3834 Rotliegend Gp	Pebbles of quartzities, granite, gneiss, micaschists, porphyry are bonded by red siliceous cement giving an extremely tight and hard formation are present and some of them reaching over 10 cm of size. No sorting is present angular to subangular. Formation is barren of fossils, but porphyry pebbles and heavy mineral composition suggest rather Permian than Devonian.	cuttings, logs, cores	3881-3884	2,5m
17/12-2	2243 Zechstein Gp	Dolomite and limestone, grey, hard to very hard slightly argillaceous and micaceous, occ. Pyritic.	cuttings, logs, cores		
	2293 Rotliegend Gp				
	2300 Undefined Gp	Sandstone grey		2331-2334m	2.7m
17/11-1	2517 Zechstein Gp.	White-pinkish grey anhydrite, partially intergrown with salt crystals with thin shale stringers locally is present in the most upper part of Zechstein sequence. Below characteristic log brake there is rock salt with claystone, deeper there is dolomitic anhydrite section and next section is typical salt rock interbedded with potash salt.	cuttings, logs		

Appendix 4: Table of cores

Table of cores				
1	2	3	4	5
Well	Cored formation	Core length [m]	Interval [m]	Core photo
6/3-2	Rotliegend	3m	4098-4091	
7/3-1	Zechstein	5m	4380-4385	<p><i>Fig. 4a:</i> Core 2, 4419 m. Mud clasts in sand matrix.</p>
	Rotliegend	46m	4415-4434; 4548-4575	<p><i>Fig. 4b:</i> Core 2, 4427 m. Very sharp edged clay clasts with sand infillings, erosional surfaces and slumping</p> <p><i>Fig. 4c:</i> Core 3, 4563 m. Wavy, irregular bedding, grading upwards to regular laminations.</p> <p><i>Fig. 4d:</i> Core 3, 4566 m. Crossbedded sequence.</p>

Table of cores (continued)

1	2	3	4	5
Well	Cored formation	Core length [m]	Interval [m]	Core photo
15/12-3	Zechstein	7m	3256-3263	
	Rotliegend	9m	4424-4433	
17/4-1	Rotliegend	2.5m	3881-3884	<p>CORE 2. 3881.5 - 3884. m. rec. 100 %</p>  <p>Core: brn red-gy red, pbls up to 10cm, s+arg matrix, mainly subang-subrnd, very tight, siliceous & ferric cement. Polymict; pebbles of Quartzite, Gneiss, Granite, Micaschist and Volcanics.</p> <p>NPD Paper No. 14</p>
17/12-2	Rotliegend// Undiff. ?	2.7m	2331-2334	

Appendix 5: Table of geochemical data

Well information			Rockeval pyrolysis								Visual kerogen					Spore color index (1-10)		
Well		Interval and its source	S1 [mg of HC/g]	S2 [mg of HC/g]	S3 [CO2/g]	TOC [%]	HI	OI	PP	PI	Tmax [°C]	alg	exi	vit	inert	Ro		
6/3-2	3229 Zechstein	4030 SWC	16.58	1.33	1.03	1,34	99	77	17.91	0.93	441							
		4040 SWC	3.10	0.43	1	0.42	102	238	3.53	0.88	435							
	4043 Kupferschiefer Fm																	
	4045 Rotliegend Gp	4089 SWC	0.20	0	0.53	0.07	0	757	0.2	1								
7/3-1	2696 Zechstein	2709-2728 C				1.62		333						30	70		4.5	
		3102-3112 C																
		3168-3182 C													30	70	0.53	4
		4151-4170 C																
		4224-4242 C																
	4381-4385 CC											5		15	80	0.52	7	
	4402 Kupferschiefer														100			
	4406 Rotliegend	4547-4550 CC																
		4548-4574 CC																
	4692 Undefined Gp (Carboniferous?)	4684-4697 C															0.67	
15/12-2	2888 Zechstein	2915 C	0.02	0.02	0.09	0.04	50	225		0.5	409							
15/12-3	3238 Zechstein Gp	3256 CC			0.63	0.25		252	0.03	0.39								
		3261 CC	0.12	0.19	0.63	0.85	22	74	0.03	0.39	430							
		3263 CC			0.37	0.1		370										
		3270 C																
		4382 Kupferschiefer Fm																0.46
		4392 Rotliegend Gp	4424 CC	0.38	0.16	0.59	0.23	70	257	0.5	0.7	368						0.5
		4428 CC	0.31	0.01	0.38	0.26	4	146	0.3	0.97							0.42	
																	0.57	

		4432 CC	0.13		0.28	0.12		233	0.1	1							Permian spores no color defined	
16/8-3 S	2734 Zechstein Gp																	
	3015 Rotliegend Gp																	
16/10-4	2550 Zechstein Gp																	
16/10-1	3116 Zechstein Gp	3120 C				0.11												
		3122 C				19.11												
		3140 C				1.6												
		3151 C				1.15												
		3152 C				0.86												
16/11-1S	2255 Zechstein Gp	2258-2264 C				3.5	23	17			421							
		2267-2270 C				5.57	4	18			425							
		2273-2277 C				0.32		121										
		2280-2295 C				5.33												
		2298-2301 C				7.07												
		2310-2328 C				4.13												
16/11-2	2269 Zechstein Gp	2286-2316 C	0.98 or 4.98?	25.29		4.6	550			0.04		85	3	12				
		2316-2340 C	0.75	19.87		3.8	523			0.04		80	3	17				
		2347-2371 C	0.62	17.35		3.67	473			0.03		85	5	10				
17/4-1	2665 Zechstein Gp																	
	3829 Kupferschiefer Fm																	
	3834 Rotliegend Gp	3834-3839 C				1.67	100	99		0.5	436							
17/12-2	2243 Zechstein Gp	2255 C	5.4	3.6			180	45		0.6	430							
17/11-1	2517 Zechstein Gp																	

Legend

CC	Conventional core	
SWC	Side wall core	
C	Cuttings	
S1		The amount of free hydrocarbons in the sample.
S2		The amount of hydrocarbons generated through thermal cracking of non-volatile organic matter.
S3		The amount of CO ₂ produced during pyrolysis of kerogen.
TOC	Total organic carbon	The amount of organic matter in a rock sample, expressed as weight percent of the rock sample.
HI	Hydrogen index	$HI = [100 \times S2]/TOC$
OI	Oxygen index	$OI = [100 \times S3]/TOC$
PP	(Petroleum potential)	S1+S2
PI	(Production Index)	$PI = S1 / [S1 + S2]$
Tmax		The temperature at which the maximum release of hydrocarbons from cracking of kerogen occurs during pyrolysis (top of S2 peak).
Alg	Alginite	Algal debris plus cysts and bodies and amorphous sapropel
Exi	Exinite	Pollen and spore exine. Plant cuticle resins and other strongly fluorescent organic matter plus amorphous herbaceous
Vit	Vitrinite	Woody tissue altered to humic compounds plus nonfluorescent structured translucent material plus amorphous vitrinite
Iner	Inertinite	Coal material including fusinite, semifusinite, pseudovitrinite, macrinite and inertodetrinite
Vo	Vitrinite Reflectivity	A measure of the percentage of incident light reflected from the surface of vitrinite particles in a sedimentary rock.